치의과학박사 학위논문

Nanofibrous engineered matrix induces odontoblast differentiation through Wnt signaling pathways

Wnt 신호전달경로를 통한 나노섬유의 상아모세포 분화 조절

2015년 2월

서울대학교 대학원

치의과학과 분자유전학전공

Saeed Ur Rahman

Nanofibrous engineered matrix induces odontoblast differentiation through Wnt signaling pathways

Saeed Ur Rahman

Molecular Genetics Major,

Department of Dental Science

The Graduate School of Seoul National University

(Directed by Prof. Kyung Mi Woo, D.D.S., PhD)

Biomaterials have an important role in tissue engineering and regenerative medicine. In this aspect, the nanofibrous engineered matrix holds high potential for cellular differentiation and tissue regeneration that mimic the morphology of natural extracellular matrix microenvironment. Nanofiber induces the differentiation of cells not only committed to specific lineages, but also undifferentiated mesenchymal stem cells. Stem cells may require the specific extracellular signals that lead to induce in different lineages. However, the mechanisms by which nanofibrous engineered matrix promotes mesenchymal stem cells response differentially that lead to specific differentiation are mostly unknown. Some specific inductive factors might be involved in the initiation of such stimuli. However, the first aim of the present study was to investigate the responsiveness of mesenchymal stem cells on the nanofibrous matrix. Here, our study demonstrated that nanofibrous engineered matrix induces the growth factors expression profile

differentially among mesenchymal stem cells at same substrate and in same culture condition. Among growth factors, Wnts and BMPs signaling molecules were highly expressed in dental pulp-derived mesenchymal stem cells on the nanofibrous matrix. Among differentiation markers, dentin sialophosphoprotein (DSPP) expression was highly increased in human dental pulp-derived stem cells (hDPSCs) on polystyrene nanofibrous matrix (PSF), bone sialoptotein (BSP) expression was increased in hADSCs, while osteocalcin (OCN) expression was increased in human bone marrow-derived stem cells (hBMSCs) on PSF during osteogenic condition. It has been reported that Wnt signaling pathway has an important role in odontoblast differentiation *in-vitro* and tooth development *in-vivo*. However, the underlying mechanism was largely unknown. Here, we found that Wnt3a induces DSPP expression directly by canonical Wnt/β-catenin signaling pathway by using the nanofibrous engineered matrix. MDPC23 pre-odontoblasts cultured on electrospun PSF exhibited intense alizarin-red staining and abundant expressions of DSPP and DMP1, indicating that PSF promoted odontoblast differentiation. Canonical Wnt signaling pathway was involved in the PSF-induced DSPP expression indicating that, PSF maintained high level of β-catenin, and the β-catenin in the cells grown on PSF was trans-localized to nucleus. Further, we investigated that PSF increased activities of an LEF/TCF reporter. Knockdown of β-catenin and treatment with rDkk1 abrogated PSF-induced DSPP expression, while the forced expression of LEF1 and treatment with LiCl enhanced DSPP expression. In addition, adding the rhWnt3a protein to the culture of dental pulp cells increased DSPP expression. Furthermore, transplantations of MDPC cells seeded on PSF to the subcutaneous tissue of nude mice confirmed the association of PSF-stimulated Wnt3a with the DSPP

expression in an *in vivo* condition. Overall, these results demonstrate that Wnt3a induces DSPP expression through canonical Wnt signaling pathway when cells cultured on nanofibrous engineered matrix.

The nanofibrous matrix that mimics the feature of natural extracellular microenvironment not only binds the cells but also exert their impact on cell survival, shape, and reorganization. Therefore, the nanofibrous matrix implicates to facilitate cellular behavior such as cellular attachment, differentiation, morphology, and activate the intracellular signaling that lead to induce these characteristics. However, the morphological alterations and actin reorganization in dental pulp cells during differentiation induced by the nanofibrous matrix was unknown. Cellular polarization is an important morphological feature of odontoblast differentiation. Here we investigated that morphological alteration of MDPC-23 cells induced by noncanonical Wnt signaling pathway that has an important role in the generation of cellular polarization. Next, we found that Wnt5a is involved in morphological alterations of cells during odontoblast differentiation. The cells height and cell processes formation on PSF was increased and was further increased with rWnt5a treatment. The cell processes formation in cells on PSF was induced through CDC42 while the stress fibers formation was induced through RhoA in cells on TCD. Knockdown of Wnt5a, Ror2 or CDC42 abrogated PSF-induced cell processes formation. The stress fiber formation was increased in cells on TCD and was further increased with rWnt5a treatment; this stress fiber formation was reduced with knockdown of RhoA. The CDC42 activation was increased in cells on PSF while RhoA activation was increased on TCD. Collectively, the results in this study provide evidence that nanofibrous engineered matrix induces odontoblast

differentiation through Wnt signaling pathways.

Key word: Nanofiber, odontoblast, Wnt3a, β-catenin, Wnt5a

Student number: 2009-31329

CONTENTS

ABSTRACT …….....…..i

CONTENTS……..…….....…..…..v

LIST OF FIGURES.……..…viii

I. Introduction ……..…….……1

II. Purpose of Study…….…….....…..6

III. Literature Review…….....7

IV. Part-1

IV.1.
Introduction…….…….…….…….....…16

IV.2. Materials and Methods……..…...….21

IV.3. Results

IV.3.1. The electrospun polystyrene exhibits nanofibrous morphology..33

IV.3.2. Electrospun nanofibrous engineered matrix induces growth factors expression in mesenchymal stem cells……..…....35

IV.3.3. Nanofibrous engineered matrix induces osteogenic differentiation markers expression in mesenchymal stem cells….…….....38

IV.3.4. Nanofibrous engineered matrix induces differentiation markers and specifically DSPP gene expression in dental pulp stem cells ….....40

IV.3.5. PSF induced-Wnt3a affects DSPP gene expression in detal pulp-derived mesenchymal stem cells …….....…..42

IV.3.6. Polystyrene nanofiber matrix accelerates odontoblast differentiation and specifically induces DSPP gene expression..….....44

IV.3.7. Canonical Wnt signaling pathway is involved in PSF-induced DSPP expression…….…….....…46

IV.3.8. DSPP gene expression is a direct target of Wnt3a ……..….50

IV.3.9. Identification of LEF1 consensus motifs in Mouse DSPP gene promoter and regulation of DSPP promoter activity increases on PSF..55

IV.3.10. ChIP assay demonstrating β-catenin binds to the LEF1 binding sequence on the DSPP promoter…….……..58

IV.3.11. Effect of Wnt3a on the transcriptional activity of DSPP promoter…….....60

IV.3.12. *In-vivo* study shows the association of Wnt3a and DSP after cell-matrix transplantation into nude mice…….….62

IV.4. Discussion……..….……64

IV.5. Conclusion……..……..…..70

V. Part-II

V.1. Introduction……....…….…..…..71

V.2. Materials and methods…….....75

V.3. Results

V.3.1. Nanofibrous engineered matrix induces Wnt5a expression…….....82

V.3.2. Nanofiber matrix induces the morphological alterations of MDPC-23 cells…….....84

V.3.3. Nanofiber-induced Wnt5a alter the morphological changes and induces cell processes formation ……..…..88

V.3.4. Effect of Wnt5a on morphological alterations of MDPC-23 cells.92

V.3.5. Ror2 mediates the Wnt5a-induced morphological alteration of MDPC-23 cells……..96

V.3.6. Knockdown of RhoA induces the morphological alterations and cell processes formation in cells on PSF ……..100

V.3.7. Effect of CDC42 on morphological alterations and cell processes formation……103

V.3.8. Nanofiber-induced Wnt5a results in activation of CDC42.....106

V.4. Discussion…….…….…108

V.5. Conclusion…….....…113

VI. Conclusion……..….114

VII. References……..……118

VIII. Abstract in Korean……..…138

List of Figures

PART. I

Figure 1. Scanning electron micrographs of nanofibrous engineered matrix…….....34

Figure 2. The responsiveness of mesenchymal stem cells during diff erentiation on nanofibrous matrix..…….....….....37

Figure 3. Osteogenic differentiation markers expressions in mesenchymal stem cells …….....….....39

Figure 4. Effect of Wnt3a on osteogenic differentiation markers expressions in mesenchymal stem cells ….....41

Figure 5. Effect of canonical Wnt signaling on DSPP expression..43

Figure 6. Polystyrene nanofiber matrix accelerates odontoblast differentiation……..45

Figure 7. Wnt3a is involved in DSPP expression in cells on PSF…..…48

Figure 8. PSF-induced DSPP gene expression is a direct target of Wnt3a……...52

Figure 9. DSPP promoter activity in odontoblast (MDPC-23) cells and the binding of β-catenin to the putative LEF-1 binding sites on the DSPP promoter……..57

Figure 10. ChIP assay analysis …….....59

Figure 11. Wnt3a affects the transcription activity of the DSPP

promoter ……..61

Figure 12. MDPC-23 cells-scaffold constructs implanted into nude mice…….…..63

PART. II

Figure 1. Polystyrene nanofibrous matrix exhibits higher expression of Wnt5a…….....83

Figure 2. Nanofibrous matrix accelerates the morphological alterations of MDPC-23 cells……...….…85

Figure 3. Nanofiber-induced Wnt5a accelerates the morphological alterations…….…....89

Figure 4. Knockdown of Wnt5a affect the morphological alterations....93

Figure 5. Knockdown of Ror2 affect the cellular morphology……..….97

Figure 6. Knockdown of RhoA alter the morphological changes of MDPC-23 cells……101

Figure 7. PSF-induced morphological alterations affected by CDC42 knockdown…….104

Figure 8. The small GTPases are activated differentially in cells on TCD and PSF during odontoblast differentiation……..…..107

I. Introduction

Biomaterial has potential applications in the field of tissue engineering. Tissue engineering is a fast growing field that pursue to repair or regenerate damaged tissue or diseased organs through the cells, scaffolds, and soluble factors [Langer and Vacanti, 1999; Atala, 2004]. The cells under controlled and appropriate conditions can provide suitable function for the synthesis of new tissues. Stem cells possess specific properties that make them suitable for application in tissue engineering. Stem cells exhibit multilineage potential necessary for regulating cell proliferation, differentiation, and phenotypic expression. Stem cells fate affected by molecular factors, such as growth factors as well as environmental factors that contribute to the control of stem cell activity. Especially, an important is the effect of the micro-environment, i.e., the extracellular matrix (ECM) that has an important role on stem cell fate, particularly the cell-ECM interaction [Daley et al., 2008]. The effect of ECM to control the cellular activity may occur through multiple mechanisms, such as ECM elasticity, ECM geometry at the micro- and nanoscale, or signals transmitted from the ECM to the cells. However, the cell-ECM interaction can transduce different signaling pathways to provide new insight into the regulation of stem cells differentiation. The ability to engineer synthetic nanofibrous scaffold to mimic the natural ECM microenvironment control cellular behavior through physical, as well as molecular interaction, may attract the interest in tissue engineering application [Metallo et al., 2007]. The majority of different studies have focused on adult stem cell population, such as mesenchymal stem cells (MSCs). Therefore, it is essential to know the response of mesenchymal stem cells to the microenvironment that possesses certain properties in the

application of tissue regeneration.

The mechanisms by which nanofibrous engineered matrix to mimic natural ECM and to direct cell differentiation and morphological alterations are not known. Here, we hypothesize that the response of cells to the nanofibrous engineered matrix can induce some specific growth factors that lead to cell differentiation and changes in morphological structure. In our study, we determined the response of different mesenchymal stem cells to the nanofibrous matrix compared to tissue culture dishes as both substrates contained the same material. The current issue is to create the most favorable micro-environment to guide the cell differentiation that has application in tissue regeneration. Our study shows that the nanofibrous engineered matrix significantly influences the cellular behavior ranging from cell differentiation to morphological alterations.

Nanofibrous scaffolds provide suitable microenvironment for cell signaling that influence cell proliferation, differentiation, and biology. The aim of designing different nanofibrous scaffolds is to simulate the best structural and most suitable environmental pattern for extracellular matrix. The electrospinning, which is an easy and economical method for designing 3D nanofibrous scaffolds, has drawn attention in tissue engineering application because it provides a more suitable and natural environment for studies of cell behavior and a suitable engineered 3D surface similar to the extracellular matrix. Nanofiber scaffolds generated through electrospinning procedure have structures similar to extracellular matrix and can display most favorable features for tissue engineering purposes. The electrospun nanofibrous matrix holds high potential for cellular differentiation and tissue engineering. In the case of bone, an attempt has been made to use nanofiber in induction of

osteoblast differentiation and tissue regeneration. As we reported previously that, the nanofibrous scaffolding promotes osteoblast differentiation and biomineralization [Woo et al., 2007]. The performance of the dental pulp cells on electrospun nanofibrous matrix undergoes to differentiation both in-vitro and in-vivo. All these information emphasized a strong association of nanofibers with odontoblast differentiation and dentin formation, but the molecular mechanisms by which nanofibrous engineered matrix induced the odontoblast differentiation is unclear.

Dentin is the mineralized tissue that protects the pulp and supports the enamel and cementum. It contains 70% mineral, 20%organic matrix, and 10% water [Yamakoshi, 2009]. Dentin is similar to bone in mechanism of formation and protein matrix composition. During the formation of dentin, an unmineralized collagen-rich matrix termed pre dentin is secreted by the odontoblast and become mineralized when apatite crystals are deposited [Huang et al., 2008]. Odontoblasts are similar to osteoblasts in that they secrete extracellular matrix protein. However, the relative proportion of these ECM proteins may differ dramatically among them during differentiation and tissue formation. Odontoblast is considering as unique cells, which organized as a single layer responsible for dentin formation [Magloire et al., 2009].

The extracellular matrix (ECM) of dentin contains a number of noncollagenous proteins (NCPs) that considered as regulators of mineralization [Buttler et al., 2003]. The non-collagenous protein includes dentin sialophosphoprotein (DSPP), bone sialoprotein (BSP), dentin matrix protein 1 (DMP1), osteopontin (OPN), and matrix extracellular phosphoglycoprotein (MEPE). All these components are small integrin-

binding ligand N-linked glycoprotein (SIBLING), are components of the extracellular matrix of bone and dentin. The SIBLING proteins are considered to play an important role in the biomineralization of dentin [Fisher et al., 2001]. The non-collagenous proteins in dentin are dominated by DSPP derived proteins, which generated by proteolytic cleavage of dentin sialophosphoprotein (DSPP). DSPP is express in teeth, predominantly by odontoblasts (MacDougall et al., 1997; Begue et al., 1998]. The importance of DSPP and their derived proteins has been proven in dentin biomineralization by the tooth defects that occur in their absence. Genetic studies have shown that DSPP is critical for proper dentin formation (Holappa et al., 2006]. Several mouse models are present to understand the functional role of specific genes in tooth development [Fleischmannova et al., 2008]. Phenotypic abnormalities in the mineralization process of dentin associated with mutations in the genes of non-collagenous proteins (NCP) [Zhang et al., 2001]. The studies have shown that the genetic defects in dentin formations are dentinogenesis imperfect (DI), and dentin dysplasia (DD). Both are autosomal-dominant disorders of the dentin caused by mutation in DSPP gene. In the DSPP knockout mice, it has been reported that DSPP deficient mice show defect in dentin mineralization [Sreenath et al., 2003]. These informations give us the evidence that DSPP is very critical for mineralization of dentin.

Several pathways are involved in odontogenesis at molecular levels like Wnt signaling, BMPs, member of the hedgehog, and fibroblast growth factor. The disruption of any of odontogenic signaling pathways can disrupt tooth development and cause dental defect [Jarvinen et al., 2006; Kim et al., 2013]. Wnt forms a large family of secreted ligands that activate several receptor-

mediated pathways. In the Wnt signaling pathway, binding of Wnt ligands to Frizzled (FZ) receptor proteins and LDL receptor-related protein (LRP) family co-receptor causes activation β-catenin. The β-catenin accumulates and translocates to nucleus and transcriptional activation occur by complexes of β-catenin and LEF/TCF transcription factor family members [Logan and Nusse, 2004]. It is believed that the Wnt signaling pathways play an important role in odontoblast differentiation and tooth development [Thesleff and Sharp, 1997; Yamashiro et al., 2007]. All these informations give us the idea that nanofibrous engineered matrix may provide sufficient artificial microenvironment and synthetic platform to induce the odontoblast differentiation through Wnt-mediated signaling pathways.

II. Purpose of Study

Nanofibrous engineered matrix is a novel concept that mimic the natural extracellular matrix microenvironment to alter the cellular activity and play supportive role in differentiation and tissue regeneration. The combinations of physical, mechanical and biological properties of synthetic nanofibrous matrix permit osteoblast and odontoblast to initiate the formation of bone and dentin respectively. The performance of the dental pulp cells on electrospun nanofibrous matrix undergoes to differentiation has been reported [Wang et al., 2011; Cavalcanti and Zeitlin, 2013]. In addition, Wnt signaling pathway is a potent factor in odontoblast differentiation and tooth development. However, the underlying molecular mechanisms were unknown. The purpose of this study was to investigate the response of cells on the nanofibrous engineered matrix during odontoblast differentiation as follows:

Part I: Nanofibrous engineered matrix induces DSPP expression through canonical Wnt signaling pathway.

Part II: Nanofibrous engineered matrix induces the morphological alterations of MDPC-23 cells through Wnt5a.

III. Literature review

III.1. Biomaterials

The body has self-healing properties, but the extent of repairing processes vary amongst different tissues and can be impaired by the severity of different injury or disease [Lanza et al., 2000]. The development of biomaterials is an important avenue of tissue engineering to repair damaged tissue and to promote regenerative processes by transporting therapeutic agents and cell populations, as well as giving structural scaffolding that confer mechanical properties to healing tissues. Material selection is important to design the appropriate scaffold to provide support for tissue regeneration. Polymers can be constructed into adoptable scaffold such as gels and fibers, which may be functionalized chemically to improve the bioactivity and easily degradable. There are two kinds of polymers can be used for tissue regenerative purposes: natural polymers, and synthetic polymers. Natural polymers widely used include collagen, fibrin, alginate, silk, HAc, and chitosan, have some drawbacks, such as immunogenicity, processing difficulty, and variability depending on their source. These liabilities have prompted the development of synthetic polymers with more compositional characteristics [Lee et al., 2007]. However, several scaffolds have been fabricated for the dental applications with a variety of natural and synthetic biomaterials, such as ceramics [Miura et al., 2003], proteins [Kumada and Zhang, 2010], metals [Lin et al., 2010], and polymers [Young et al., 2002].

Synthetic polymers are attaining the popularity because they have a high mechanical stability, processing capability, biocompatibility and

biodegradability [Ma, 2008]. These features allow a polymer scaffold to be used into biological systems and designed to mimic the natural extracellular matrix (ECM) microenvironment. The metallic scaffolds have been considered for bone-related functions, due to attractive physical properties and their good ability to promote tissue growth. The most commonly known materials in this class are tantalum (Ta) and titanium (Ti). These structures showed mechanical properties closer in texture to bone, as well as inducing osteoblast adhesion, proliferation and differentiation [Takemoto et al., 2005; Xue et al., 2007].

The other class of biomaterials called biocomposites that are designed with the aim of advantageous key properties from two classes of materials, in which natural or synthetic polymers are often combined with inorganic components, such as CaPs or bioglasses [Mieszawska et al., 2010]. The calcium phosphate (CaP) bioceramics are inherently slow degrading and have stiff properties, and they must be combined with other polymers to yield better structures. The commonly used CaP ceramics are b-tricalcium phosphate (TCP), hydroxyapatite (HA), and biphasic calcium phosphate (BCP) [Guo et al., 2009; Sohier et al., 2010].

Biomaterials play critical roles in modern strategies in tissue engineering and regenerative medicine and have designable biophysical and biochemical milieus that direct cellular behavior and function [Langer and Tirrell, 2004; Hubbell, 1995]. Polymeric nanofiber matrix is among the most encouraging biomaterials for native ECM analogs. The microscaled polymeric nonwoven matrix has already been used in tissue engineering because of its high porosity and high surface area [Kim et al., 1994]. The processes with which nanoscale polymeric fibers are synthesized by electrospinning technology is

the simplest, cost-effective, and efficient method, has excited interest in the field of biomaterials and tissue engineering. The nanofibers can be designed to promote the cell functions such as cell adhesion, proliferation, differentiation, and tissue neogenesis [Ma, 2008].

III.2. Electrospinning

Electrospinning is a technology for polymer processing. It has been explored for last several decades. Special needs in biomedical and advanced research related applications have stimulated renewed interest and studies on electrospinning. The principle use of electrospinning method is to use an electric field to synthesize the nanofiber from the polymer solution. High voltages are using to develop sufficient surface charge to reduce the surface tension in a polymer fluid. Electrospinning usually make nonwoven matrix sheet. The 3-D nanofibrous engineered matrix can be produced to prolong the time, and the thickness of the nanofibrous matrix increases with electrospinning time. Most of the biomaterials are widely used in tissue engineering have been fabricated into the nanofiber via electrospinning. The synthetic as well as naturally occurring polymers can be electrospun into nanofibers by electrospinning [Li et al., 2002; Matthews et al., 2002, Wnek et al., 2003].

III.3. Role of nanofiber in cell differentiation and tissue regeneration

The biological processes of the cells need continuous flow of signals from the extracellular surrounding microenvironment. These signals are important for fulfillment of specific genetic program. It is essential for cells to know that cells in all tissues are in contact with their ECM. Without this contact, cells grown in suspension fail to differentiation. Therefore, understanding of

cell differentiation and cell functions means the understanding of cell-to-cell and cell to extracellular matrix (ECM) communication mechanisms. There are at least two essential means by which the ECM can affect cellular behavior. One of these is the cell to ECM interaction that may directly regulate cell functions through receptor-mediated signaling. The other is that by which the ECM can alter the mobilization of growth or differentiation factors, thus modulation of cell proliferation and controlling cell phenotype [Taipale and Keski, 1997].

During tissue development and homeostasis, pluripotent stem cells interact with various signals to determine their specific lineages. Among the numerous factors affecting cells differentiation, nanofibrous matrix can play an essential role to induce cell differentiation [Kshitiz et al., 2011]. Nanomaterials stimulate the osteogenic differentiation of human mesenchymal stem cells (hMSCs), even in the absence of osteogenic induction media [Dalby et al., 2007], suggesting that nano topography may be satisfactory to guide cellular differentiation. In addition, it has been reported that the osteogenic differentiation of hMSCs is enhanced by culture on nano-structured surfaces with osteogenic induction media [You et al., 2010]. The ability to synthesize properly controlled the nanofibrous matrix holds the potential to direct cell function. The role of nanofibrous structure promoting differentiation toward other lineages has also been studied. The influence of nano topography on cellular response has been studied using a variety of surface topographies and cell types including osteoblasts [Webster et al., 2000; Martin et al., 1995], odontoblasts, fibroblasts [Cousins et al., 2004], macrophages [Rice et al., 2003], neural cells [Fan et al., 2002], and endothelial cells [Buttiglieri et al.,2003]. Previous studies have mentioned

about the cells-material interactions used osteoblast-like cells [El-Ghannam et al., 1997; Matsuura et al., 2000].

III.4. Odontoblast differentiation

Odontoblast is similar to osteoblast in several ways. The study of odontoblast cell response is important for the dentinogenesis. Besides being possible sources of large amounts of specific molecules involved in dentinogenesis [Hanks et al., 1998], an odontoblast-like cell line may have potential usefulness in studies the effects of biological and synthetic biomaterials on cell function. Several different kinds of stem cell sources have been considered for the odontoblast differentiation. The most useful ones are dental pulp stem cells (DPSCs), stem cells from exfoliated deciduous teeth (SHED), and periodontal ligament stem cells (PDLSCs) [Miura et al., 2003]. Odontoblasts and osteoblasts cells show nearly identical genetic profiles. There is prominent difference between the process of odontogenesis and osteogenesis. First, pre-odontoblasts cells require signals from the epithelial cells during development to differentiate into odontoblasts. Second, odontoblasts need to align on the existing dentin or on the surface of the matrix to generate dentin whereas osteoblast does not show any such polarity. It is very important to know if these differences affect by scaffold for odontogenic cells [Arinzeh et al., 2005; Batouli et al., 2003]. Significant research has been conducted to observe the behaviors of cells in the presence of nano topographic cues. However, the molecular mechanisms governing these processes remain elusive. Precise nanofibrous matrix control the cellular behavior will likely allow better understanding of signaling and cellular functions and motivate novel strategies to manipulate cell behavior such as proliferation and differentiation. The number of different molecule

families and even intact biomolecule classes remain under investigation in cell differentiation and tissue regeneration. Many signals involved in embryonic development, such as Wnts, BMPs, sonic hedgehog, and Notch may be important signaling pathway that may play essential roles in cell differentiation and tissue regeneration.

III.5. Wnt signaling pathway

Wnt proteins are a large family of cysteine-rich secreted glycosylated ligands. At the cellular level, cell proliferation and differentiation are regulated by Wnt as well as cell morphology and tissue development. There are two main types of Wnt signaling pathway that are classified as canonical (Wnt/β-catenin) and non-canonical (planar cell polarity (PCP), the Wnt-calcium (Wnt/Ca2+) pathways, Wnt5a/Ror2 signaling) [Katoh, 2005; Nusse, 2005; DasGupta, 2005]. The WNT/β-catenin pathway initiates a signaling cascade that is important in both normal development and throughout life. Wnt/β-catenin signaling modulates many cellular functions such as cell proliferation, differentiation, and migration playing important roles in organ development and tissue homeostasis.

Wnt forms a large family of secreted ligands that activate several receptor-mediated pathways. In the Wnt/β-catenin pathway, the Wnt ligands binds to Frizzled (FZ) receptors and LDL receptor related protein (LRP) family co-receptors causes β-catenin stabilization, nuclear translocation, and transcriptional activation by complexes of the β-catenin and LEF/TCF transcription factors [Logan and Nusse, 2004]. Because Wnt signaling controls a variety of adult and development processes, understanding the role of Wnt signaling and the mechanisms that regulate Wnt signaling is of

critical importance. It is reported that the Wnt signaling pathway plays an important role in tooth development [Thesleff and Sharpe, 1997]. Several Wnt genes are widely expressed in oral and dental epithelium, while some others are upregulated in the developing teeth [Sarkar and Sharpe, 1999; Dassule et al., 2000; Kratochwil et al., 2002]. Lef1 knockout mice arrest tooth morphogenesis at the bud stage [Kratochwil et al., 2002]. The inactivation of β-catenin at epithelium or epithelial expression of Dkk1, an inhibitor of the canonical Wnt signaling, lead to abnormal tooth patterning at the bud stage [Liu et al., 2008]. Mesenchyme-specific inactivation of β-catenin also observed a critical role of canonical Wnt signaling in the activation of odontogenic potential in early tooth development [Chen et al., 2009]. It is reported that the Wnt/β-catenin signaling plays multiple roles in various stages of tooth morphogenesis [Liu and Millar, 2010]. However, it is still largely unknown about the detailed mechanism of Wnt/β-catenin signaling in odontoblast differentiation. Moreover, it has been reported that the Lef-1 overexpression induce the odontoblast differentiation of dental pulp cells, and constitutive β-catenin stabilization in the dental mesenchyme can lead to dentin formation [Yokose and Naka, 2010; Kim et al., 2011]. These reports strongly suggest that the modulation of canonical Wnt signaling may play an important role in odontoblast differentiation. Non-canonical signaling can be initiated by WNT–Frizzled receptor interactions; alternatively, RYK and ROR receptor tyrosine kinases can also act as WNT receptors to activate β-catenin-independent signaling [Angers and Moon, 2009]. ß-catenin-independent signaling can also regulate small GTPases, such as RhoA, Rac and cell division control protein 42 (CDC42), in a Dishevelled-dependent manner [Lai et al., 2009].

III.6. Dentin Sialophosphoprotein

The noncollagenous proteins (NCPs) of the dentin matrix are considered to play a critical role in modulating the mineralization of dentin. A family of bone and dentin noncollagenous proteins that has attracted attention is the small integrin-binding ligand, N-linked glycoprotein (SIBLING) proteins. This group comprises DSPP, dentin matrix protein 1 (DMP1), bone sialoprotein (BSP), and osteopontin (OPN). DSPP is a SIBLING family member that makes dentin matrix distinguishable from the bone. It is transcribed from a single mRNA that synthesizes DSP and DPP of a large precursor molecule [Ritchie and Li, 2001]. Because of the presence of these proteins in dentin matrix, DSPP is cleaved posttranslationally by a proteinase. The expression of DSP and DPP show tooth-specific in the newly differentiated odontoblasts in predentin and dentin matrix. DSPP very rarely expresses in osteoblasts than in odontoblasts [Qin et al., 2002].

DSP, discovered by Butler et al. [Butler et al., 1981], while DPP, discovered by Veis and Perry [Veis and Perry, 1967], may modulate mineralization. In odontoblast these proteins express, and binds to collagen at the mineralization site and may modulate the binding of other NCPs to the growing mineralized crystals in a specific manner [Slinskey et al., 1999]. There are three DSPP-derived variants, DSP, DPP, and DSP-PG, each of these molecules may play an essential role in the mineralization of dentin. Conversion of DSPP to DSP and DPP in dentin may require the activation and the activating molecules. The extent and rate and of biomineralization may be controlled by the activation and structural changes involving DSPP. Mutations in the human DSPP gene lead to DGI-II and DGI-III, in which the dentin is severely affected. Studies with DSPP-null mice have provided

evidence for defects in the mineralization of dentin. Therefore, the DSPP is very important for normal dentinogenesis [Sreenath et al., 2003].

IV. Part-1. Nanofiberous engineered matrix induces odontoblast differentiation and specifically DSPP expression through canonical Wnt signaling pathway

IV.1. Introduction

Biomaterials play vital roles to facilitate cellular behavior and function in tissue engineering and regenerative medicine. In tissue engineering, considerable efforts have been directed to develop organized nanofibrous scaffolds that mimic the morphology of natural ECM microenvironment to enhance cells recruiting, differentiation and tissue neo-genesis [Lutolf and Hubbell,2005; Ma,2008]. Nanofiberous scaffolds have been developed by several methods under the hypothesis that synthetic nanofibrous matrix would mimic a morphological function of collagen fibrils and create a more favorable micro-environment for cells [Ma et al., 2005; Chen et al., 2013], that can physically simulate an extracellular matrix (ECM) and functioning as a network for cell adhesion, proliferation, and differentiation [Li et al., 2002; Bao et al., 2011]. Nanofibers are the most reported materials that have important role in tissue engineering applications, and have been investigated for manipulating stem cells fate in osteogenic differentiation and bone tissue regeneration [Smith et al., 2010; Jose et al., 2010; Mata et al., 2010; Chen and Chang, 2011]. Previously, the synthetic nanofibrous matrices for bone and dentin regeneration were investigated, and reported that nanofibrous scaffolding architecture promotes osteoblast/odontoblast differentiation and biomineralization in vitro and vivo [Woo et al., 2007; Park et al., 2010; Lee et al., 2012]. Especially, in an in-vivo study, the bone and dentin formations was observed inside the nanofibrous scaffolds where no adjacent, pre-existing bone and dentin tissues, suggesting that nanofibrous scaffolds may

have the differentiation-inductive effect to osteoblast and odontoblasts. Importantly, nanofibrous matrix enhanced the differentiation of not only the cells committed to specific lineages but also undifferentiated mesenchymal stem cells. The engineered 3D extracellular matrix (ECM) scaffold induced differentiation of human dental pulp stem cells (DPSCs) without the need for addition of exogenous growth factors [Cavalcanti et al., 2013; Ravindran et al., 2014]. It has been demonstrated that synthetic nanofibrous scaffold promoted the odontogenic differentiation and biomineralization of human dental pulp stem cells both in vitro and vivo and suggested a promising scaffolds for dentin regeneration. [Wang et al., 2011; Cavalcanti et al., 2013]. However, the mechanisms by which nanofibrous engineered matrix enhances the differentiation of mesenchymal stem cells (MSCs) and the induction of bone and dentin formation still largely remain to be found. Stem cells may require the appropriate extracellular signals to trigger that lead to induce different lineage commitment. Differentiation induction factors can initiate an important class of such stimuli.

It is well known that soluble factors including growth factors, small molecules, and cytokines can exert robust and accurate effects in to cell microenvironments. Among them, growth factor induces the differentiation of MSCs into the cells of specific lineages and supports its terminal differentiation. Mimicking the natural processes of wound healing and development is a strategy that is frequently utilized in tissue engineering. During tooth development, cell signaling pathways associated with fibroblast growth factor, BMPs, sonic hedgehog, and Wnts participate in the processes of tooth development in a precisely regulated manner [Thesleff and Sharpe.,1997; Liu et al.,2008]. Bone morphogenetic proteins (BMPs) are

secretory growth factors signaling molecules that belong to the transforming growth factor-b (TGF-b) superfamily. BMPs can produce important signaling functions such as induce cell proliferation, differentiation, or apoptosis. The activity of BMP is required in early tooth development from lamina to the bud stage [Ducy and Karsenty, 2000; Wang et al., 2012; Yang et al., 2012; Clough et al., 2014]. The tooth development at the lamina/early-bud stage arrested when BMP signaling inhibitor such as Noggin has been overexpression in the dental epithelium at the tooth initiation stage [Wang et al., 2012]. In contrast, an atypical canonical BMP signaling pathway exists that has functionally operated in the dental mesenchyme during early odontogenesis [Yang et al., 2014]. The Bmp genes, including Bmp-2, -4, and -7, are expressed in the epithelium or mesenchyme of the developing tooth. Upon treatment of BMP4 or BMP7, the mesenchyme stem cells lead to odontoblast differentiation and robustly increased DSPP expression, a significant component of odontoblast differentiation [Wang et al., 2010; Jiang et al., 2014]. BMP2 mutant mice exhibited severe defects in odontogenesis and dentin formation. The odontoblasts in the Bmp2 knockout mice did not mature appropriately and failed to proper dentin formation [Zhang et al., 2013].

Wnt signaling pathway also plays essential roles in tooth development. Several Wnt genes are mainly expressed in the dental epithelium and mesenchyme [Liu et al., 2008]. During tooth development, nuclear beta-catenin is observed in both the dental epithelium and the underlying mesenchyme, and the canonical Wnt signaling pathway is activated at various stages of tooth morphogenesis [Liu et al., 2008]. The functional significance of Wnt/β-catenin has been studied extensively. During tooth root

formation, β-catenin is strongly expressed in odontoblast-lineage cells and is required to differentiate odontoblasts for root formation. Knockout of β-catenin lead to disruption of Wnt/β-catenin signaling in odontoblasts and arrested tooth root development, and mutant mice exhibited striking tooth phenotypes with erupted molars lacking roots and aberrantly thin incisors [Kim et al., 2013]. The inhibition of canonical Wnt signaling either by deleting Lef-1 or overexpressing Dkk1 arrests tooth morphogenesis at the late bud stage [van Genderen et al., 1994; Sasaki et al., 2005], and overexpression of Lef-1 accelerated odontoblast differentiation of dental pulp cells [Yokose and Naka., 2010]. The oral epithelium expressing constitutively active beta-catenin results in the formation of multiple teeth, following transplantation to the kidney capsule [Jarvinen et al., 2006].

The applications of MSCs in tissue engineering have been extensively studied. The MSCs can be isolated from tissues such as bone marrow, adipose tissue, and dental pulp tissue [Conget and Minguell, 1999; Zuk et al., 2002; Bluteau et al., 2008]. They are the multi-potent cells that can differentiate to the types of cells according to their micro-environments, and the differentiation capacity can be affected by the originated tissue. It has been reported that dental pulp-derived mesenchymal stem cells (DPSCs) were more prone to be differentiated into odontoblasts than osteoblasts, compared with bone marrow-derived mesenchymal stem cells (BMSCs) [Gronthos et al., 2000]. DPSCs is considered as a mesenchymal stem cell (MSC) present in adult teeth showing similar characteristics to the bone marrow derived MSCs characterized by odontoblast differentiation and similar genes expression profile [Davies et al.,2014]. Conversely, differentially expressed genes between DPSCs and BMSCs have also been

reported [Shi et al., 2001]. The hypothesis underlying this study is that the response of mesenchymal stem cells derived from various tissues might be different to their microenvironment such as nanofibrous matrix that leads to induce cell differentiation through specific molecular mechanisms.

In this study, we aimed to address the molecular events that underlies the responsiveness of different mesenchymal stem cells on nanofibrous engineered matrix, under the hypothesis that nanofibrous engineered matrix induces the expression of Wnts and BMPs that can lead further to induce the cellular differentiation. First, the expression of the molecules involved in the Wnt and BMP signaling in human dental pulp-derived stem cells, bone marrow-derived stem cells, and human adipose-derived stem cells (hDPSCs, hBMSCs, hADSCs) on electrospun polystyrene fiber (PSF) matrix were examined. Then, based on the results, we evaluated the effects of Wnt3a, which is preferential highly expressed in hDPSCs cultured on nanofibrous matrix. Based on the odontogenic differentiation of hDPSCs, we confirmed the findings with a murine odontoblast-like cell line MDPC-23 and found that nanofibrous engineered matrix induces the odontoblast differentiation through canonical Wnt signaling pathway.

IV.2. Materials and Methods

IV.2.1. Materials and Reagents

Polystyrene (Mw ~280,000) was purchased from Sigma (St. Louis, MO). N-N Dimethylformamide was from Georgiachem (Suwanee, GA). Dulbeco's Modified Eagle's Medium and fetal bovine serum (FBS) were purchased from Hyclone (Logan, UT). Penicillin-streptomycin solution was obtained from GibcoBRL (Carlsbad, CA). L-ascorbic acid and glycerol 2-phosphate were from Sigma (St. Louis, MO). Quant-iT Picogreen reagent kit was purchased from Invitrogen (Eugene, OR). Alizarin Red S, and Cetylpyridinium chloride were purchased from Sigma (St. Louis, MO). RNA isoplus reagents, PrimeScript™ RT reagent kit, and SYBR® Premix Ex TaqTM were purchased from Takara (Kyoto, Japan). Anti-β-catenin antibody, anti-p-β-catenin antibody and normal rabbit IgG were purchased from Cell Signaling Technology (Danvers, MA). Anti-Wnt3a antibody, anti-DSP antibody, and β-actin HRP-conjugated mouse monoclonal IgG1 antibody were from Santa Cruz Biotechnology (Santa Cruz Biotechnology, CA). Alexa Fluorr® 488 conjugated-goat anti-rabbit and Alexafluor 546-conjugated phalloidin were purchased from Molecular probes (Eugene, OR). ECL chemiluminescence reagent was purchased from iNtron Biotechnology (Sungnam, Korea). Genefectine reagent was from Genetrone Biotech (Qwangmyeong, Korea). Lithium chloride was from Sigma (Sigma, St. Louis, MO). Dual-Glo Luciferase assay kit was from Promega (Promega, Madison). Mouse Wnt3a ELISA kit and ELISA substrate were purchased from R&D Systems (Minneapolis, MN). Rhodamine phalloidin was from Molecular Probe (Eugene, OR). siRNA against Wnt3a and β-catenin (GENOME SMART pool) were purchased from Dharmacon (Dharmacon,

Lafayette, CO). Protease inhibitor cocktail tablets (Complete) were purchased from Roche (Basel, Switzerland). Protein G Agarose/Salmon Sperm DNA was purchased from Millipore (Billerica, MA), DNA purification kit was purchased from Zymo Research (Irvine, CA). Biotinylated anti-rabbit IgG, and vectastain ABC reagent were purchased from Vector laboratories (Burlingame, CA). Mounting medium was purchased from DAKO (Carpinteria, CA).

IV.2.2. Electrospinning

Electrospinning requires an optimization condition to obtain uniform polystyrene nanofibers to avoid the bead morphology [Tamer and Flemming, 2008]. Homogeneous polymer solution was prepared by dissolving polystyrene in N, N-Dimethylformamide (DMF). The solution was dissolved for overnight at room temperature to obtain enough viscosity required for electrospinning. While electrospinning processes, the solution were placed in 10ml syringe fitted with a metallic needle of 0.2mm of inner diameter and applied high voltage of 30kV. The flow rate of the polymer solution was 0.5ml/hour and the distance between the tip and the collector was 20cm. The fiber was collected on a rotating metal drum covered with aluminum foil. The electrospun nanofibers were dried to remove the residual DMF. The electrospinning of polystyrene was repeated three times to make sure of the reproducible nanofibers.

IV.2.3. Scanning electron microscopy

For scanning electron microscopy (SEM) analysis, the electrospun polystyrene nanofibers were attached to the bacterial culture dishes (BCD) with DMF and dried for overnight to evaporate the solvent. The polystyrene

nanofiber were sputter coated with gold using Ion sputter “Au-Pb” target for 120 seconds and examined using scanning electron microscopy (Hitachi, S-4700, Japan),at an accelerating voltage of 15 kV.

IV.2.4. Cell Culture

Bone marrow-derived mesenchymal stem cells (hBMSCs), human dental pulp-derived stem cells (hDPSCs), human adipose-derived stem cells (hADSCs), and mouse pre-odontoblast cells (MDPC-23) were cultured with a concentration of $5X10^5$ cells in DMEM supplemented with 10% (v/v) FBS using 60mm tissue culture dishes (TCD). The cells were induced to differentiate in 60 mm TCD or 12 w% PSF attached to BCD applied the differentiation media (DMEM with 10% (v/v) FBS, 100 units/ml penicillin/streptomycin, 50 μg/ml ascorbic acid, and 10 mM β-glycerol phosphate) and incubated at 37°C under 5% CO_2. For the experiments to examine the effect of phosphate compound contained in differentiation media, the cells were cultured in DMEM media with or without of ascorbic acid or β-glycerol phosphate.

IV.2.5. Alizarin Red Staining and Quantification

The calcium deposition of dental pulp cells on different substrates was analyzed by Alizarin Red S staining. The MDPC-23 cells were seeded on six wells cell culture plates without and with attached PSF. After overnight changed the media and allowed to stay for differentiation. After 7 days and 12 days of differentiation washed the cells three times with cold PBS, fixed with 70% ice-cold ethanol for 1 hour, washed with deionized water and stained with 40mM Alizarin red S (pH 4.2) for 20 min at room temperature. The samples were rinsed with deionized water and lastly washed with PBS.

Images of the stains were captured showing the calcium deposition. The stained plates were washed several times with deionized water, desorbed in 10% cetylpyridinium chloride (Sigma) for 1 hour, and read the absorbance at 490 nm in a spectrophotometer to measure the quantification.

IV.2.6. Reverse Transcription-PCR and Quantitative Real-Time PCR

hDPSCs, hBMSCs, hADSCs, and MDPC-23 cells were harvested and total RNA were isolated using RNA isoplus reagents. RNA concentration was determined by Nanodrop. The first-strand cDNA was synthesized using PrimeScript™ RT reagent kit according to the manufacturer's instructions. For quantitative real-time PCR, amplification reactions were analyzed in real time on 7500 Real-time PCR system using SYBR® Premix Ex TaqTM according to the protocol described in the kit. The relative levels of each target gene mRNAs were normalized to those of glyceraldehyde-3-phosphate dehydrogenase (GAPDH). The primers sequences were used in this study are listed in Table 1 and 2.

IV.2.7. Western Blot Analysis

The western blot analysis was performed as described previously [Oh et al., 2011]. The whole-cell lysates were prepared from MDPC-23 cells cultures on PSF and TCD. At fourth day of cells differentiation, cells were washed with 1X cold PBS and lysed with Lysis buffer (1XPBS, 0.5% sodium deoxycholate, 0.1% SDS, 10 mg/ml phenymethylsulfonyl fluoride, 30 up/ml aprotinin, 100 mM sodium orthovanadate, and complete protease inhibitor cocktail tablet). The samples were subjected to 10-12% SDS-PAGE and transferred on to polyvinylidene difluoride (PVDF) membrane. The membranes were blocked with 5% non-fat skim milk in TBST buffer (10

mMTris– HCl, pH 7.5, 100 mM NaCl, 0.1% Tween-20) for 60 minutes at room temperature. After washing, the membranes were incubated with primary antibody with appropriate dilution (1:1000) for overnight at 4^{o}C. The samples were incubated with an HRP-conjugated secondary antibody at room temperature for 60 min. Immunoreactivity was determined using the ECL chemiluminescence reagent. β-actin HRP-conjugated mouse monoclonal IgG antibody was used as a loading control.

IV.2.8. β-catenin/Tcf luciferase assay

Cells were seeded on 24 wells culture plate on PSF and without PSF control wells (without PSF) at a density of 1×10^{5} cells per well. After overnight changed the media and added differentiation media. Two days later transfected the cells with Topflash or Fopflash constructs by using Genefectine reagent (Genetrone Biotech). Six hours after transfection, changed the media and added fresh differentiation media without antibiotics to the transfected cells and were stimulated the treatment group with LiCl (20mM) for last 24 hours. Cells were lysed after 36 hours of transfection with Dual-Glo Luciferase reagent Lysis Buffer, transferred to a 96-well plate, and measured the firefly Luciferase activity. The Renilla luciferase was recorded after addition of Dual-Glo Stop and Glo Reagent as instructed by the manufacturer. The ratio of TOP/FOP activity was calculated by the ratio of firefly/Renilla luciferase.

IV.2.9. Immunofluorescence and confocal microscopy

To determine the DSP, Wnt3a, and the nuclear translocation of β-catenin in dental pulp cells, MDPC 23 cells were seeded on PSF and TCD at 5×10^{3} cells/cm^{2} in growth media. The cells were induced to differentiate to

osteogenic condition using osteogenic differentiation media. To know about nuclear translocation of β-catenin the cells were treated with LiCl 20mM for last 24 hours of culture. While to determine the effect of wnt3a, cells were treated with anti-wnt3a antibody to culture. Cells were fixed with 4% formaldehyde for 15 min and incubated with PBS containing 0.1% Triton X-100 (PBS-T) for 10 minutes to permeabilize the cells and then incubated in PBS-T for 1 hour to block non-specific binding. The cells were incubated with appropriate primary antibody for 2 hours followed by Alexa Fluorr® 488 conjugated-goat anti-rabbit secondary antibody for 1 hour. The samples were incubated with rhodamine phalloidin for 20 minutes to visualize the actin; coverslips were mounted in a mounting medium with DAPI to identify nuclei. After each incubation, the samples were washed with PBS three times for 5 min each. The samples were examined using a laser scanning confocal microscope (LSCM). The experiments were in triplicates for at least three times.

IV.2.10. Knockdown Assays with siRNA

To knockdown the expression of Wnt3a or β-catenin, scrambled pooled siRNA against wnt3a or β-catenin were used. Cells were seeded in 60mm culture plates on PSF and TCD, after overnight the differentiation media was added. Two days later the cells were transfected with each specific siRNA in accordance with the manufacturer’s instruction. The cells were harvested after 48 hours of transfection and determined the expression of DNA and proteins.

IV.2.11. DNA Constructs and Site-directed Mutagenesis of LEF1 binding Sites

The DSPP promoter regions, D-791(bp-791 to +54), D-624 (bp -624 to + 54), D-435 (bp -435 to + 54), D-260 (bp -260 to + 54), and D-225 (bp -225 to + 54) was cloned in to the pGL3 vector by standard protocol. Site-directed mutagenesis was carried out to mutate the LEF1 binding sites. To produce the mutants plasmids, M-624 and M-435, was generated by site-specific mutangenesis of D-624 and D-435 constructs as a template. Mutant oligonucleotides designated for specific sites (mutated bases in lowercase) are listed as L1 (forward 5'-TCAGAAAGGTTTCCTGAAGTTAtgGgTTATAAATTCTTTTAAAGATCCC-3'); and reverse 5'-GGGATCTTTAAAAGAATTTATAAcCcaTAACTTCAGGAAACCTTTCTGA -3'); and L2 (forward 5'-GGTGACAGAGTCTAAGTGGCTtgTgTCAGATATATCACACTGATTATC-3'); and reverse 5'-GATAATCAGTGTGATATATCTGAcAcaAGCCACTTAGACTCTGTCACC-3').

IV.2.12. Transient Transfection Assay

For transient transfection studies, DSPP promoter constructs of D-791, D-624, D-435, D-260, and D-225 or an empty plasmid pGL-3 basic as a control were co-transfected with pRL-TK vector (promega) into MDPC-23 cells using the Genefectine reagent. Six hours after post-transfection, the cells were deprived in differentiation media without antibiotics for 36 hours prior to harvesting. Luciferase activity was measured by Dual-Glo Luciferase Reagents (Promega) as described by the manufacturer. Briefly, 300µl of Dual-Glo luciferase reagents was added to cells culture on TCD and PSF in 24 well plates containing 300 µl of medium, mixed well to lyse completely

and waited for 10 minutes. Mixture of 150 µl was dispensed into each well of 96 well assay plates and measured the firefly luciferase activity with a GloMax-Multi Detection System machine (Promega). After measuring the firefly luciferase, a volume of 75 µl of Dual-Glo Stop and Glo Reagent was added to each well of the same plate, mixed, and the Renilla luciferase activity was measured. The promoter activity was obtained by the ratio of firefly/Renilla luciferase for each construct. The same method was used to wild-type (D-624, D-435) or mutant reporter plasmids (M-624, M-435). Transfection was carried out in quadruplicate, and the data are expressed as the relative luciferase activity±S.D.

IV.2.13. Chromatin Immunoprecipitation (ChIP)

A ChIP assay was performed in this experiment according to the instructions provided by kit (Protein G Agarose/Salmon Sperm DNA). Briefly MDPC-23 cells seeded in 60mm dishes on PSF and TCD. At four days of differentiation, cells were washed with PBS and incubated for 10 min at RT with 1% formaldehyde, and quenched the reaction with 1/15 volume of 2M glycine (final concentration is 0.125M). After collected the cells from the dishes and washing with cold PBS, swelling the cells with swelling buffer added protease inhibitor for 20 min in ice. To get the nucleus, glass tissue grinder were used, collected the pellet. 1% SDS nuclei lysis buffer with protease inhibitor were added to the pellet and sonicated in ice to break the DNA to get fragments and saved 1% of each sample as input fraction. The samples were diluted 10 folds with ChIP dilution buffer added protease inhibitor. Immunoprecipitation was performed by adding protein G beads and 20ul of anti-β-catenin rabbit polyclonal antibody. For the negative control used 0.2ul of normal rabbit IgG. Washed the immunoprecipitated material and cross-

linked were reversed. Then the recovered material with proteinase K was treated, and the DNA fragement was purified by kit. The purified DNA was amplified by PCR using the primers for all three regions are as follows; Region A; sense 5′-CCCAAAACCTTTATGTCAGTGT-3′ and antisense 5′-ACGACTGGCTATTTAAGACCCC-3′; region B; sense 5′-CCTAGAGTTTTCTTAGATTGCCG-3′ and antisense 5′-GAGGCTGTAATAACGCCCCA-3′; region C; sense 5′-GAGTGGGGCGTTATTACAGC-3′ and antisense 5′-CGTGACAATTTTGTACCTGC-3′.

IV.2.14. Immunohistochemistry

Immunohistochemistry for DSP and Wnt3a was performed on 4μm thick paraffin sections. After subcutaneous implantation, the samples were harvested and fixed in 4% paraformaldehyde in PBS at 4℃ for overnight. Then the paraffin block were made by the general process. After deparaffinization, samples were treated with 0.3% H_2O_2 for 30min at room temperature and washed with PBS. The specimen were incubated with 1% BSA in PBS for 1h and then incubated with a dilution of 1:50 of primary antibodies specific for DSP and Wnt3a in 1% BSA. For negative control IgG1 were used. The sample were incubated for 90 min and washed with PBS followed by 1:100 dilution of secondary antibody, Biotinylated anti-rabbit IgG for 1 h. The samples were washed with PBS to remove the excess secondary antibody and treated with vectastain ABC reagent for 30 min. The sections were mounted using ultramount aqueous permanent mounting medium. Images of immunohistochemical staining of DSP and Wnt3a were obtained.

IV.2.15. Statistical analysis

Data from the repeated experiments are presented as the mean and standard deviation. Statistical analyses were performed using the analysis of variance (ANOVA) method. Differences were considered to be significant if the p value was <0.05.

Table 1. Sequences of primers used in RT-PCR

Molecules	Primer sequences
mDSPP	5′- AACACATCCAGGAACTGCAGCACA -3′
	5′- TGACTCGGAGCCATTCCCATCTCT -3′
mDMP1	5′-AACTGGACAGTGATGAGGAGGAC-3′
	5′- TTTAGATTCTTCCGACCTAG -3′
mBSP	5′- GAGACGGCGATAGTTCC -3′
	5′- AGTGCCGCTAACTCAA-3′
mWnt3a	5′- CATGCACCTCAAGTGCAAATG -3′
	5′- TGAGGAAATCCCCGATGGT -3′
mWnt5a	5′- CATGTCTTCCAAGTTCTTCC -3′
	5′- CTGTCCTTGAGAAAGTCCTG -3′
mWnt10a	5′- TCTCAAGAATGGTTGTCCTC -3′
	5′- ATCAGATCTGGACTGTCTGG -3′
mWnt5b	5′- GGAGAGGAAGAGCTTAGGAG -3′
	5′- TGTGGAATAAGTCCAGTTCC -3′
mH3f3	5′- CTGCGCTTCCAGAGTGCAGCT-3′
	5′- AGCACGTTCTCCGCGTATGCG-3′
mGapdh	5′- AGGTCGGTGTGAACGGATTTG-3′
	5′- TGTAGACCATGTAGTTGAGGTCA-3′

Table 2. Sequences of primers used in RT-PCR

Molecules	Primer sequences
hDSPP	5′- ATGAGGATGTCGCTGTTGTCC -3′
	5′- TCCAGTGCCTGGTGTTACCT -3′
hWnt3a	5′- AGTATTCCTCCCTGGGCTCG-3′
	5′- TGCCAATCTTGATGCCCTCG-3′
hWnt5a	5′- GCAGTACATCGGAGAAGGCG -3′
	5′- GCTGCCTATCTGCATCACCC -3′
hWnt10a	5′- ACC TCC GCC TCC CCC -3′
	5′- GTGTTGGCATTCGTGGATGG -3′
hBMP2	5′- GGCACCCGGGAGAAGGAGGA -3′
	5′- CCTGGGGAAGCAGCAACGCT -3′
hBMP4	5′- ATGTGGGCTGGAATGACTGG -3′
	5′- GCACAATGGCATGGTTGGTT -3′
hBMP7	5′- CCCGTGGCTGTCTCTTCATT -3′
	5′- TGCACCCATCAGACCTCCTA -3′
hGapdh	5′- GCCGCATCTTCTTTTGCGTCGC-3′
	5′- CCGTTCTCAGCCTTGACGGTGC-3′

IV.3. Results

IV.3.1.The electrospun polystyrene exhibits nanofibrous morphology

The nanofibrous engineered matrix was synthesized from polystyrene polymer. We examined the physical characteristics of electrospun polystyrene nanofibrous matrix. SEM micrograph of electrospun nanofiber showed that uniformly nanofibers have obtained from 12% of polyotyrene is DMF solvent under optimized spinning conditions (Fig. 1A). Then we examined the diameter of nanofibrous engineered matrix and found that the average diameter of the nanofiber was 284±85 nm (Fig. 1B).

A

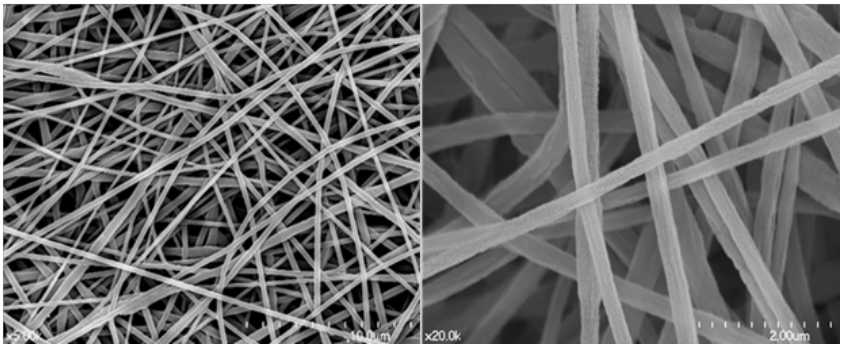

B

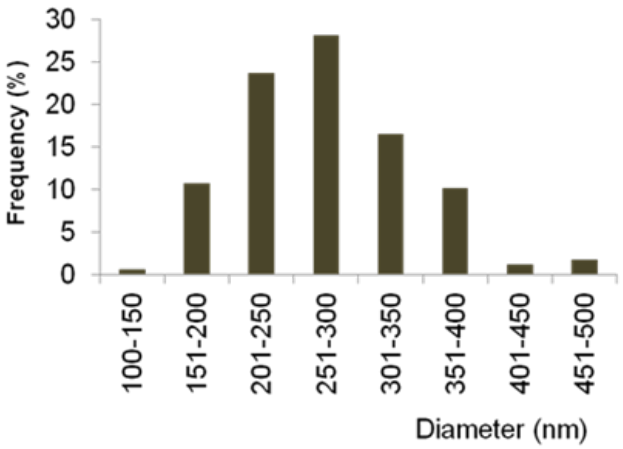

Figure 1. Scanning electron micrographs of nanofibrous engineered matrix. Polystyrene nanofiber mesh produced by electrospinning. Scanning Electron micrograph of electrospun nanofibrous matrix at low and high magnification (A). The average fibers diameter of the nanofibrous matrix (B).

IV.3.2. Electrospun nanofibrous engineered matrix induces growth factors expression in mesenchymal stem cells

hDPSCs, hBMSCs, and hADSCs were cultured on the PSF and TCD in four different kinds of media such as basal media (BM) without differentiation induction components, growth media with ascorbic acid (A.A), growth media with β-glycerophosphate (βGP), and differentiation media (DM) contain both ascorbic acid and β-glycerophosphate, and examined the response of these stem cells on the nanofibrous matrix, which mimic the natural ECM microenvironment. Real-time PCR was performed to analyze different growth factors genes expressions. At same culture conditions, hDPSCs, hBMSCs, and hADSCs upregulated the Wnt and BMP signaling molecules expression differentially on PSF compared to TCD in differentiation condition. Among Wnt signaling molecules, Wnt3a expression was markedly increased in hDPSCs on PSF while in hBMSCs the Wnt3a expression was increased on PSF but comparatively was decreased than hDPSCs while in hADSCs it decreased in both on TCD and PSF compared to other cell types (Fig. 2A). Wnt5a expression was highly increased in hDPSCs cells on PSF in differentiation media compared to TCD as well as compared to basal media. While hADSCs induced Wnt5a expression higher compared to hBMSCs (Fig. 2B). PSF induced Wnt10a expression in hADSCs and hDPSCs compared to TCD while in hBMSCs Wnt10a expression was less than other two kinds of cells (Fig. 2C). Further, we examined the BMP signaling molecules. Among BMP signaling molecules, BMP2 expression was higher in hDPSCs cells and was further increased in cells on PSF compared to hBMSCs and hADSCs (Fig. 2D). The expression of BMP4 was highly increased in hDPSC on PSF at

differentiation state while in hBMSCs it also increased compared to hADSCs (Fig. 2E). The expression of BMP7 was upregulated in hADSCs on PSF compared to hDPSCs and hADSCs (Fig. 2F). Our results demonstrated that the nanofibrous matrix induced Wnt and BMP signaling molecules differentially in dental pulp-derived, bone marrow-derived mesenchymal stem cells, and adipose-derived stem cells at osteogenic differentiation state. PSF induced Wnt3a expression highly in hDPSCs compared to other molecules as well as compared to other cells types.

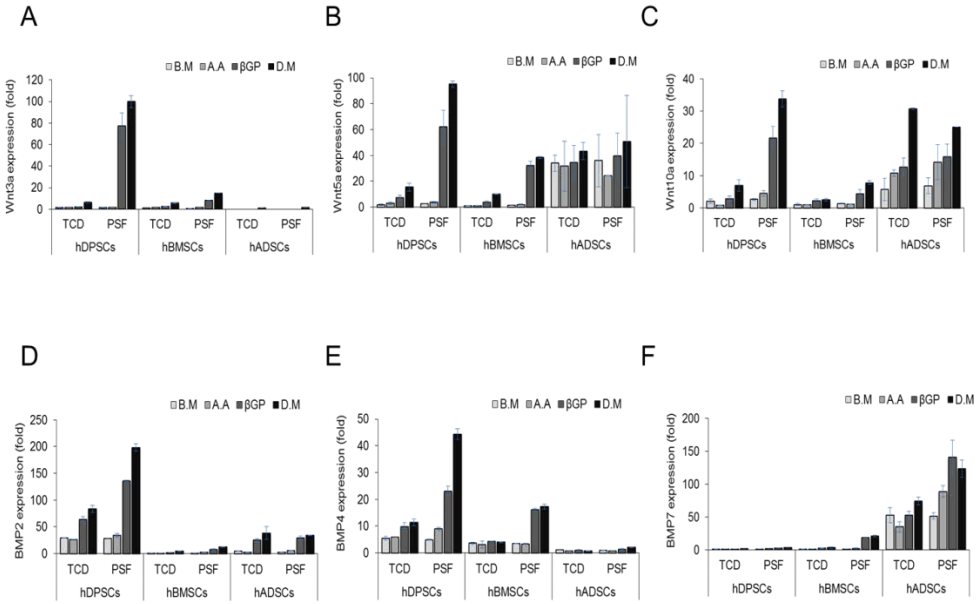

Figure 2. The responsiveness of mesenchymal stem cells during differentiation on nanofibrous matrix. Three different kinds of stem cells (hADSCs, hBMSCs, and hADSCs) were cultured on TCD and PSF in four different kinds of media such as basal media (BM), ascorbic acid (A.A), β-glycerophosphate (βGP), and differentiation media (DM) which contain both ascorbic acid and β-glycerophosphate, and determined different growth factors genes expression by quantitative real-time PCR. Real-time PCR analysis for Wnt3a (A), Wnt5a (B), Wnt10a (C), BMP2 (D), BMP4 (E), and BMP7 (F) were performed. Data are presented in fold change ± SD of the representative of three independent experiments.

IV.3.3. Nanofibrous engineered matrix induces osteogenic differentiation markers expression in mesenchymal stem cells

To determine the responsiveness of different menenchymal stem cells on nanofibrous matrix during osteogenic differentiation state, we cultured the hDPSCs, hBMSCs, and hADSCs in four different kinds of media. The osteogenic differentiation markers were examined and found that nanofibrous matrix induces DSPP expression highly in hDPSCs at osteogenic state (Fig. 3A). While in the hBMSCs, PSF induces OCN expression higher compared to other cells (Fig. 3B). The BSP expression is highly increased in hADSCs in osteogenic media in cells on PSF (Fig. 3C).

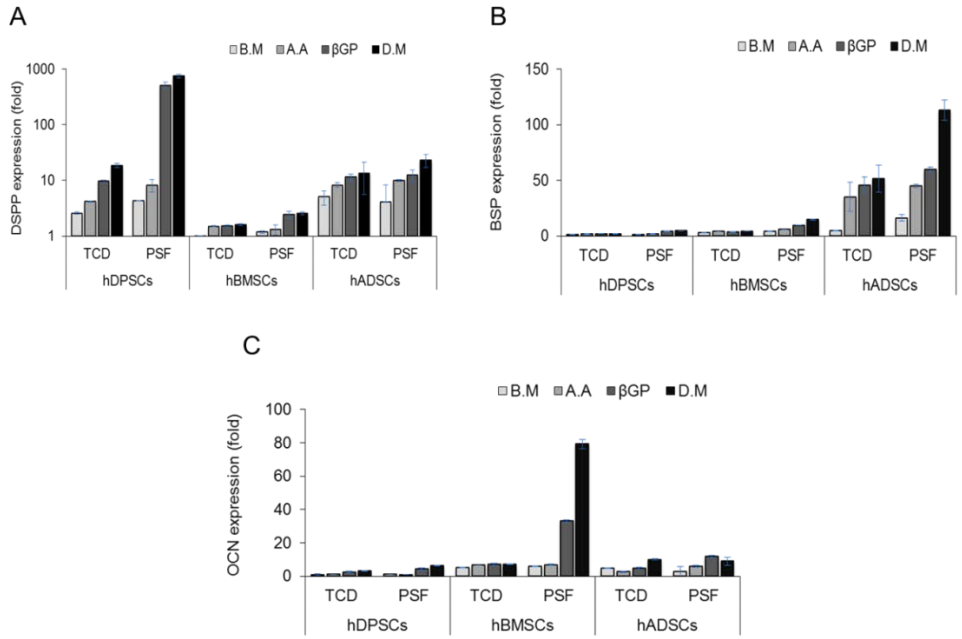

Figure 3. Osteogenic differentiation markers expressions in mesenchymal stem cells. The hDPSCs, hBMSCs, and hADSCs were cultured on the TCD and PSF with differentiation media conditions. Osteogenic differentiation markers genes expressions were examined by quantitative real-time PCR. Real-time PCR analysis for DSPP (A), BSP (B), and OCN (C) were performed. Data are presented in fold change ± SD of the representative of the repeated experiment.

IV.3.4. Nanofibrous engineered matrix induces differentiation markers and specifically DSPP gene expression in dental pulp stem cells

hDPSCs, hBMSCs, and hADSCs were cultured on the PSF and TCD. The cells were treated with rBMP2 or rhWnt3a and examined the osteogenic differentiation markers genes expression. Here we found that PSF-induced DSPP expression was upregulated when the hDPSCs were treated with rhWnt3a compared to hBMSCs and hADSCs (Fig. 4A). While the BSP gene expression was highly increased with treatment of rBMP2 in hBMSCs and hADSCs compare to hADSCs when cultured on PSF (Fig. 4B). The OCN gene expression was highly increased in hBMSCs with the treatment of rBMP2 in cells on PSF compared to control as well as compared to other groups (Fig. 4C). These results demonstrated that the treatment of rhWnt3a induces DSPP expression highly in hDPSCs on PSF.

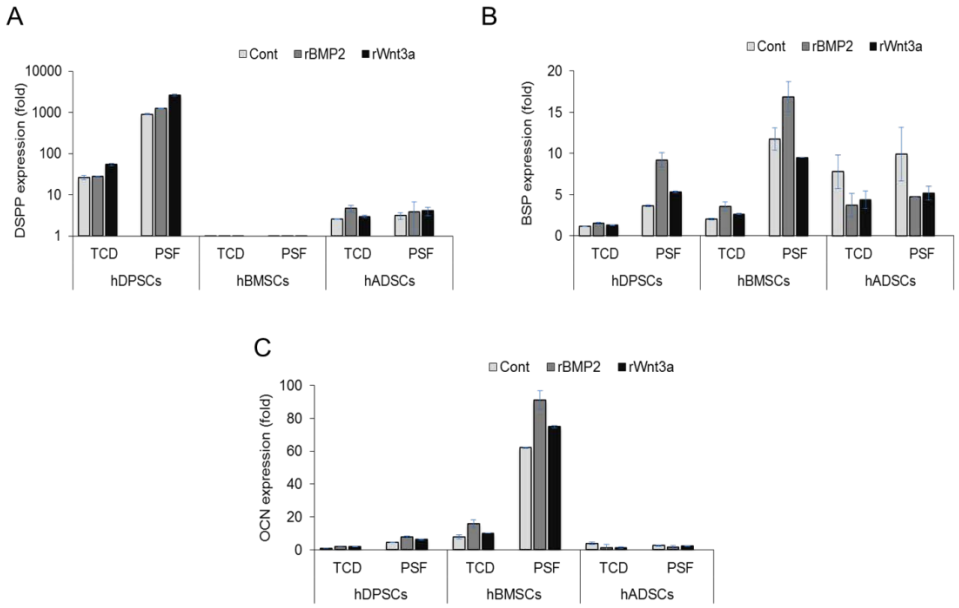

Figure 4. Effect of Wnt3a on osteogenic differentiation markers expressions in mesenchymal stem cells. The stem cells were cultured on TCD and PSF with or without of rBMP2 or rhWnt3a in osteogenic differentiation media, and examined osteogenic differentiation markers genes expression by quantitative real-time PCR. Real-time PCR analysis for DSPP (A), BSP (B), and OCN (C) were performed. Data are presented in fold change ± SD.

IV.3.5. PSF induced-Wnt3a affects DSPP gene expression in detal pulp-derived mesenchymal stem cells

To identify whether canonical Wnt signaling is involved during odontoblast differentiation, human DPSCs was cultured on PSF and TCD and determined the Wnt3a gene expression. Analysis revealed a highly increased of Wnt3a gene expression on PSF (Fig. 5A). DSPP is consider as one of the most important and dominant marker of odontoblast differentiation and dentin mineralization [Guo et al., 2014]. DSPP gene expression was increased more than 100 folds in cells on PSF compared to TCD (Fig. 5B). Further, we examined the effect of canonical Wnt signaling on DSPP expression. Inhibition of canonical Wnt signaling either by treatment with Dkk1 protein or anti-Wnt3a antibody abrogated PSF-induced DSPP expression (Fig. 5C, D).

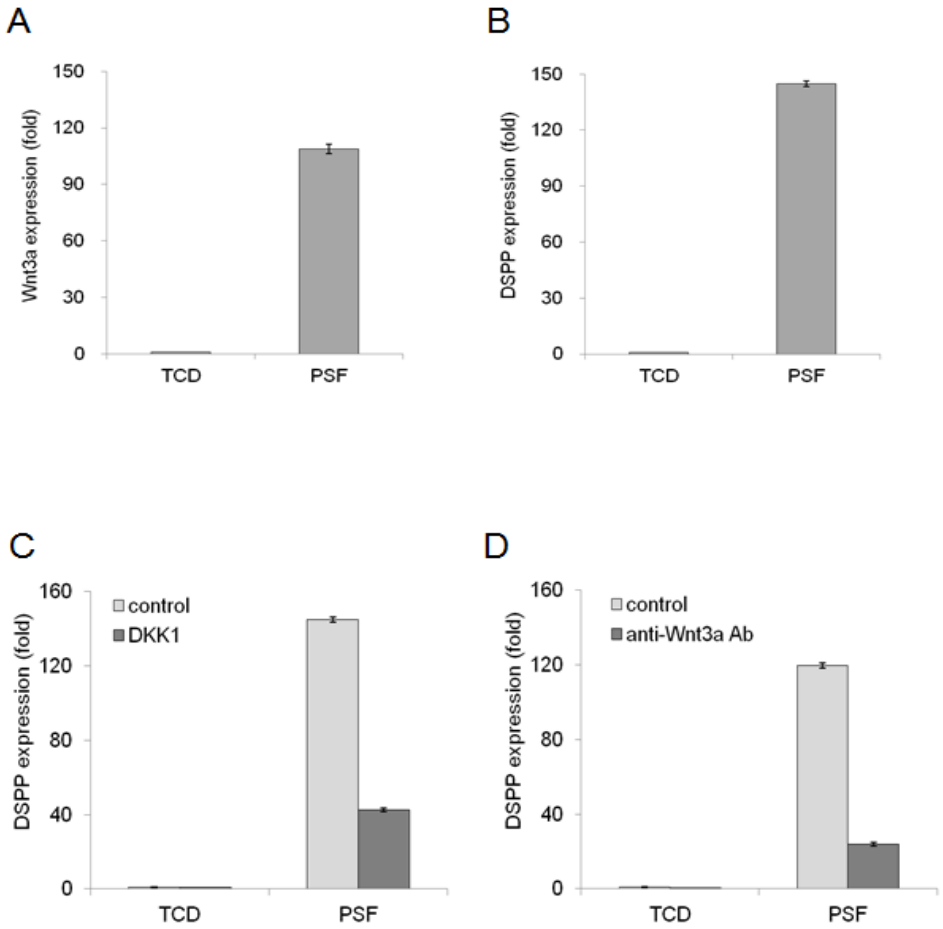

Figure 5. Effect of canonical Wnt signaling on DSPP expression. The hDPSCs cells were cultured on TCD and PSF with or without treatment of DKK1 or ani-Wnt3a antibody. Real-time PCR for Wnt3a (A), DSPP (B), and DSPP after DKK1 treatment (C), DSPP after ant-Wnt3a antibody treatment (D) was performed. Data are the mean ± SD of the repeated experiments.

IV.3.6. Polystyrene nanofiber matrix accelerates odontoblast differentiation and specifically induces DSPP gene expression

The Alizarin Red Staining was used to characterize the nodule formation of MDPC-23 cultured on nanofibers for 7 days & 12 days (Fig. 6A). The images of ARS of cells culture on PSF observed the red bright stains shows the presence of calcium. Moreover, the cells cultured for 12 days showed more positive and brighter red staining on PSF than those on TCD. Moreover, the cells cultured for 7 and 12 days showed more positive and brighter red staining on PSF than those on TCD. The result revealed that the PSF induced the differentiation of MDPC-23 cells and enhanced in 12 days culture compared to control. The calcium deposition was higher on PSF both in 7 days and 12 days culture than those on TCD measured quantitatively, analysis of the ARS stain collection using 10% cetylpyridinium chloride and measured by their absorbance. The measured absorbance of the sample collected from PSF was significantly ($p < 0.05$) higher than control. Moreover, the eluents collected from PSF 12 days sample showed absorbance significantly ($p < 0.05$) higher than those on TCD. Further, the expressions of odontoblast differentiation markers genes (DSPP, DMP1, and BSP) at 4 day of differentiation were examined using quantitative real-time PCR. DSPP mRNA expression was observed abundantly and significantly ($p < 0.05$) increased in cells on PSF compared to control group (Fig. 6B). In addition, DMP1 was increased 8 fold and BSP increased 50 fold, both genes expressed significantly ($p < 0.05$) in cells on PSF compared to TCD.

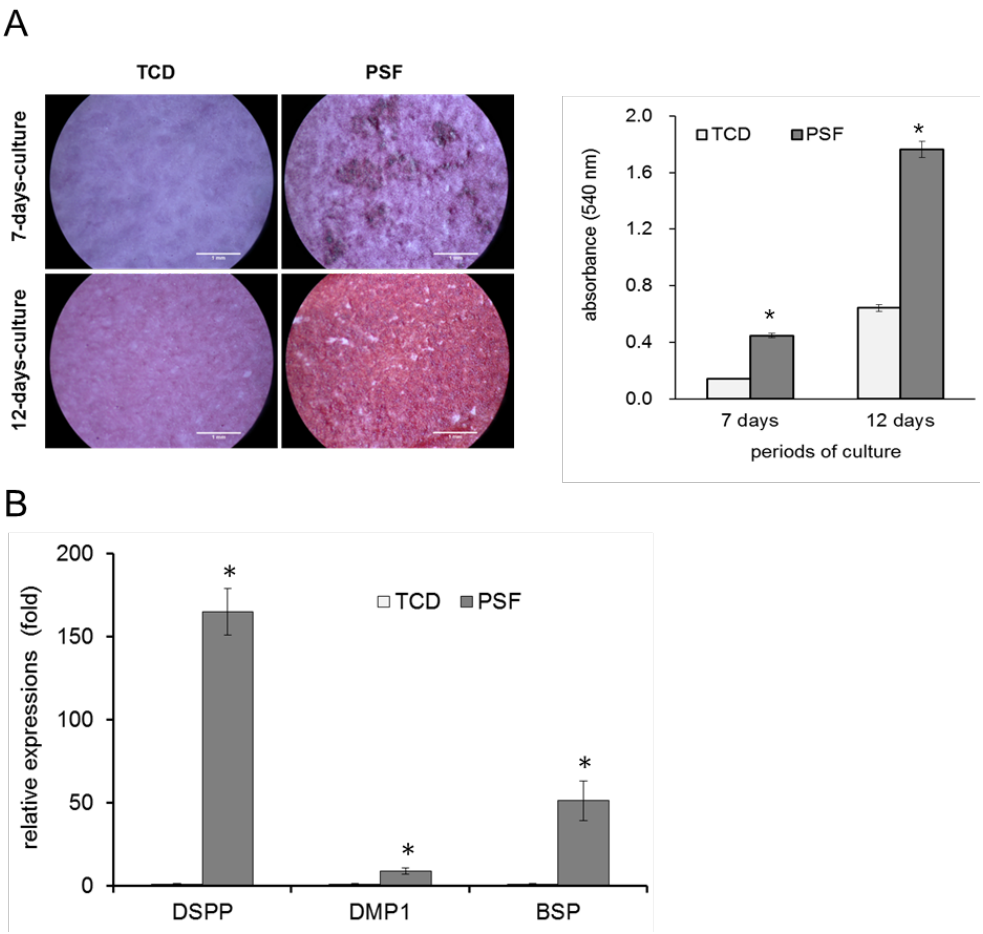

Figure 6. Polystyrene nanofiber matrix accelerates odontoblast differentiation. MDPC-23 cells were cultured on TCD and PSF for 7 days and 12 days. Odontoblast differentiation was shown by alizarin red stain and quantification of mineral deposition in MDPC-23 cells on PSF and TCD (A). Expression of odontoblast differentiation markers (DSPP, DMP1, and BSP) was determined by quantitative real time PCR (B). Data are the mean ± SD of triplicate independent experiments. *Significantly different from the control ($p < 0.05$).

IV.3.7. Canonical Wnt signaling pathway is involved in PSF-induced DSPP expression

Our results suggested that PSF induced canonical wnt signaling followed by stabilization of β-catenin in MDPC-23 cells under odontoblast differentiation. The western blot analysis revealed that the amount of β-catenin was higher in cells on PSF and the p-β-catenin which undergoes to degradation was increased in control group (Fig. 7A). The TopFlash luciferase reporter gene assay was performed to determine the β-catenin mediated transcriptional activation of TCF/LEF. The cells on PS nanofibers transfected with TopFlash induced the luciferase activity, and the addition of LiCl enhanced the β-catenin induced TopFlash reporter activity in both groups. By contrast, there was no transcriptional activation observed in cells on PS nanofiber and TCD transfected with TopFlash even with treatment of LiCl (Fig. 7B). To verify whether canonical Wnt signaling were functional in the MDPC-23 cells cultured on PSF. The immunoflourescence analysis revealed that the amount of β-catenin translocate to the nucleus was higher in cells on PSF determined by nuclear stain DAPI. The β-catenin appeared at the peripheral sites of cells in control group. Activation of canonical Wnt signaling pathway can be achieved by lithium chloride (LiCl), which inhibits glycogen synthase kinase -3β activity and is able to increase β-catenin stabilization and induces nuclear translocation to interacts with TCF/LEF family members making in complexes, where it bind with specific response elements on the promoter of Wnt downstream target genes [Zhu et al., 2014; Kahn, 2014]. MDPC-23 cells were treated with LiCl, rWnt3a, or α-Wnt3a antibody for last 24 hours and the β-catenin was determined by immunoflourescence. Nuclear accumulation of β-catenin was increased among both groups by treatment

with LiCl, and rWnt3a while this translocation of β-catenin to the nucleus was abrogated with α-Wnt3a antibody treatment (Fig. 7C). We further tested whether PSF induced canonical Wnt signaling pathway operates odontoblast differentiation; the cells were treated with LiCl and examined the DSPP expression. As shown in Fig. 7D, the DSPP mRNA expression was increased with the LiCl treatment and more accelerated in the PSF group. Further, we determined either canonical wnt signaling is a direct downstream target of DSPP expression. Several evidence support that the active β-catenin form a complex with LEF1 to activate transcription. Our results indicated the over expression of LEF1 increased DSPP expression significantly ($p < 0.05$) in the cells on PSF (Fig. 7E). To confirm that canonical wnt signaling is involved in DSPP expression, the cells were treated with wnt signaling inhibitor DKK1. The treatment of DKK1 reduced the expression of DSPP significantly ($p < 0.05$) on PSF compared to non-treated group (Fig. 7F). We further confirmed whether DSPP mRNA expression affected by inhibition of functionling wnt signaling molecule. Knockdown of β-catenin by siRNA abrogated the DSPP mRNA level specifically more highly suppressed in the cells on PS nanofibers (Fig. 7G). These results suggested that nanofibrous matrix accelerates canonical wnt signaling functionally followed by induction of DSPP expression that required β-catenin activities.

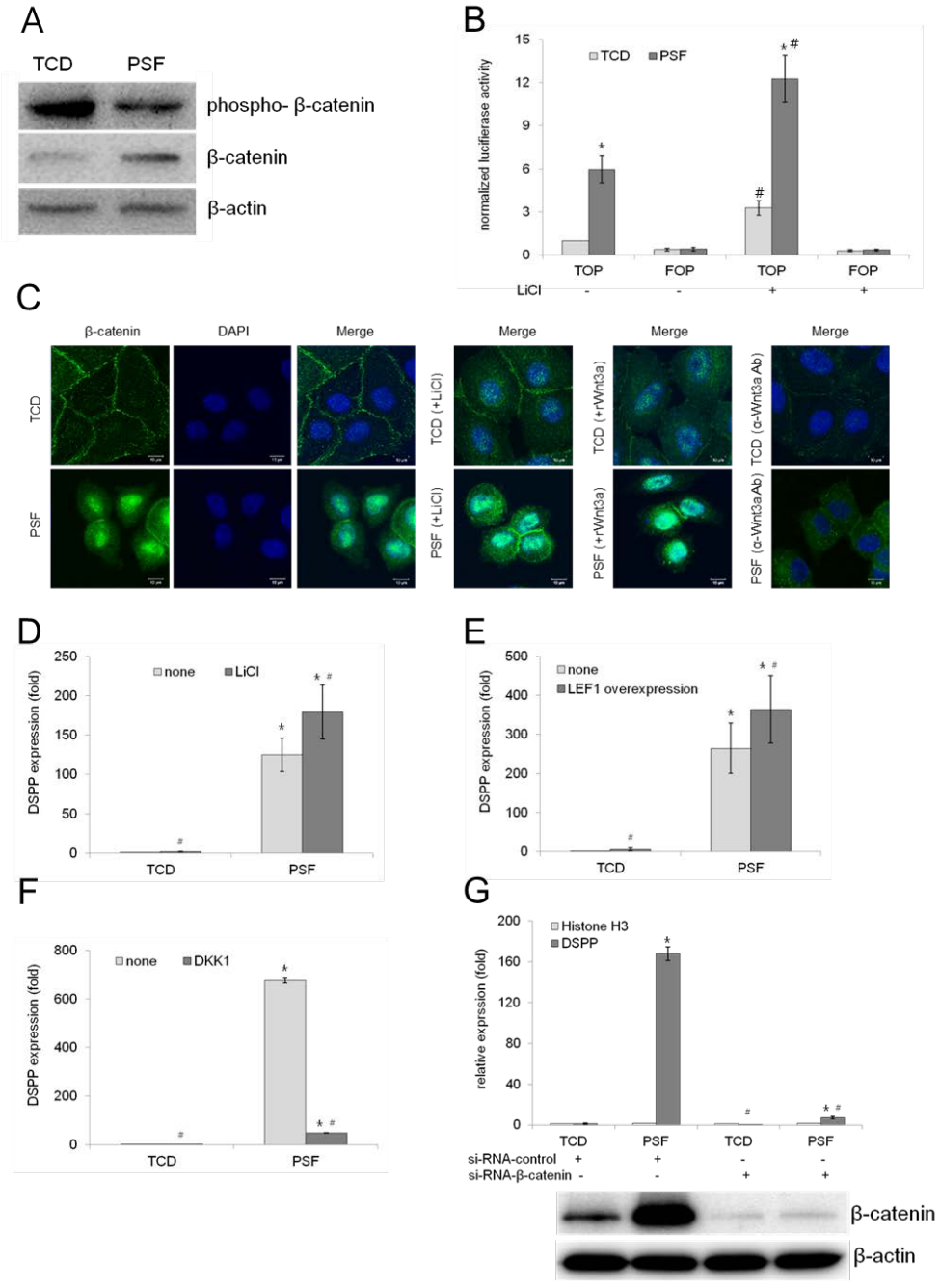
A
TCD
PSF
phospho- β-catenin
β-catenin
β-actin
B
TCD
PSF
normalized luciferase activity
TOP
FOP
TOP
FOP
LiCl
C
β-catenin
DAPI
Merge
TCD
PSF
TCD (+LiCl)
PSF (+LiCl)
TCD (+rWnt3a)
PSF (+rWnt3a)
TCD (α-Wnt3a Ab)
PSF (α-Wnt3a Ab)
D
none
LiCl
DSPP expression (fold)
TCD
PSF
E
none
LEF1 overexpression
DSPP expression (fold)
TCD
PSF
F
none
DKK1
DSPP expression (fold)
TCD
PSF
G
Histone H3
DSPP
relative exprssion (fold)
TCD
PSF
TCD
PSF
si-RNA-control
si-RNA-β-catenin
β-catenin
β-actin

Figure 7. Wnt3a is involved in DSPP expression in cells on PSF. MDPC 23 cells were cultured on TCD and PSF and determined the total β-catenin and p- β-catenin by western blot analysis (A). Cells were transfected with Topflash (wild-type) or Fopflash (mutant) reporter plasmids and cultured in differentiation media with or without of LiCl for last 24 h and luciferase activities were measured in cell lysates and normalized to a Renilla transfection control (B). Cells cultured on PSF and TCD without or with LiCl, rWnt3a, or α-Wnt3a antibody treatment for 4 days and the nuclear translocation of β-catenin was detected by immunofluorescence (C). Real-time PCR for DSPP expression was performed in cell on TCD and PSF with or without of LiCl treatment (D), or LEF1 overexpression (E), or rDKK1 treatment (F). The cells were transfected with siRNA against β-catenin and determined the DSPP expression by real-time PCR analysis (G). Data are the mean ± SD of repeated experiments. *Significantly different from the control ($p < 0.05$). # Significantly different from the groups treated with non-treated ($p < 0.05$).

IV.3.8. DSPP gene expression is a direct target of Wnt3a

The above results suggested that canonical Wnt signaling pathway is involved in odontoblast differentiation specifically DSPP expression in cells on PS nanofibrous matrix. The mRNA expression of several Wnt signaling molecules identified that PSF induced the mRNA expression of Wnt3a, Wnt5a, Wnt5b, and Wnt10a. Among them the Wnt3a mRNA expression was significantly ($p < 0.05$) higher in cells on PSF than control (Fig. 8A). Further, we determined the Wnt3a protein in the media by ELISA assay and confirmed that the amount of secreted Wnt3a protein was higher on PSF compared to control group (Fig. 8B). Next, we confirmed that DSPP expression is a direct target of Wnt3a. The PS nanofibers were attached to half of plate while the remaining half area was without PSF used as a control. The amount of Wnt3a and DSP proteins were higher in the samples on PSF compared to TCD as determined by immunostaining using confocal microscopy. The expression of Wnt3a and DSP proteins were higher in cells on PSF compared to TCD. This expression of DSP protein was reduced with treatment of anti-Wnt3a antibody to the culture (Fig. 8C, D). Next we examined the treatment of rhWnt3a increased DSPP expression and was highly increased up to more than 100 folds with 100ng/ml and 500ng/ml of rhWnt3a treatment compared to non-treated group, and DSPP expression was observed higher in rhWnt3a treated group compared to rBMP2 treated group (Fig. 8E). Next, we determined the effect of Wnt3a treatment on DSPP expression with different time points, the cells were treated with rhWnt3a for last 24 hours of culture and determined DSPP expression at different time points. DSPP expression was robustly increased at 8 hour's time point and continuously increased up to 24 hours compared to control group (Fig. 8F).

Further, we confirmed the effect of Wnt3a on DSPP expression and found that the treatment of anti-Wnt3a antibody abrogated the PSF-induced DSPP expression (Fig. 8G). To confirm whether Wnt3a is directly involved in DSPP expression during odontoblast differentiation, therefore, we examined the DSPP mRNA expression after using knockdown of Wnt3a by siRNA. As shown in Fig. 8H, knockdown of Wnt3a reduced the expression of DSPP mRNA significantly ($p < 0.05$) while no effect happened to the H3f3a mRNA expression.

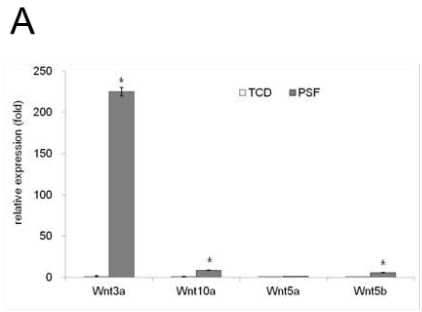
A
250
200
150
100
50
0
relative expression (fold)
TCD
PSF
Wnt3a
Wnt10a
Wnt5a
Wnt5b

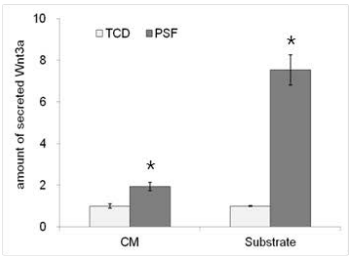
B
10
8
6
4
2
0
amount of secreted Wnt3a
TCD
PSF
CM
Substrate

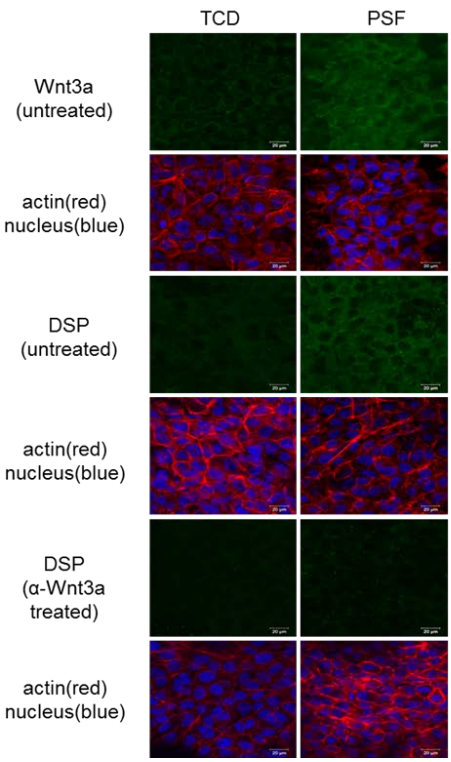
C
TCD
PSF
Wnt3a (untreated)
actin(red) nucleus(blue)
DSP (untreated)
actin(red) nucleus(blue)
DSP (α-Wnt3a treated)
actin(red) nucleus(blue)

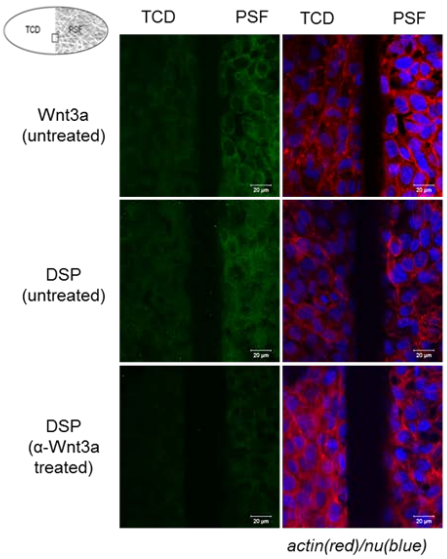
D
TCD
PSF
TCD
PSF
Wnt3a (untreated)
DSP (untreated)
DSP (α-Wnt3a treated)
actin(red)/nu(blue)

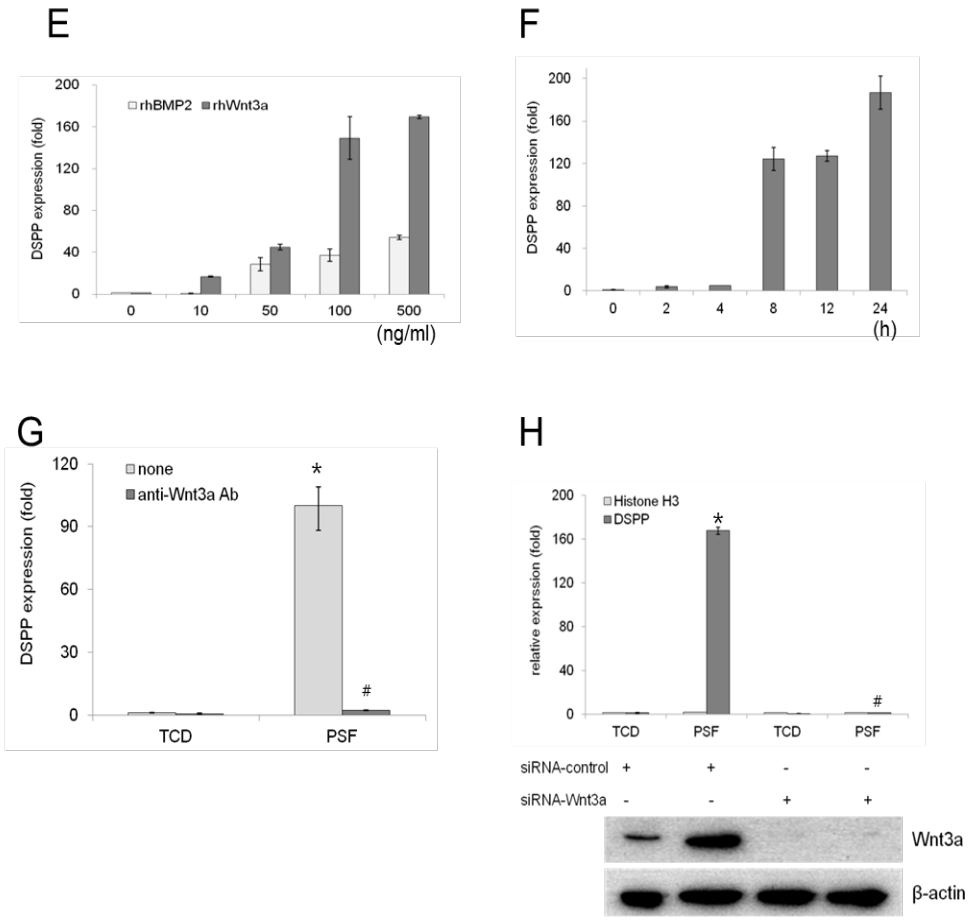

Figure 8. PSF-induced DSPP gene expression is a direct target of Wnt3a. MDPC-23 cells were culture on TCD and PSF for four days. Real-time PCR for different Wnts molecules expression was performed (A). The amount and secretion of Wnt3a was determined by ELISA assay (B). Wnt3a and DSP proteins were observed by immunofluorescence in cells on TCD and PSF, as well as DSP expression was also observed in cells on TCD and PSF after treatment of anti-Wnt3a antibody to the culture (C, D). Real-time PCR for DSPP gene expression was determined in samples with or without rhBMP2

or rhWnt3a treatment (E), different time interval treatment of rhWnt3a 100ng/ml (F), and after treatment with anti-Wnt3a antibody (G). After knockdown of Wnt3a gene by siRNA, determined the DSPP expression by real-time PCR analysis (H). Data are the mean ± SD of repeated experiments. *Significantly different from the control ($p < 0.05$).

IV.3.9. Identification of LEF1 consensus motifs in Mouse DSPP gene promoter and regulation of DSPP promoter activity increases on PSF

We analyzed the DSPP proximal promoter by TESS and found four putative LEF1 binding sequences between the -791 and putative transcription start site (+1). All of these four binding sites are well conserved among human, mouse, and rat DSPP promoters. Based on these observations, serial deletions of the DSPP promoter at the 5´end were transiently transfected in to odontoblast cells cultured on PS nanofibrous matrix and TCD. Luciferase assay analysis of the first DSPP construct (D-791) revealed that no changes was observed in the transcriptional activity in cells on TCD and PSF suggesting that there might be repressor binding region include in D-791 promoter construct. Further, luciferase assays of the DSPP promoter constructs revealed (Fig. 9A) that an initial deletion of the DSPP promoter at the 5' end increased the transcriptional activity compared to the full-length DSPP promoter. The D-624 construct showed greater transcriptional activity in cells on nanofibrous matrix compared to TCD. Further, another deletion construct D-435 also increased the transcriptional activity with respect to the full length. The transcriptional activity was reduced in D-435 compared with D-624. There were no changes observed in the transcriptional activity of the rest deletion construct (D-260, and D-225) of DSPP promoters in cells on PSF and TCD. Further we observed wether the L1 (site1) and L2 (site2) putative binding sites are important for the regulation of DSPP gene. DNA constructs of D-625 and D-435 were mutated at L1 and L2 binding sites generated M-624 and M-435 respectively and were transfected to MDPC-23 cells cultured on PSF and TCD. As shown in Fig. 9B, the promoter activity of the M-624 was strongly reduced compared to wild type in cells on PSF.

While the M-425 shown reduced transcriptional activity than D-425. Taken together these results suggest that two putative binding sites (L1 and L2) for LEF1 are essential for the expression of DSPP gene.

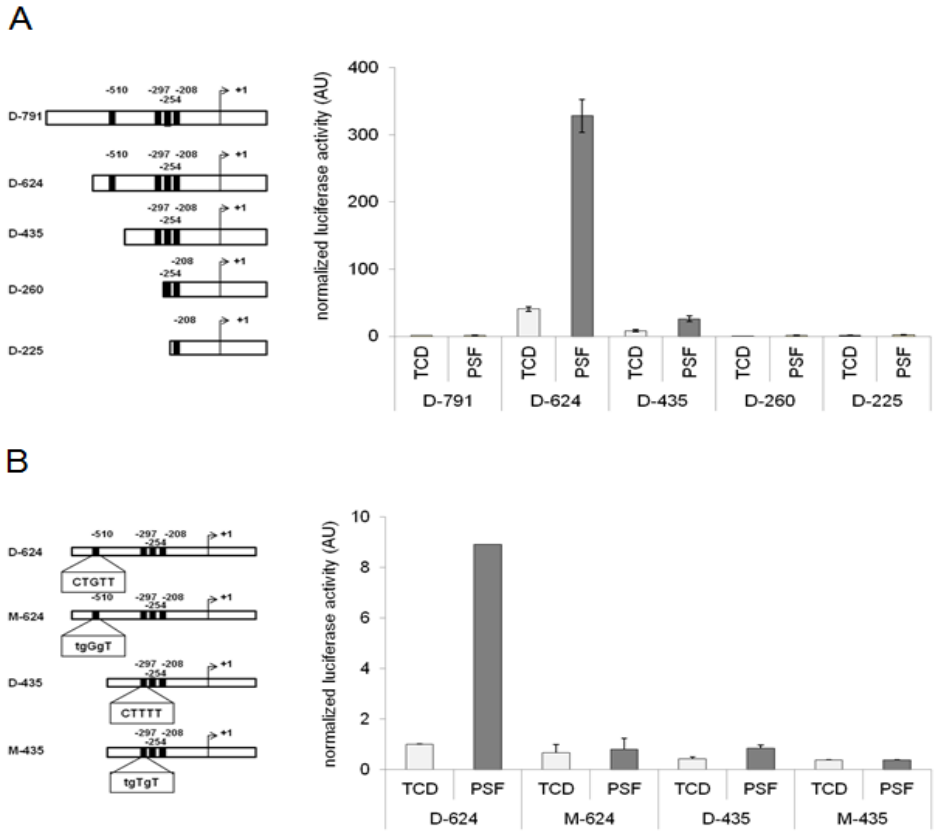

Figure 9. DSPP promoter activity in odontoblast (MDPC-23) cells and the binding of β-catenin to the putative LEF-1 binding sites on the DSPP promoter. MDPC-23 cells were cultured on TCD and PSF. Transient transfection were performed with luciferase reporter vector containing the DSPP promoter region (D-791 and 4-serial deletion constructs D-624, D-435, D-260, D-225) and empty plasmid as a control. DSPP promoter activity was quantified in terms of relative luciferase activity. Renilla luciferase vector was used as an internal control (A). Illustration of wild-type and mutants DSPP promoter gene constructs. The diagram shows the position and sequence of LEF1 responsible elements with mutated sequences shown in lowercase type (B).

IV.3.10. ChIP assay demonstrating β-catenin binds to the LEF1 binding sequence on the DSPP promoter

To determine wether β-catenin interacts directly with the TCF/LEF binding sites in vivo, ChIP assays was performed. After harvesting the cells, chromatin was prepared from cells and immunoprecipitated with antibody specific for β-catenin. Following anti-β-catenin antibody-immunoprecipitated protein-DNA complexes de-cross-linking, the purified DNA was used as a template, using specific primers for PCR corresponding to the regions of mouse DSPP promoter. As shown in Fig. 9, we identified two regions, A and B where the β-catenin make complex to the TCF/LEF binding sequence increased on PSF compared to TCD. While no difference observed at region C of cells on PSF to those on TCD.

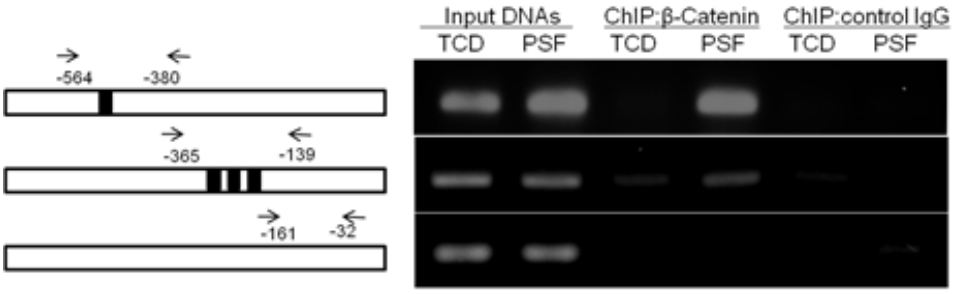

Figure 10. ChIP assay analysis. The schematic representation of region A, and region B show the binding sites for the LEF1 on the mouse DSPP promoter and the arrows represents the primers used in the Chip assay. Chromatin immunoprecipitation was performed to confirm the binding of β-catenin to the putative binding sites on the DSPP promoter.

IV.3.11. Effect of Wnt3a on the transcriptional activity of DSPP promoter

To determine whether Wnt3a treatment affect the DSPP promoter activity in wild type or mutant constructs, we transfected cells with different constructs and treated with rhwnt5a or rhBMP2. The transcriptional activity was significantly increased in D624 transfected group with rhWnt3a treatment compared with BMP2 treated group, while in D435 transfected group the luciferase activity was also increased significantly with treatment of rhWnt3a (Fig. 11A). We determined that Wnts signaling and BMP signaling inhibitors treatment affected the transcriptional activity of DSPP promoter. The noggin treatment decreased the transcriptional activity while the DKK1 treatment highly decreased the transcriptional activityin both D624, and D435 groups (Fig. 11B). Further, we examined the effect of LiCl on the DSPP promoter activity. The transcriptional activity was increased significantly with treatment of LiCl in wild type (D624) group while no changes observed in mutant (M624) group (Fig. 11C).

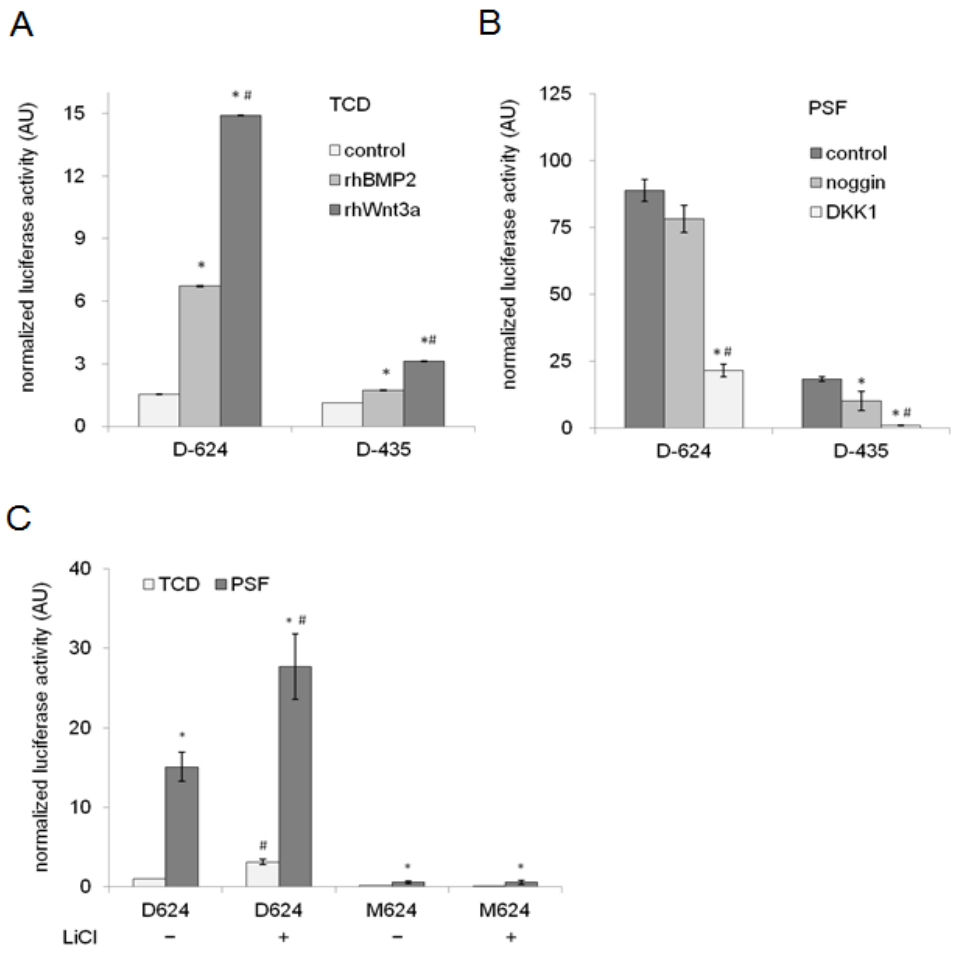

Figure 11. Wnt3a affects the transcription activity of the DSPP promoter. MDPC-23 cells were cultured on TCD and PSF. The cells were transfected with DSPP promoter constructs and determined the luciferase activity after treatment with rhBMP2 or rhWnt3a (A), rNoggin or rDKK1 (B), and LiCl treatment (C). While the untreated groups used as a control. Data are presented in the mean ± SD of repeated experiments. *Significantly different from the control ($p < 0.05$). # Significantly different from the groups treated with non-treated ($p < 0.05$).

IV.3.12. *In-vivo* study shows the association of Wnt3a and DSP after cell-matrix transplantation into nude mice

The samples were retrieved after 8 days of subcutaneous implantation in nude mice. The H-E staining indicated the MDPC-23 cells grew on the nanofibrous matrix. The immunohistochemical staining for DSP indicated the ECM matrix deposition of the cells on nanofibers. Meanwhile the Wnt3a was abundantly detected in MDPC-23 cells (Fig. 11). These results indicate that both DSP and Wnt3a were functional and expressed at higher level in cells on nanofibrous matrix to make the extracellular matrix.

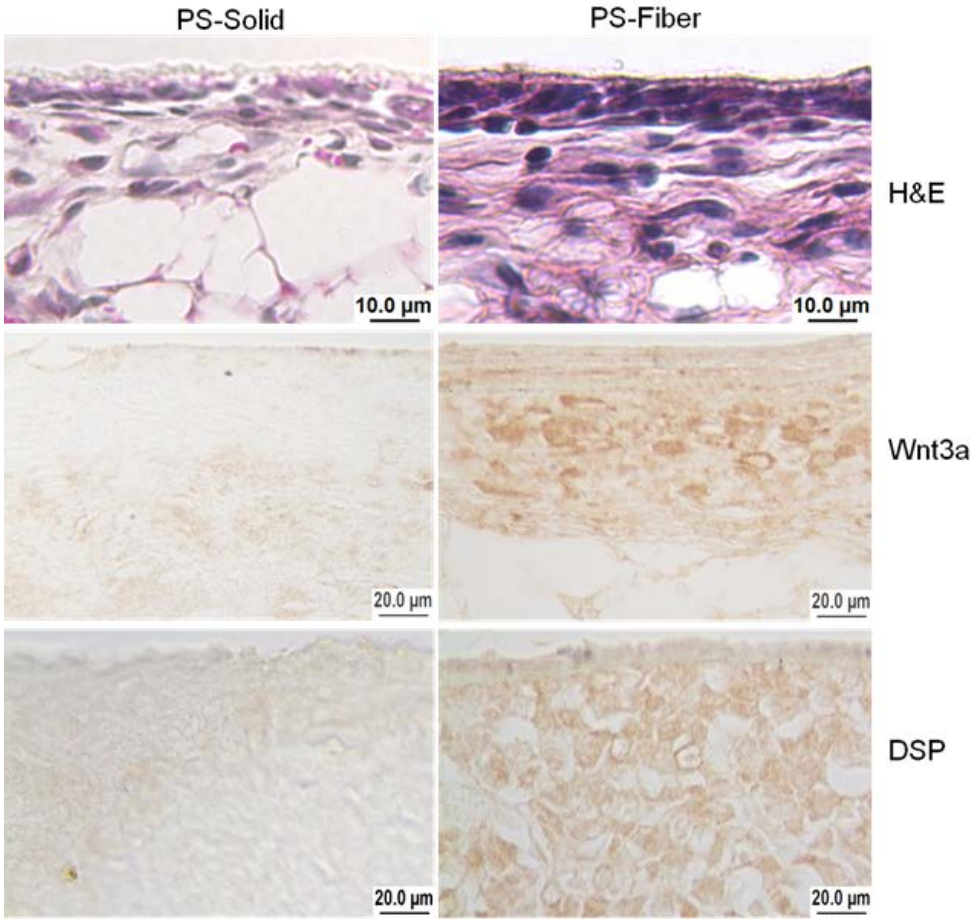

Figure 12. MDPC-23 cells-scaffold constructs implanted into nude mice. The H-E staining demonstrating the cells overlaying on the surface of interconnected nanofibers. The Wnt3a and DSP proteins were clearly detected by immunohistochemical staining. The immunostaining indicated the absence of Wnt3a, and DSP in the control group.

IV.4. Discussion

The stem cells respond profoundly to their microenvironment. Here we investigated the developments in nanofibrous engineered matrix that affect the cellular response to induce specific growth factors and transduce molecular events intracellularly that leads to differentiation and has potential applications in biological research and tissue engineering.

The combination of physical, mechanical and biological properties play a dynamic role in odontoblast and osteoblast differentiation to form dentin and bone respectively. Therefore, the cell-matrix interaction implicates extracellular molecules to control cell behavior such as cellular attachment, activate intracellular signaling that lead to differentiation. Nano-biomaterial is novel concepts that mimic the natural ECM microenvironment to alter the interactive cellular activity and play an essential role in differentiation and tissue neo-genesis [Lee et al., 2014]. To engineer material that mimics the natural EMC, several technologies have been developed to designate biomaterials with succession. Electrospinning is one of the most up growing methods used to fabricate the nanofibrous materials [Li et al., 2002] that provide the nanometer scale fibrous structure to the cells [Wei and Kasper, 2014]. The electrospun nanofibers have high potential for cellular differentiation and tissue engineering. In the case of bone, an effort has been made by the nanofiber to induce osteoblast differentiation and bone regeneration [Woo et al., 2009; Ma et al., 2011]. Previously we have reported that nanofibrous scaffolding promotes osteoblast differentiation and biomineralization [Woo et al., 2007]. Odontoblast is similar to osteoblast in ways to secrete extracellular matrix proteins. However, the relative proportion of their response to microenvironment may differ during

differentiation.

In our study, we examined the performance of dental pulp-derived, bone marrow-derived, and adipose-derived mesenchymal stem cells on electrospun nanofibrous matrix undergoes to induction of growth factors differentially on same culture condition. However, the dental pulp stem cells showed strong expression of Wnt and BMP signaling molecules on the nanofibrous matrix. Among Wnts, Wnt3a expression was highly increased in DPSCs on PSF. The performance of the dental pulp cells on electrospun nanofibers undergoes to differentiation both *in-vitro* and *in-vivo* [Yang et al., 2009; Wang et al., 2010]. All these information emphasize a strong association of nanofibrous matrix with odontoblast differentiation and dentin formation, But the molecular mechanism was unclear that how nanofibers induced the odontoblast differentiation. Here for the first time we investigated that the nanofibrous engineered matrix induced odontoblast differentiation specifically DSPP expression through canonical Wnt signaling pathway.

Here in our study, the polystyrene nanofibrous matrix were successfully developed by electrospinning has diameter of less than 500nm indicating uniformly observed by SEM. Several researchers have focused on the application of the nanofibrous matrix in terms of cellular differentiations and tissue regeneration [Shin et al., 2004; Xin et al., 2007; Woo et al., 2009; Yang et al., 2009; Ma et al., 2011]. Here we investigated the molecular mechanisms and compared the properties of odontoblast cells seeded on the nanofibrous matrix with those on TCD while both substrates are composed of the same material (polystyrene). Another important difference observed in the extent of ARS-calcium expression analyzed qualitatively and

quantitatively showed higher calcium concentration on PSF. Furthermore, the data indicated that the odontoblast differentiation of the seeded MDPC-23 increased on PSF. DSPP is a dominant member of the non-collagenous matrix protein of dentin and is important for proper dentin formation and biomineralization [Yamakoshi, 2008]. It is highly expressed and secreted by odontoblasts, the cells that are responsible for dentin formation. In our study, DSPP mRNA expression in MDPC-23 was increased 100 fold on PSF than TCD and 10 times more than cells exposed to rBMP2 treated measured by qRT-PCR analysis. Like DSPP, DMP1 and BSP also belong to the small integrin-binding ligand N-linked glycoprotein (SIBLING) gene family [Fisher et al., 2001]. DMP1 and BSP expression were increased 8- and 50-fold respectively on PSF than those of TCD. Therefore our data indicate that PS nanofibrous matrix induced the odontoblast differentiation markers particularly DSPP gene expression relatively much higher than other molecules, which is considered to have an important role in odontoblast differentiation and biomineralization.

The Wnt signaling has been observed during odontoblast differentiation that goes further to dentin formation. Wnt5a and Wnt6a have been illustrated to induce the differentiation of human dental papilla cells and promoted biomineralization, while Wnt10a seems to be critical for dentinogenesis and tooth morphogenesis in regulating the odontoblast differentiation [Yamashiro et al., 2007; Liu et al., 2008; Wang et al., 2010; Peng et al., 2010]. However, Wnt signaling pathway is a potent factor in tooth development and odontoblast differentiation. β-catenin, a main component of canonical Wnt signaling pathway is strongly expressed in odontoblast and is required for odontoblast differentiation during tooth root formation, and its disruption

lead to arrest tooth root formation [Kim et al., 2013]. In addition, DSPP is exclusively expressed during dentin formation. DSPP might be a direct target of canonical Wnt signaling pathway when cells seeded on nanofibrous engineered matrix. Based on these observations we examined genes expression of Wnt signaling molecules during odontoblast differentiation on PS nanofibrous matrix and TCD. In this study, we proved that induction or inhibition of Wnt signaling pathway using inducers or inhibitors altered DSPP gene expression in cells on PSF.

Further, we confirmed that DSPP is a direct target of canonical Wnt signaling using MDPC-23 cells as a model. The stabilization and nuclear translocation of β-catenin were increased in cells on PSF while real-time PCR analysis revealed that canonical Wnt signaling molecules exhibited higher expression on PSF particularly Wnt3a. We confirmed here that canonical Wnt signaling stimulates DSPP expression. DSPP mRNA expression was increased by treatment with Wnt3a protein. Overexpression of LEF1 or treatment with LiCl up regulated the DSPP expression during odontoblast differentiation, as it has been suggested that overexpression of Lef-1 accelerate the odontoblast differentiation of dental pulp cells [Yokose and Naka, 2010]. Our study further indicates that the β-catenin induced transcriptional activity of LEF1 was higher on PSF and increased by treatment with LiCl, whereas FopFlash did not show any changes. Conversely, treatment of cells with Wnt signaling inhibitors such as rDKK1 or anti-Wnt3a antibody abrogated PSF-induced DSPP expression. Meanwhile, siRNA knockdown of Wnt3a or β-catenin suppressed the expression of DSPP mRNA.

Previous studies have identified from deletion studies that murine DSPP gene promoter contain positive and negative regulatory region [Feng et al.,

1998; Ritchie et al., 2002; Unterbrink et al., 2002]. In this study, we demonstrated the mouse DSPP gene reporter activity strongly increased in cells on PSF when the promoter region -791 to -625 was deleted (from D -791 to D -624). We, therefore, hypothesized that downstream of -625 contain critical regions that includes activator binding regions which up-regulates the DSPP promoter activity in MDPC-23 during odontoblast differentiation on PSF. Upstream of -625 may contain a repressor binding region that down-regulated the promoter activity in MDPC-23. We found YY1 potential binding element at -635 that may act as a repressor of transcription [Shrivastaval and Calame, 1994]. Furthermore, we have found four consensuses LEF1 sites in the DSPP gene promoter and identified the effect of these LEF1 sites on the DSPP promoter region. Moreover, we investigated the effect of these LEF1 sites in the mouse DSPP promoter. Substitution mutations of these LEF1 binding region resulted in a decrease of DSPP promoter activity as compared to wild type. Additionally we focused on DNA-protein binding assay indicated that β-catenin binds at two regions of TCF/LEF response elements downstream of -624 of DSPP promoter particularly more highly in cells on PSF and represented as region A, B, and C. These three regions A, B, and C located between nt -564 to nt -380, and nt -365 to nt -139, and nt -161 to nt -32 respectively upstream of DSPP transcription start site. Our data indicated that the β-catenin interact with the TCF/LEF1 motifs to make complex at region A and B of the DSPP promoter may dictate the DSPP transcription in MDPC-23 during odontoblast differentiation on PSF compared to those on TCD. While there was no difference observed in the DNA-protein complex at region C of the DSPP promoter in cells between both groups. The in-vitro culture system as a model to investigate the odontoblast differentiation and development, the

potential of this model is critical to be confirmed in vivo. For this confirmation, we performed the animal study and found that the H & E and immunohistochemical staining for DSP verified the differentiation and matrix formation by odontoblast on nanofibrous engineered matrix. Meanwhile, the Wnt3a also showed strong positively immunohistochemical staining. Therefore, our results suggest that polystyrene nanofibrous engineered matrix induces DSPP expression through canonical Wnt signaling pathway.

IV.5. Conclusion

In conclusion, this study demonstrated that polystyrene nanofibrous engineered matrix induces the DSPP expression in human dental pulp stem cells and murine dental papilla-derived cells. We found that this expression of DSPP is under the control of Wnt3a. Overall, our results indicate that nanofibrous engineered matrix induces odontoblast differentiation and specifically DSPP gene expression through canonical Wnt signaling pathway in MDPC-23 cells.

V. Part-II. Nanofiberous engineered matrix induces morphological alterations through Wnt5a

V.1. Introduction

The cells reside in their proper extracellular matrix (ECM) formed by the cells not only binds the cells together, but also exert their impact on cell survival, shape, migration, and development. ECM is a dynamic network of different molecules secreted by cells and provides three-dimensional ultra-structure [Hynes, 2009; Gentili and Cancedda, 2009]. The ability to mimic the physical, chemical, and mechanical properties of the natural extracellular matrix is an essential requirement for tissue engineering. Accumulating evidence indicates that the nanofibrous engineered matrix can modulate the cell responses leading to tissue regeneration [Lutolf et al., 2003; Anselme et al., 2010]. Nanofibrous engineered matrix provides microenvironment that respond extracellular and intracellular cell communication and signaling which influence cell contact, proliferation, and differentiation. The nanofibrous matrix has improved physical or biomechanical features and has been used in tissue engineering of various organs. Nanofibrous matrices are among the available biomaterials can be used broadly in bioengineering. The combinations of physical, mechanical and biological properties play a vital role in odontoblast and osteoblast differentiation to form dentin and bone respectively [Wang et al., 2010; Wang et al., 2011]. Therefore, the cell-matrix interaction implicates extracellular molecules to control cell behavior such as cellular attachment, differentiation, morphology, and activate intracellular signaling that has an important application in tissue engineering [Biggs et al., 2009; Nikkhah et al., 2012]. It has been documented that nanofibrous scaffold promoted the odontogenic differentiation and

biomineralization of dental pulp stem cells both *in-vitro* and *in-vivo* and suggested an important scaffold for dentin regeneration [Wang et al., 2011; Cavalcanti and Zeitlin, 2013].

Odontoblasts are considered as specialized cells that are responsible for proper dentin formation. Cells elongation, cytological polarization, cellular process formation, and functional changes occur during odontoblast differentiation. Odontoblasts are aligned and polarized along the interface between dental pulp and dentin and exhibit long processes extending into the mineralized matrix, which give tubular characteristics to dentin, these two morphological features are specific for odontoblasts [Linde and Goldberg, 1993; Tjaderhane et al., 2013]. Functionally odontoblast has distinct processes whereby secretion occurs. The odontoblast process consists of one main trunk with various branches along its length, and is defined by a plasma membrane that contain predominantly cytoskeletal components [Ruch et al., 1995; Teti et al., 2013]

Several signaling pathways and different transcription factors regulate differentiation of odontoblast that undergoes tooth formation during tooth development. Among them Bone morphogenetic proteins (BMP), Wnt signaling, members of the Hedgehog (Hh), and Fibroblast growth factors (FGF) have a vital role in tooth development. Disruption of any of these pathways during odontogenesis can affect tooth development. The evidence from animal models indicated that Wnt signaling pathway plays an important role in tooth morphogenesis, and continuous tooth generation is induced by activated Wnt signaling [Wang et al., 2011]

Wnt signaling pathway plays an important role in proliferation,

differentiation, migration, cell survival, and cell polarity to control various cellular functions by activating intracellular signaling cascades. Wnt5a is most widely studied member of Wnt family protein and has an important role in the developmental process of various organs. Mice lacking Wnt5a gene exhibit smaller and abnormally patterned teeth and show delayed odontoblast differentiation [Lin et al., 2011]. The genetic evidence indicated that Wnt5a is required for skeletal development and observed the shortening of limbs in Wnt5a-null mice [Yamaguchi et al., 1999]. Wnt5a has gained importance for their role in odontoblast differentiation and is specifically expressed in the differentiating odontoblast in mice and human. Wnt5a is involved in various cellular functions through regulation of multiple signaling pathways [Veeman et al., 2003; Peng et al., 2010].

It has been indicated from the observations that Wnt5a overexpression in Xenopus oocyte leads to an increase in intracellular calcium without affecting β-catenin level [Slusarski et al., 1997; Kuhl et al., 2000]. The increased in intracellular calcium induced by Wnt5a activates the Ca^{2+} dependent effector molecules such as calcium/calmodulin-dependent kinase II (CamKII), protein kinase C (PKC), or calcineurin (CaCN) which in turn activate translocation of NFAT to the nucleus. Nuclear Factor of Activated T cells (NFATc) is a transcription factor exist in the cytoplasm as a phosphorylated form in unstimulated cells. An increase in intracellular calcium level leads to activate the phosphate calcineurin and induces NFATc dephosphorylation leading to translocation to the nucleus, where it make complexes with other factors to regulate target genes. NFAT has an essential role in bone regeneration and the transcriptional program of osteoblasts [Hogan et al., 2003; Zayzafoon, 2006]. It has been documented that NFATc

is a downstream target of Wnt5a. The noncanonical Wnt signaling pathway that induces intracellular Ca^{2+} has shown to promote the nuclear translocation of NFATc [Saneyoshi et al., 2002]. However, the Wnt5a has an important role in cytoskeleton remodeling, cell migration, and coordinates with planer cell polarity pathway in regulating cell polarity.

It was unclear whether dental pulp cells induce morphological alterations and actin reorganization when seeded on the nanofibrous engineered matrix that provide 3D culture microenvironment. Under the hypothesis that the nanofibrous engineered matrix induces the morphological alterations, we cultured pre-odontoblast MDPC-23 cells on the electrospun polystyrene nanofibrous matrix compared to TCD, both substrates contained same material. The principal purpose of this study was to investigate the effects of nanofibrous matrix on morphological alterations and specifically cells processes formation and actin reorganization during odontoblast differentiation, and what mechanism involved in these characteristics.

We demonstrated that PSF induced the Wnt5a expression followed by the morphological alterations of odontoblast, the cells exhibited increased in height and displayed a columnar, elongated appearance and have increased cell processes formation. Then based on these observations, we found that Wnt5a is involved in morphological alterations through small GTPases pathway.

V.2. Materials and methods

V.2.1. Materials & reagents

Polystyrene (PS) tissue culture plates were purchased from BD Falcon (Franklin Lakes, NJ). Dulbecco's modified Eagle's medium (DMEM) was purchased from Hyclone (Logan, UT) Fetal bovine serum (FBS), HEPES buffer solution, and penicillin-streptomycin solution were purchased from GibcoBRL (Carlsbad, CA). L-Ascorbic acid, glycerol 2-phosphate, phosphatase inhibitor cocktails, dimethylformamide (DMF), and tetrahydrofuran (THF) were purchased from Sigma (St. Louis, MO). RNA isoplus reagents, PrimeScript™ RT reagent kit, and SYBR® Premix Ex TaqTM were purchased from Takara (Kyoto, Japan). Protease inhibitor cocktail tablets complete was from Roche (Basel, Switzerland). CellMask™ plasma membrane stain and Phalliodin-Alexafluor488 were purchased from Molecular Probes (Eugene, OR). Recombinant human/mouse Wnt5a protein was purchased from R&D Systems (Minneapolis, MN). The siRNAs against Wnt5a, Ror2, and non-targeting siRNAs were purchased from Dharmacon (Lafayette, CO). Anti-Wnt5a, anti-Ror2, anti-NFATc1, anti-Actin, and HRP-conjugated IgG antibodies were purchased from Santa Cruz Biotechnology (Santa Cruz, CA). The small GTPases activation assay kit was purchased from Cytoskeleton (Denver, CO).

V.2.2. Preparation of the nanofibrous matrix

A polystyrene (PS) fiber matrix was prepared by electrospinning as previously described [39]. Briefly, the polystyrene was dissolved in dimethylforamide (DMF), and a 12% (weight/volume) PS solution was added into a 10-mm syringe with a stainless steel syringe needle (30 G). The

electric potential and the distance to the collector were 30 kV and 20 cm, respectively. The fiber was collected on a rotating metal drum covered with aluminum foil. After electrospinning, a very small amount of DMF was spread on the bottom of a petri dish and a PS sheet was placed over it. Then, a PS sheet fixed onto a petri dish was dried in a clean bench at room temperature. Subsequently, the PS sheet on a petri dish was washed with 70% ethanol and then dried to remove any residual DMF. Afterward, it was dried again in a clean bench.

V.2.3. Cell culture

MDPC-23 mice odontoblast-like cell line [Hanks et al., 1998] was used in this study. The cells were maintained in Dulbecco's modified Eagle's medium (DMEM) supplemented with 10% heat-inactivated fetal bovine serum. For each experiment, the cells were seeded on tissue culture polystyrene (TCPS) and PSF at a density of 5 X 10^5 cells per 60-mm dish. Approximately 12 h after cell seeding, the cells were cultured in a differentiation medium (growth medium plus 10 mM β-glycerophosphate and 50 μg/ml ascorbic acid) for up to 14 days.

2.4. Scanning electron microscopy

The matrices were rinsed in PBS and fixed using 2.5% glutaraldehyde in 0.1 M cacodylate buffer (pH 7.4). After freeze-drying, the specimen was dehydrated by dipping it in increasing concentrations of ethanol and then by critical point drying. After drying, the specimens were sputter-coated with gold-palladium and observed under an SEM at 12 kV (FE-SEM Hitachi S-4700, Japan).

V.2.5. Confocal microscopy

To determine the alteration of cell morphology, MDPC-23 cells were seeded on PSF-attached BCD 6.5mm^2 pieces at a concentration of 1X10^4 cells per piece in 48 well cell culture plates. While for the control group, the cells were straightly seeded on TCD 6.5mm^2 pieces at the same cells concentration. After overnight, the media were changed and cultured in differentiation media up to 14 days. The cells were washed with phenol-red free DMEM without FBS for 2 times and then treated with freshly prepared working solution of the CellMask™ plasma membrane stain in warm physiological buffer (phenol-red free DMEM without FBS) from the 1000X concentrated Cell Mask stain solution for 60 min in incubator at 37^{o}C. The cells were washed 2 times with 1XPBS including calcium and magnesium and were fixed with 4% formaldehyde for 10 min at room temperature in dark condition and then washed again for 3 times with 1XPBS. The cells were treated with Phalliodin-Alexafluor 488 and DAPI (1mg/ml stock) with a dilution of 1:50 for 30 minutes at room temperature in dark condition. After washing the samples with 1XPBS including Ca and Mg, coverslips were mounted using mounting medium with DAPI to identify nuclei and sealed with glove. The images were taken to determine the morphology of cells by Confocal Laser Scanning Microscopy (Zeiss, LSM 700). The height of the cells was determined from the Z-stacked images of the cells. After each incubation, the samples were washed with 1XPBS three times for 5 min each. All of the steps performed at room temperature. The samples were examined using a laser scanning confocal microscope (LSCM). The experiments were in triplicates for at least three times repeated.

V.2.6. Measurement of Cells height and nuclei position

To determine the cells height and nuclei position, the cells were cultured on TCD and PSF and after 4 days of differentiation treated with CellMask™ plasma membrane stain. Then after fixation, the samples were treated with Phalliodin-Alexafluor 488 and DAPI (1mg/ml stock) with a dilution of 1:50 for 30 minutes at room temperature in dark condition. The samples were fixed to the glass slides and mounted using mounting medium and sealed with glove. In order to determine the cells height, the bottom of the cells were taken at zero points and adjusted the confocal laser scanning microscopy with 0.16μm interval of each stacked section. The number of stacked interval from bottom to top of each cell was measured. At same time the position of nucleus was determined either in lower, middle, or upper part of cell basis on the height of each respective cell height. The numbers of cells for each group were estimated 100 in number, and each experiment was performed at least 3 times.

V.2.7. Extraction of total RNAs and RT-PCR

The cells were cultured on TCD and PSF in the differentiation medium. Total RNAs were extracted using RNA isoplus reagents, and the cDNA was synthesized using PrimeScripts RT reagent kit according to the manufacturer's instructions. Quantitative real-time PCR was performed on a Real-time PCR system using SYBR® Premix Ex TaqTM according to the protocol described in the kit. The relative expression of each target gene mRNAs was normalized to those of glyceraldehyde-3-phosphate dehydrogenase (GAPDH). Each experiment was duplicated at least three times. The primers sequences are listed in Table 3.

V.2.8. Western blot analysis

Whole cell lysates were prepared, and western blot analyzes were performed to detect the specific protein. The cell lysates were prepared using a buffer of 10 mM Tris-Cl (pH 7.5), 150 mM NaCl, 1 mM EDTA (pH 8.0), 1% Triton X-100, 1 mM phenyl-methylsulfonyl fluoride, 50 mM NaF, 0.2 mM Na_3VO_4, a phosphatase inhibitor, and a complete protease inhibitor cocktail tablet. The samples were subjected to 10-12% SDS–PAGE and then transferred onto a polyvinylidene difluoride membrane. The membrane was blocked by 5% nonfat dried milk and incubated with each primary antibody. This procedure was followed by incubation with an HRP-conjugated specific secondary antibody. Immunoreactivity was determined by using the ECL chemiluminescence reagent. For the loading control, anti-β-actin HRP-conjugated mouse monoclonal IgG antibody was used.

V.2.9. Knockdown with siRNAs

siRNAs were used to knockdown the expression of Wnt5a, Ror2, RhoA, and CDC42. Non-targeting siRNA was used as a control. MDPC23 cells were seeded at density of 5 x 105 cells per 60-mm culture dish and transfected with each specific siRNA in accordance with the manufacturer’s instruction.

V.2.10. Small GTPases activation assay

The activity of small GTPases was measured by pull-down assay kit and followed the protocol as described by the manufacturer (Cytoskeleton, Inc). Briefly, the cells were cultured on TCD and PSF and induced for osteogenic differentiation. At 4th day of differentiation the cells were harvested and lysed using lysis buffer contained protease inhibitor. Lysates were centrifuged for 1 min at 14000 rpm at 4°C. After centrifuged the protein quantitation was measured, and 20 μg of protein lysate from each sample

were used for total specific small GPTase protein determination. Equal amount of protein lysate from the remaining supernatants were incubated with rhotekin-RBD beads for RhoA activation assay while equal amount of protein lysate was mixed with PAK-PBD beads for CDC42 activation assay. The samples were incubated on rotator for 1 hour at 4°C, centrifuged 1 min at 3000 rpm, and removed the supernatant. After washing the beads once with 300 µl each of wash buffer, centrifuged at 4000 rpm at 4°C for 3 min, removed the supernatant, and added 30 µl of 2x sample buffer to each tube and thoroughly resuspended the beads. The samples were boiled for 2 min and determined by western blot analysis.

V.2.11. Statistical analysis

All data are presented as the average mean ± standard deviation (SD). The statistical analysis was performed using Student's t-test. The difference between groups was considered significant if the p value was less than 0.05.

Table 3. Sequences of primers used in RT-PCR

Molecules	Primer sequences
mWnt5a	5′- CATGTCTTCCAAGTTCTTCC -3′
	5′- CTGTCCTTGAGAAAGTCCTG -3′
mZO-1	5′- TTCCGGGGAAGTTACGTGC -3′
	5′- GACAAA AGTCCGGGAAGCGT -3′
mClaudin-1	5′- TATGACCCCTTGACCCCCAT -3′
	5′- AGAGGTTGTTTTCCGGGGAC -3′
mNestin	5′- TAGAGGTGACCCTTGGGTTAGA -3′
	5′- TAGAGGTGACCCTTGGGTTAGA -3′
mGapdh	5′- AGGTCGGTGTGAACGGATTTG -3′
	5′- TGTAGACCATGTAGTTGAGGTCA -3′

V.3. Results

V.3.1. Nanofibrous engineered matrix induces Wnt5a expression

The polystyrene nanofibrous matrix was synthesized by electrospinning and determined the morphology by scanning electron microscopy showing random nanofiber morphology (Fig. 1A). It has been reported that Wnt5a is specifically expressed in the differentiating odontoblasts [Peng et al., 2010]. MDPC-23 cells were cultured on TCD and PSF. The cells cultured on nanofibrous matrix significantly increased Wnt5a expression determined by quantitative real-time PCR (Fig. 1B) and western blot analysis (Fig. 1C) compared to cells cultured on TCD.

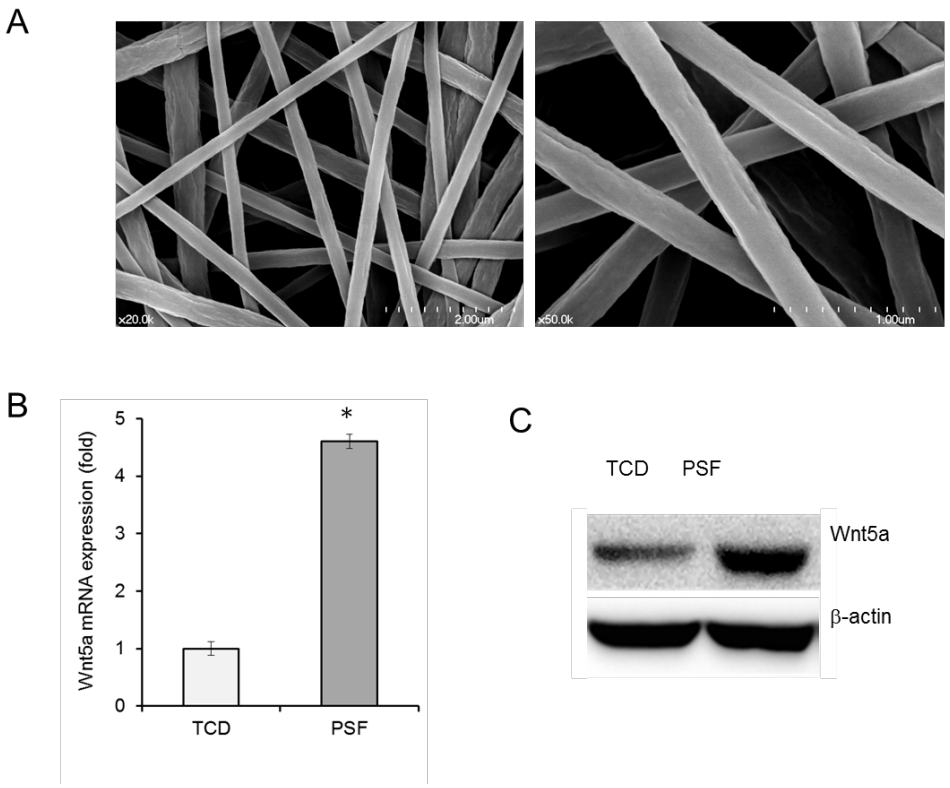

Figure 1. Polystyrene nanofibrous matrix exhibits higher expression of Wnt5a. Scanning Electron micrograph of electrospun nanofibrous matrix at low and high magnification (A). MDPC-23 cells cultured on TCD and PSF in osteogenic media condition and determined the relative mRNA expression (B) and protein expression (C) of Wnt5a determined by quantitative real-time and western blot analysis respectively. Data represent the mean ± SD (*, $p<0.05$).

V.3.2. Nanofiber matrix induces the morphological alterations of MDPC-23 cells

In the present study, we observed that murine dental papilla-derived MDPC-23 cells cultured on nanofibrous matrix increased cells height significantly (Fig. 2A) compared to TCD. Next, we determined the polarization of cells to upper third parts of cells increased significantly in cells on PSF while no changes observed in cells on TCD (Fig. 2B). The morphology of cells on TCD at 4 days of differentiation showed long actin stress fibers formation distributed throughout of cells (Fig. 2C). Next, we found that actin stress fibers formation was reduced in cells cultured for 10 days on TCD (Fig. 2D). The cells on PSF for 4 days of differentiation induced cell processes and reduced actin stress fiber formation determined by confocal laser scanning microscopy (Fig. 2E). Our results showed that the cell processes formation was highly increased in cells cultured for 10 days on nanofibrous matrix (Fig. 2F). Further, we investigated that tight junctions molecules ZO-1, and Claudin-1 expression was significantly increased in cells on PSF compared to cells on TCD and this expression was further increased with time dependent manner. The nestin expression was much higher in cells on PSF (Fig. 2G).

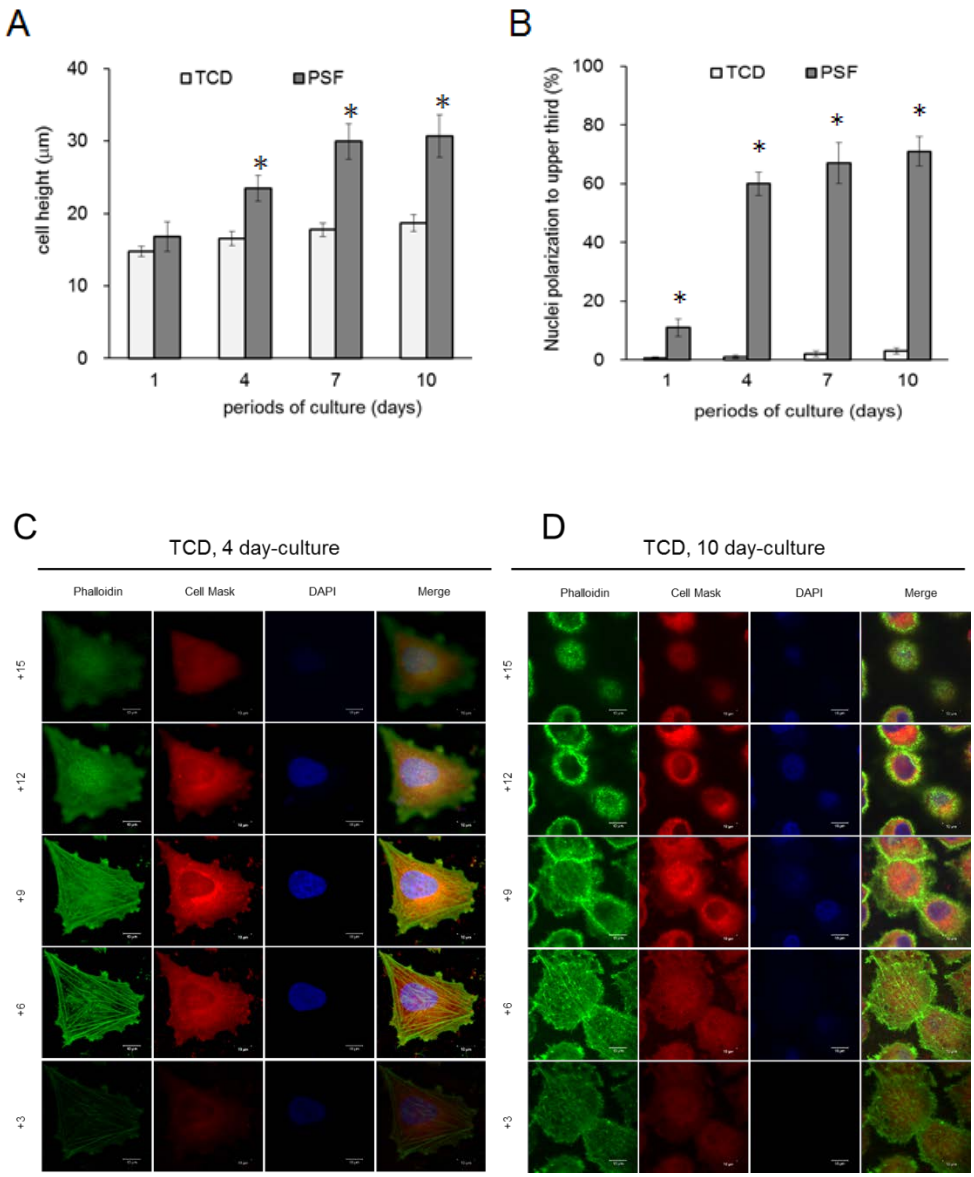
A
TCD
PSF
cell height (µm)
periods of culture (days)
B
Nuclei polarization to upper third (%)
periods of culture (days)
C
TCD, 4 day-culture
D
TCD, 10 day-culture
Phalloidin
Cell Mask
DAPI
Merge
+15
+12
+9
+6
+3

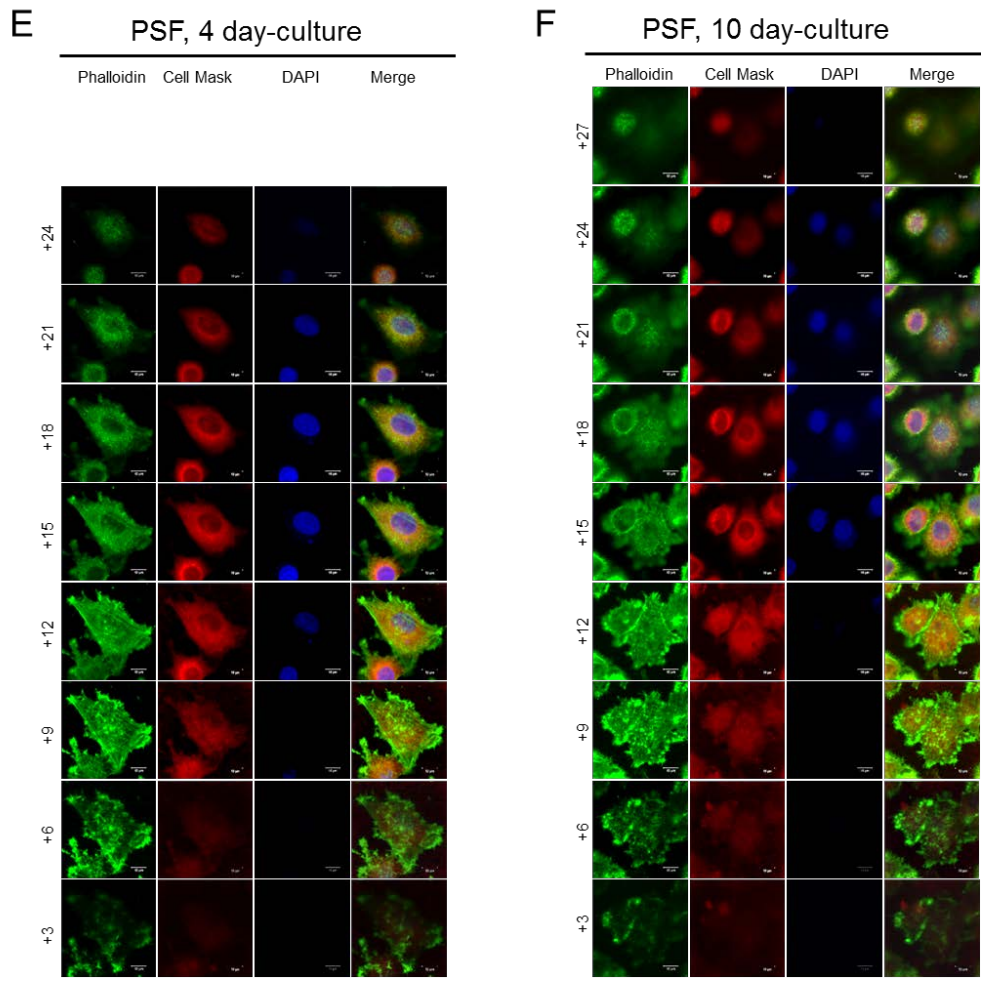
E
PSF, 4 day-culture
Phalloidin
Cell Mask
DAPI
Merge
+24
+21
+18
+15
+12
+9
+6
+3
F
PSF, 10 day-culture
Phalloidin
Cell Mask
DAPI
Merge
+27
+24
+21
+18
+15
+12
+9
+6
+3

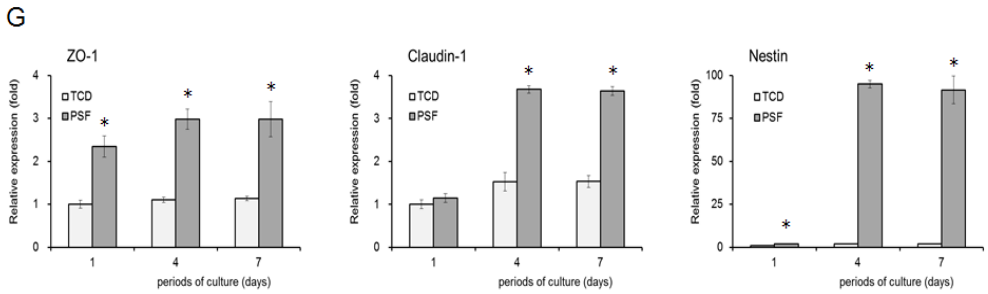
G
ZO-1
Claudin-1
Nestin
TCD
PSF
Relative expression (fold)
periods of culture (days)

Figure 2. Nanofibrous matrix accelerates the morphological alterations of MDPC-23 cells. MDPC-23 cells were cultured on TCD and PSF for up to 10 days in osteogenic media. The height of cells (A), and nuclei polarization (B) was determined from Z-stacked measuring using confocal microscopy. The cells were cultured for 4 days and 10 days on TCD and PSF and fixed with 4% formaldehyde, the samples were then treated with Alexa flour 488-phalloidin and Cell Mask membrane stain, the images were taken from bottom to top of cells with 3µm interval using confocal microscopy to determine the morphology of cell on TCD (C, D) and PSF (E, F). The relative mRNA expression of ZO-1, Claudin-1, and Nestin was determined by quantitative real-time PCR analysis (G). Data represent the mean ± SD (*, $p<0.05$).

V.3.3. Nanofiber-induced Wnt5a alter the morphological changes and induces cell processes formation

In order to determine the effect of Wnt5a on cell morphology, the cells were treated with rWnt5a. The cell height on PSF was increased significantly compared to TCD and was further increased after treatment with rWnt5a compared to non-treated cells on PSF (Fig. 3A). We examined the nuclei polarization to upper third part of cells was increased in cells on PSF and this polarization was further increased with rWnt5a treatment (Fig. 3B). Among the tight junctions molecules the ZO-1 expression was further increased with rWnt5a treatment in cells on PSF and the same effect was shown for Claudin-1 expression (Fig. 3C, D). When we treated the cells with rWnt5a, the cells induced long actin stress fibers formations on TCD determined by confocal microscopy (Fig. 3E). Further we determined that rWnt5a promoted the formation of abundant cell processes formation on nanofibrous matrix which were absent in the cells on TCD (Fig. 3F).

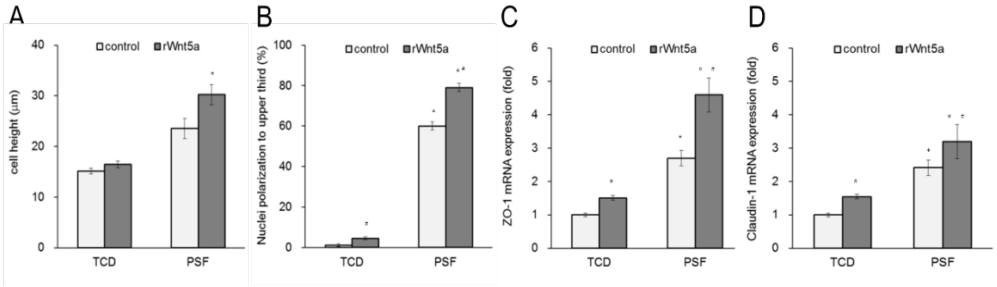
A
control
rWnt5a
cell height (μm)
40
30
20
10
0
TCD
PSF
B
control
rWnt5a
Nuclei polarization to upper third (%)
100
80
60
40
20
0
TCD
PSF
C
control
rWnt5a
ZO-1 mRNA expression (fold)
6
5
4
3
2
1
0
TCD
PSF
D
control
rWnt5a
Claudin-1 mRNA expression (fold)
6
5
4
3
2
1
0
TCD
PSF

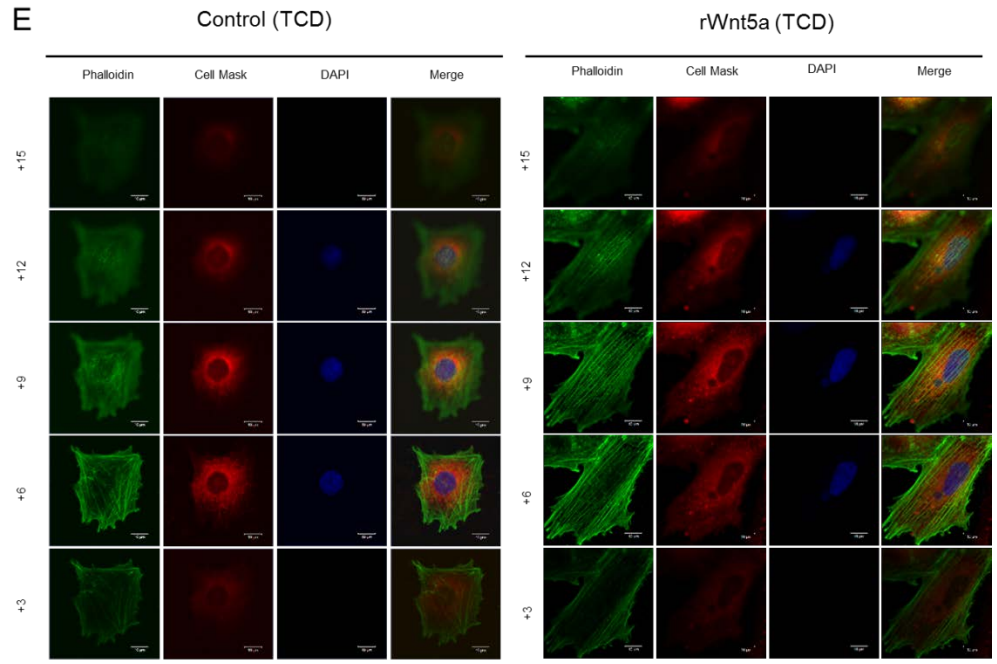
E
Control (TCD)
rWnt5a (TCD)
Phalloidin
Cell Mask
DAPI
Merge
+15
+12
+9
+6
+3

F

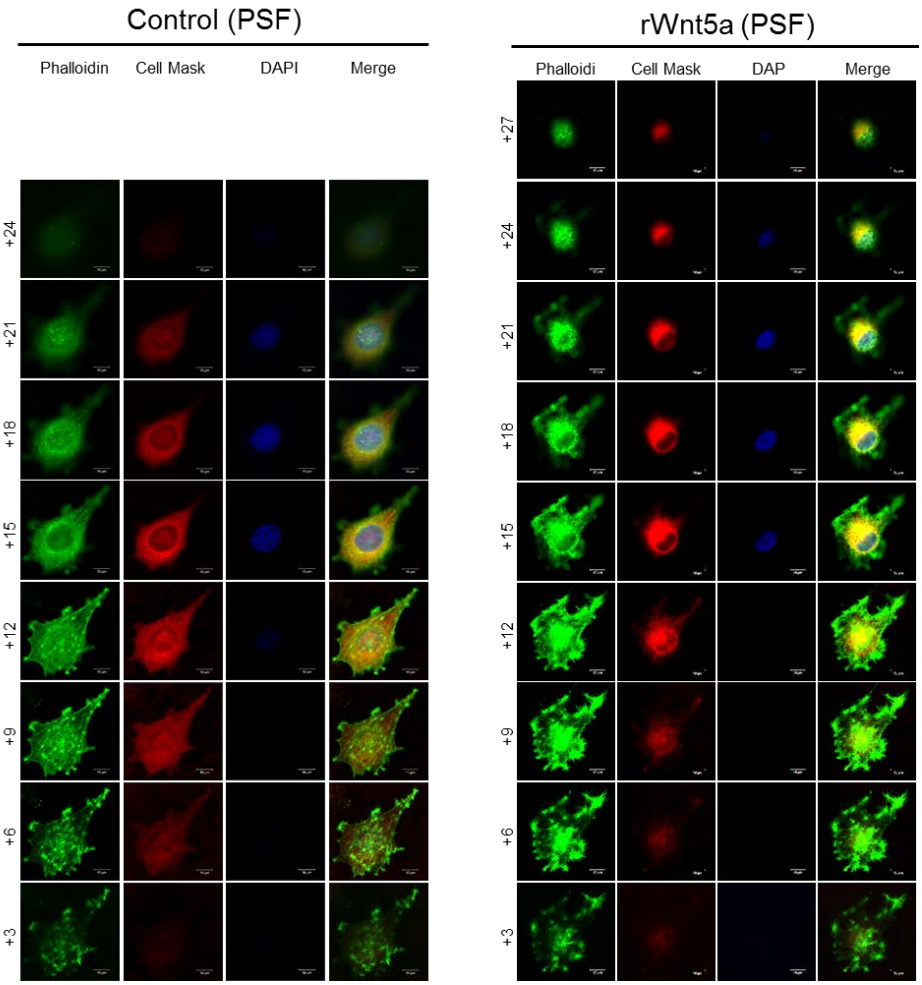
Control (PSF)
Phalloidin
Cell Mask
DAPI
Merge
+24
+21
+18
+15
+12
+9
+6
+3
rWnt5a (PSF)
Phalloidi
Cell Mask
DAP
Merge
+27
+24
+21
+18
+15
+12
+9
+6
+3

Figure 3. Nanofiber-induced Wnt5a accelerates the morphological alterations. The cells were cultured on TCD and PSF. The height of cells and nuclei polarization was determined using confocal microscopy (A, B). The relative mRNA expression of ZO-1 (C), and Claudin-1 (D) was determined by quantitative real-time PCR analysis. The cells were cultured on TCD and PSF and were treated with rhWnt5a, cells were then fixed and stained with phalloidin and cell mask membrane stain, and images were taken from bottom to top of cells with 3µm interval using confocal microscopy to determine the cell morphology on TCD (E) and PSF (F). Data represent the mean ± SD. *Significantly different from the control ($p < 0.05$). #Significantly different from the groups treated with non-treated ($p < 0.05$).

V.3.4. Effect of Wnt5a on morphological alterations of MDPC-23 cells

The above results suggested that Wnt5a is involved in induction of morphological alterations and actin reorganization. We examined the cells height and nuclei polarization after knockdown of Wnt5a using siRNA. As shown in Fig. 4A, knockdown of Wnt5a reduced the cells height significantly. The number of cells showing nuclei polarization to upper third parts was reduced after knockdown of Wnt5a (Fig. 4B). Next, we demonstrated that ZO-1 and claudin-1 molecules expression was reduced after knockdown of Wnt5a (Fig. 4C, D). We further confirmed whether knockdown of Wnt5a affected the cell processes formation and actin rearrangement, the actin stress fibers were absent in cells on TCD after knockdown of Wnt5a (Fig. 4E). The knockdown of Wnt5a leads to complete loss of cell processes formation in cells on PSF determined by confocal microscopy (Fig. 4F). To knockdown of Wnt5a gene, we used siRNA against Wnt5a and determined the knockdown effect by western blot analysis (Fig. 4G).

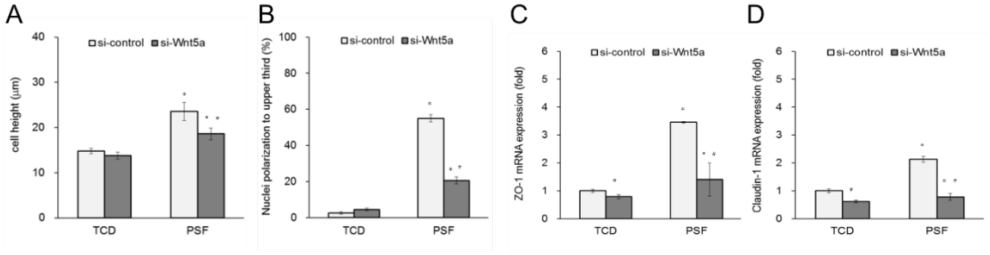
A
B
C
D
si-control
si-Wht5a
cell height (μm)
Nuclei polarization to upper third (%)
ZO-1 mRNA expression (fold)
Claudin-1 mRNA expression (fold)
TCD
PSF

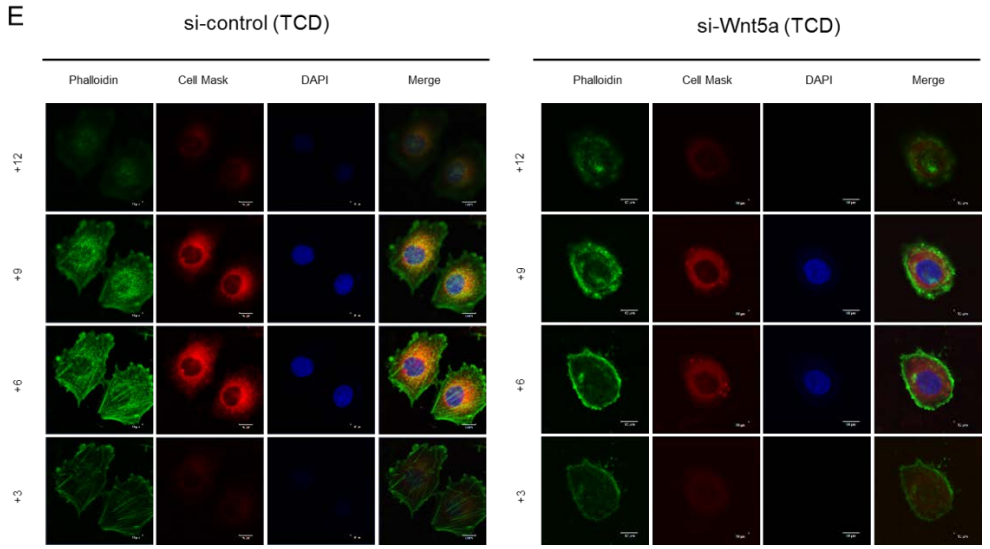
E
si-control (TCD)
si-Wnt5a (TCD)
Phalloidin
Cell Mask
DAPI
Merge
+12
+9
+6
+3

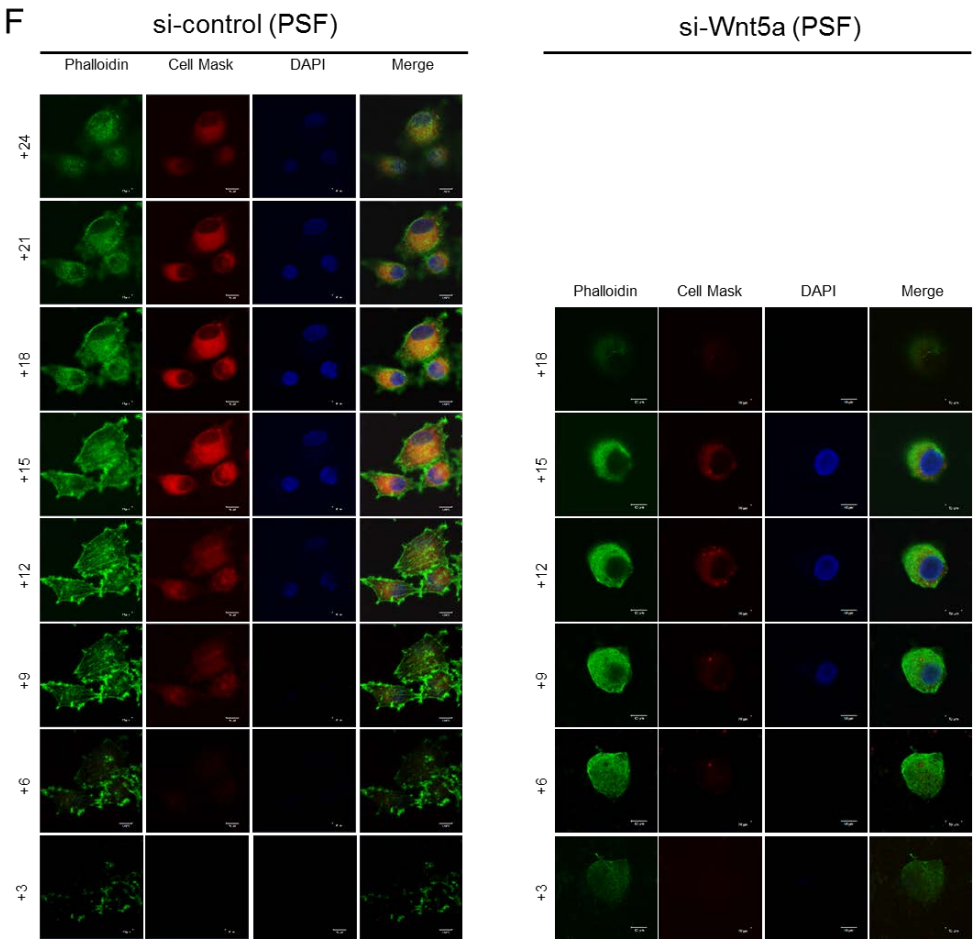
F
si-control (PSF)
si-Wnt5a (PSF)
Phalloidin
Cell Mask
DAPI
Merge
+24
+21
+18
+15
+12
+9
+6
+3

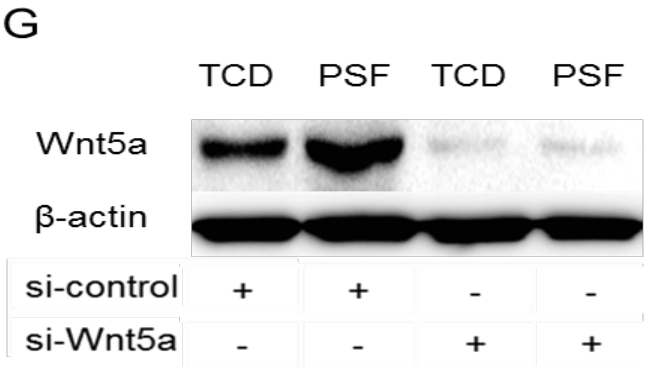
G
TCD
PSF
TCD
PSF
Wnt5a
β-actin
si-control + + - -
si-Wnt5a - - + +

Figure 4. Knockdown of Wnt5a affect the morphological alterations. MDPC-23 cells were cultured on TCD and PSF. After knockdown of Wnt5a by siRNA, the cells height and nuclei polarization of cells were measured using confocal microscopy (A, B). The relative mRNA expression of ZO-1 (C), and Claudin-1 (D) was determined by quantitative real-time PCR. The cells were cultured on TCD and PSF and were transfected with siRNA against Wnt5a, then the cells were fixed and treated with phalloidin, cell mask membrane stain, and DAPI, the images were taken from bottom to top of cells with 3μm interval by confocal microscopy to determine the morphology of cells on TCD (E) and PSF (F). To determine the effect of siRNA against Wnt5a, the cells were cultured on TCD and PSF and were transfected with siRNA against Wnt5a, and determined the Wnt5a expression by western blot analysis (G). Data represent the mean ± SD. *Significantly different from the control ($p < 0.05$). $^{\#}$Significantly different from the groups transfected with non-transfected ($p < 0.05$).

V.3.5. Ror2 mediates the Wnt5a-induced morphological alteration of MDPC-23 cells

Ror2, an orphan tyrosine kinase is known to mediate Wnt5a-initiated non-canonical signaling pathway [Oishi et al., 2003]. To verify whether Ror2 is involved in Wnt5a-induced morphological alterations and cell processes formation, we determined that the cells height was reduced after knockdown of Ror2 (Fig. 5A). The number of cells exhibited nuclei at upper third part of cells was reduced after knockdown of Ror2 (Fig. 5B). As shown in Fig. 5C and D, the knockdown of Ror2 by siRNA abrogated the tight junction molecules ZO-1 and claudin-1 expressions respectively. Further, we examined whether Ror2 is directly involved in Wnt5a-induced cellular morphology. The cells treated with rWnt5a in the presence of Ror2 knockdown exhibited similar effect of cells height as of si-Ror2 alone (Fig. 5E). The same effect was examined for nuclei polarization as shown in Fig. 5F. The cells exhibited similar effect of ZO-1 and claudin-1 mRNA expressions after knockdown of Ror2 with or without rWnt5a treatment (Fig. 5G, H). Next we investigated the actin stress fiber formation in cells on TCD was absent in Ror2 knockdown samples without or with rWnt5a treatment (Fig. 5I). Further, we confirmed whether Ror2 is involved in Wnt5a-induced cell processes formation in cells on PSF, we demonstrated that cell processes formation was completely absent in Ror2 knockdown without or with rWnt5a treatment (Fig. 5J). To knockdown of Ror2 gene, we used siRNA against Ror2 and determined the knockdown effect by western blot analysis (Fig. 5K). These results suggested that Wnt5a is involved in morphological alterations that were confirmed by inhibition of functionling noncanonical Wnt signaling pathway.

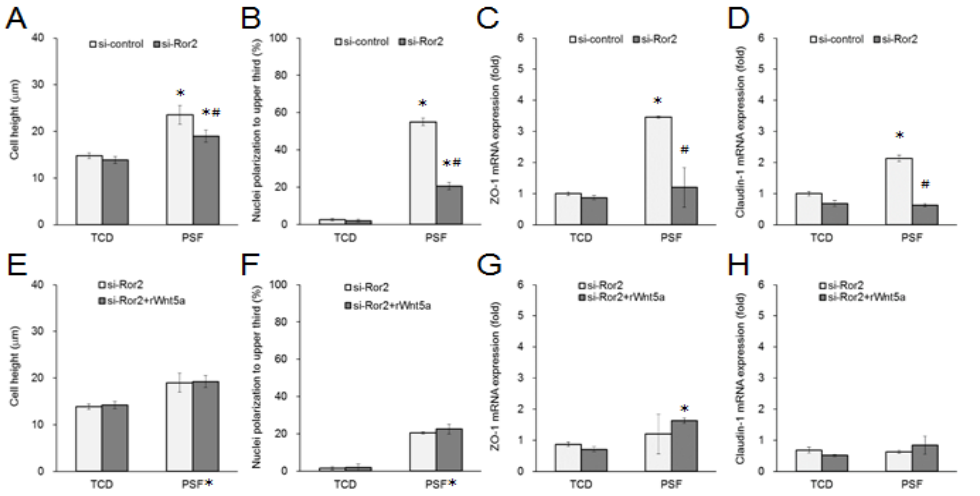
A
si-control
si-Ror2
Cell height (μm)
TCD
PSF
B
Nuclei polarization to upper third (%)
C
ZO-1 mRNA expression (fold)
D
Claudin-1 mRNA expression (fold)
E
si-Ror2+rWnt5a
F
G
H

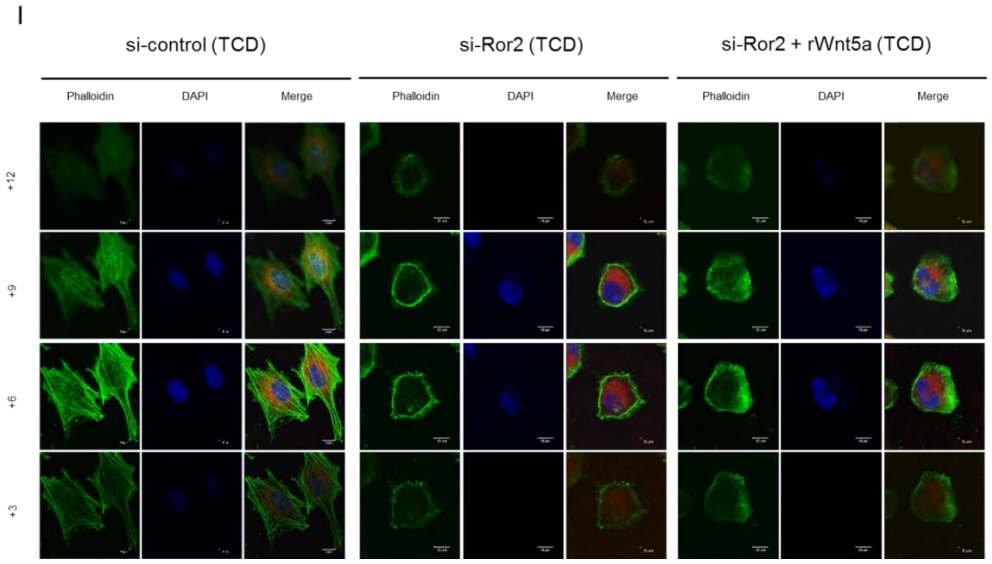
I
si-control (TCD)
si-Ror2 (TCD)
si-Ror2 + rWnt5a (TCD)
Phalloidin
DAPI
Merge
+12
+9
+6
+3

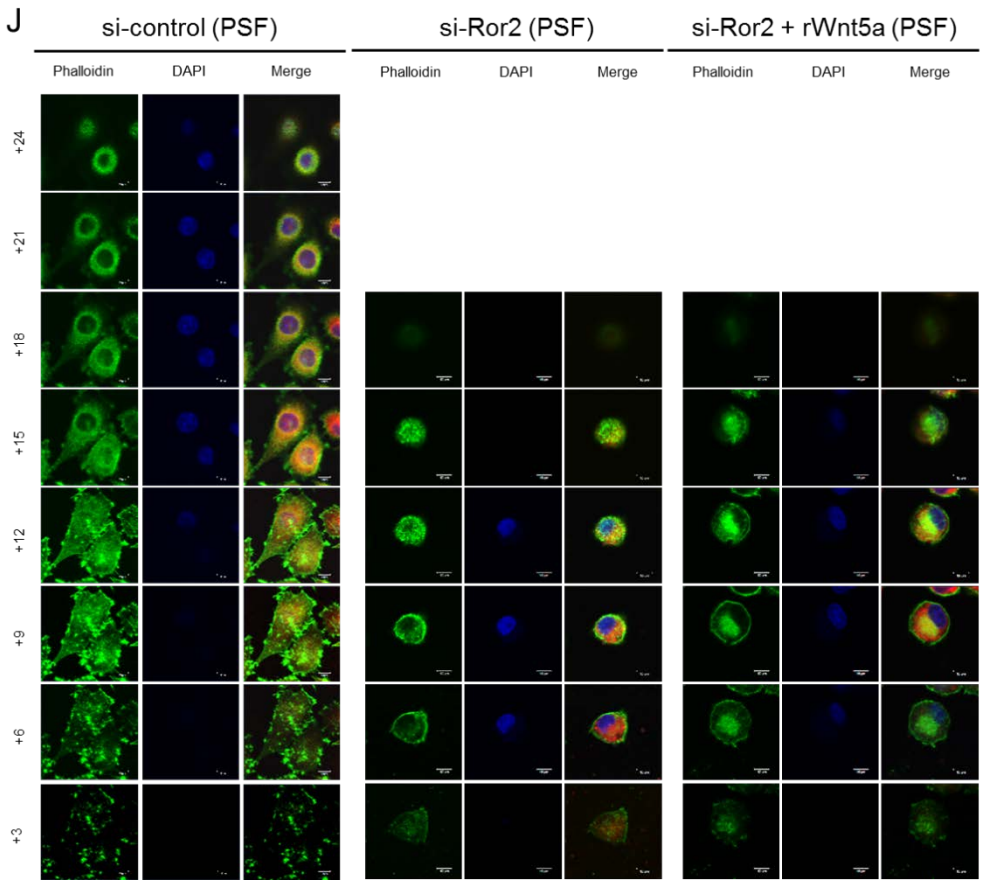
J
si-control (PSF)
si-Ror2 (PSF)
si-Ror2 + rWnt5a (PSF)
Phalloidin
DAPI
Merge
+24
+21
+18
+15
+12
+9
+6
+3

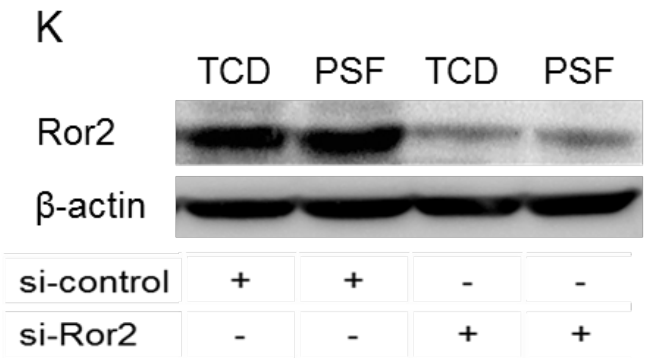
K
TCD
PSF
TCD
PSF
Ror2
β-actin
si-control
+
+
-
-
si-Ror2
-
-
+
+

Figure 5. Knockdown of Ror2 affect the cellular morphology. MDPC-23 cells were transfected with siRNA against Ror2 and allowed to culture with or without rWnt5a treatment. The height of cells (A, E), and nuclei polarization (B, F) of cells was determined by confocal microscopy. The relative mRNA expression of ZO-1 (C, G), and Claudin-1 (D, H) was determined by quantitative real-time PCR. After knockdown of Ror2 by siRNA, the cells were fixed and treated with phalloidin, cell mask membrane stain, and DAPI, the images of the cells were taken from bottom to top of cells with 3μm interval using confocal microscopy to determine the morphology of cells on TCD (I) and PSF (J). To determine the effect of siRNA against Ror2, the cells were cultured on TCD and PSF and were transfected with siRNA against Ror2, and determined the Ror2 expression by western blot analysis (K). Data represent the mean ± SD. *Significantly different from the control ($p < 0.05$). $^{\#}$Significantly different from the groups transfected with non-transfected ($p < 0.05$).

V.3.6. Knockdown of RhoA induces the morphological alterations and cell processes formation in cells on PSF

We next determined the effect of small GTPase RhoA. The cells height was increased after knockdown of RhoA by siRNA in cells on nanofibrous matrix (Fig. 6A). The number of cells exhibited nuclei at upper third part of cells was increased after knockdown of RhoA (Fig. 6B). The height of cells was further increased with rWnt5a treatment in RhoA knockdown samples (Fig. 6C); the same effect was observed for nuclei polarization as shown in Fig. 6D. It has been reported that RhoA activity is important for stress fiber formation [Katoh et al., 2007]. In order to determine the effect of RhoA we examined that actin stress fiber formation was completely reduced in cells on TCD after knockdown of RhoA, and treatment of rWnt5a did not alter the actin stress fiber formation in RhoA knockdown samples on TCD (Fig. 6E). Further, we examined whether RhoA knockdown had effect on cell processes formation in cells on PSF. The cells on PSF increased the cell processes formation after knockdown of RhoA and further increased with rWnt5a treatment (Fig. 6F).

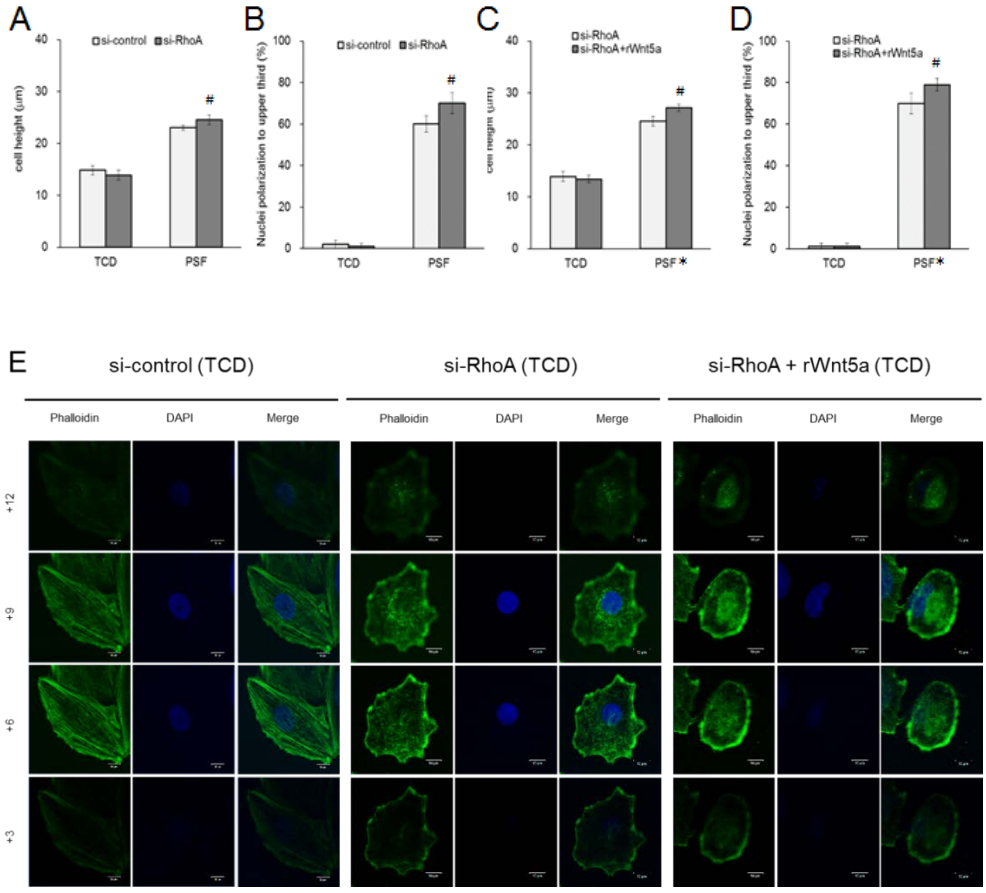
A
si-control
si-RhoA
cell height (μm)
TCD
PSF
B
Nuclei polarization to upper third (%)
C
si-RhoA
si-RhoA+rWnt5a
D
E
si-control (TCD)
si-RhoA (TCD)
si-RhoA + rWnt5a (TCD)
Phalloidin
DAPI
Merge
+12
+9
+6
+3

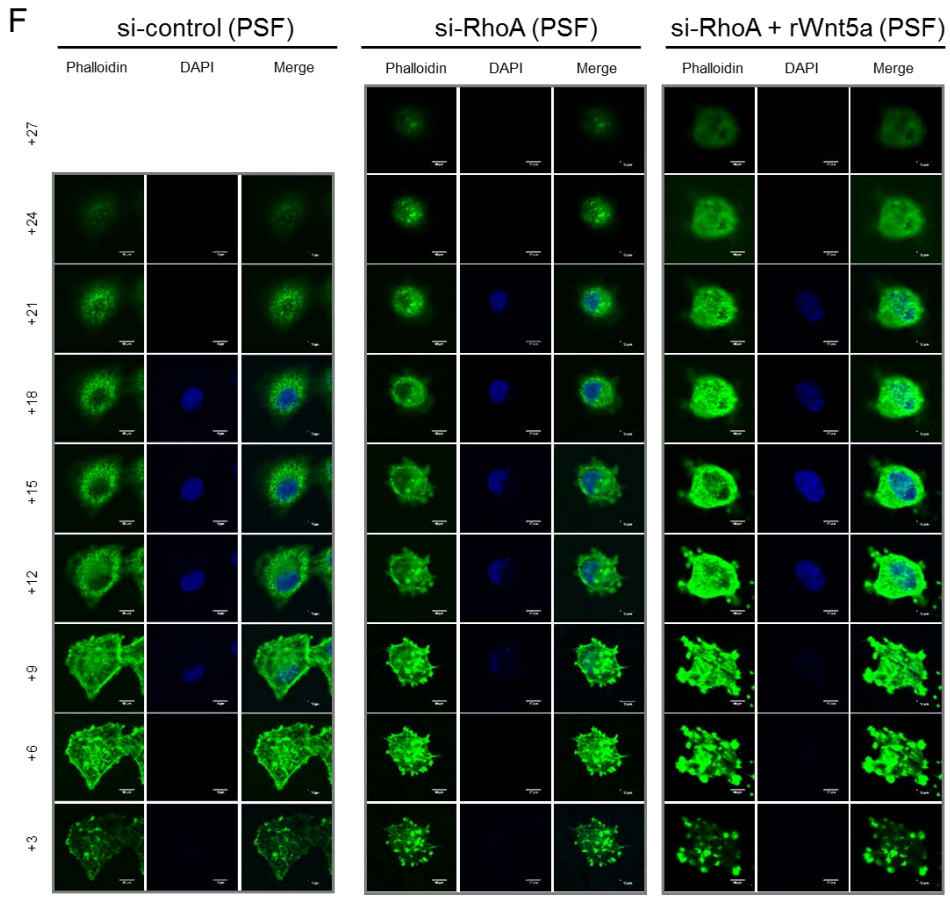

Figure 6. Knockdown of RhoA alter the morphological changes of MDPC-23 cells. The cells were transfected with siRNA against RhoA and allowed to differentiate further with or without rWnt5a treatment. The height of cells (A, C), and nuclei polarization (B, D) of cells was determined using confocal microscopy. The cells were cultured on TCD and PSF and were transfected with siRNA against RhoA with or without rWnt5a treatment, cells were fixed and treated with phalloidin, cell mask membrane stain, and DAPI, the images of the cells were taken from bottom to top of cells with 3µm interval by confocal microscopy of the cells on TCD (E) and PSF (F). Data represent the mean ± SD, (*, and # represent $p<0.05$).

V.3.7. Effect of CDC42 on morphological alterations and cell processes formation

Another member of small GTPases, CDC42 has important role in organization of actin cytoskeleton. We examined the involvement of CDC42 in Wnt5a-induced morphological alteration and cell processes formation. The cells height was decreased after knockdown of CDC42 by siRNA in cells on nanofibrous matrix (Fig. 7A). Similar effect was observed for nuclei polarization as shown in Fig. 7B. Further we examined whether rWnt5a treatment affect the cells height and nuclei polarization in CDC42 knockdown samples. There was no change observed in cells height and nuclei polarization without or with rWnt5a treatment in CDC42 knockdown samples (Fig. 7C, D). The long actin stress fiber formation was increased in cells on TCD after CDC42 knockdown and was further increased with rWnt5a treatment (Fig. 7E). Next we demonstrated that cell processes formation was completely absent in cells on PSF after knockdown of CDC42 by siRNA, and treatment of rWnt5a did not rescued this effect of CDC42 knockdown in cells on PSF (Fig. 7F).

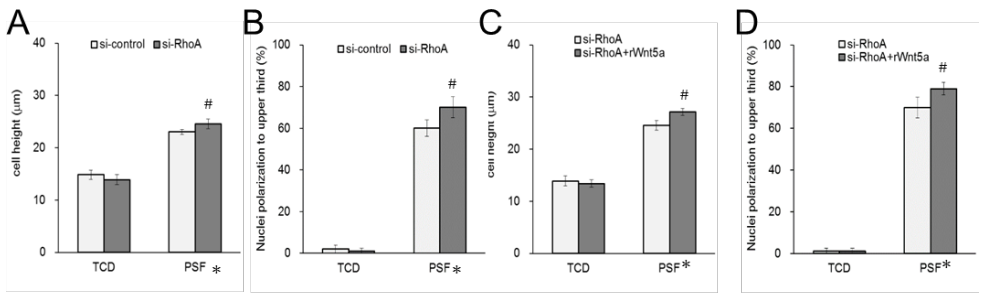
A
cell height (μm)
si-control
si-RhoA
TCD
PSF
B
Nuclei polarization to upper third (%)
C
ceii neigni (μm)
si-RhoA+rWnt5a
D

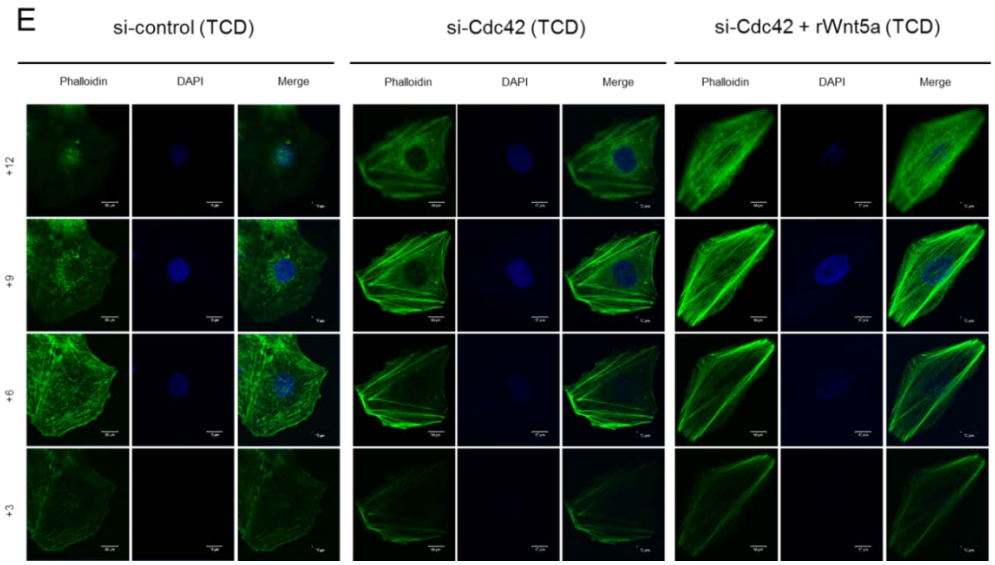
E
si-control (TCD)
si-Cdc42 (TCD)
si-Cdc42 + rWnt5a (TCD)
Phalloidin
DAPI
Merge
+12
+9
+6
+3

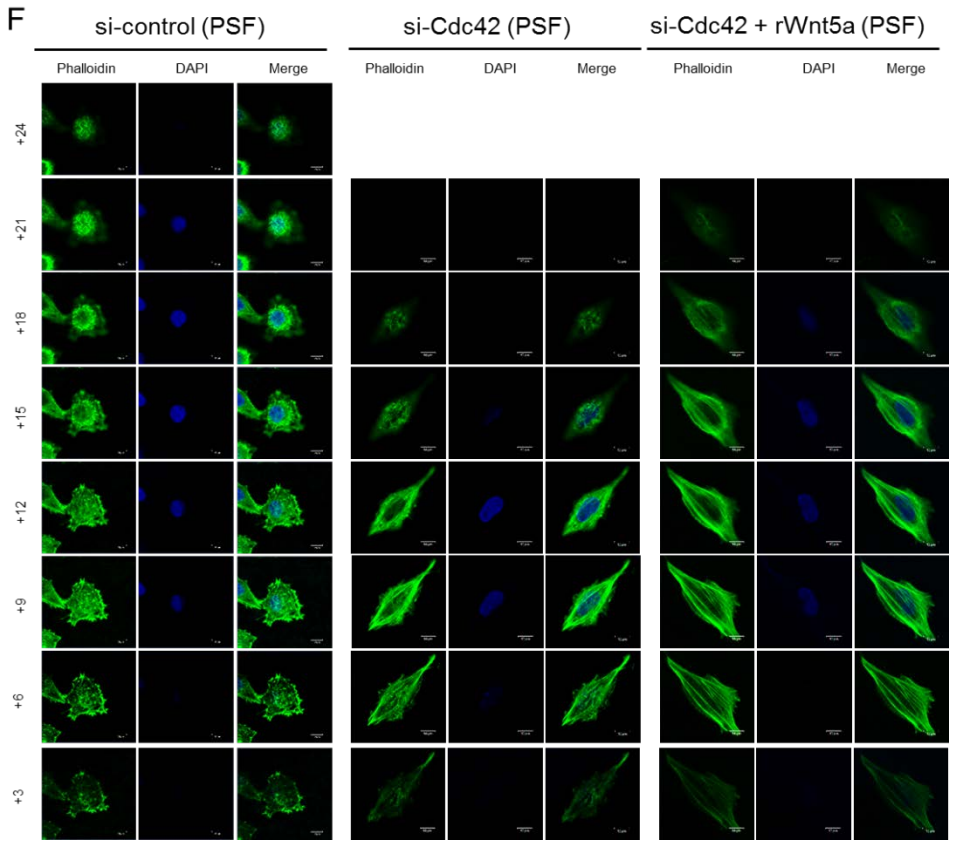

Figure 7. PSF-induced morphological alteration affected by CDC42 knockdown. MDPC-23 cells were cultured on TCD and PSF and were transfected with siRNA against CDC42 and the cells were allowed to differentiate further with or without rWnt5a treatment. The height of cells (A, C), and nuclei polarization (B, D) of cells were measured using confocal microscopy. After knockdown of CDC42 by siRNA with or without rWnt5a treatment, the cells were fixed and stained with phalloidin, cell mask membrane stain, and DAPI, the images of the cells were taken from bottom to the top of cells with 3 μm interval using confocal microscopy to determine the morphology of cells on TCD (E) and PSF (F). Data represent the mean ± SD. (*, and #, $p<0.05$).

V.3.8. Nanofiber-induced Wnt5a results in activation of CDC42

The Rho GTPases have been shown to be important regulators of the actin cytoskeleton system [Takai et al., 2001]. The activity of small GTPases RhoA, and CDC42 were determined using pull down assay. As shown in Fig. 8 the cells on TCD increased RhoA activation when treated with rWnt5a, in contrast no changes observed in RhoA activation in cells on PSF. The activity of CDC42 was increased in cells on PSF compared to TCD and was further increased with rWnt5a treatment. Knockdown of RhoA increased the activity of CDC42 in cells on PSF. In contrary, the CDC42 knockdown increased the activity of RhoA in cells on TCD (Fig. 8).

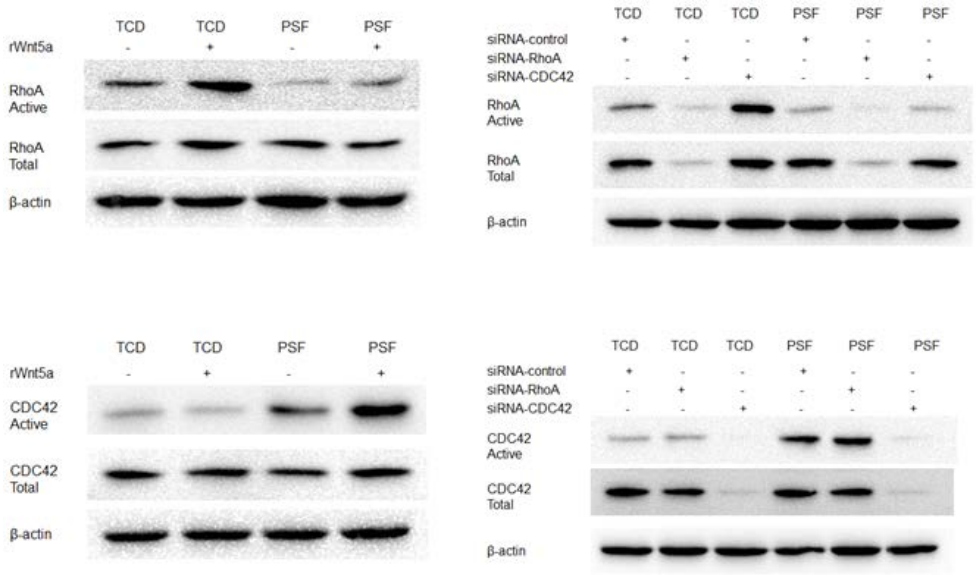

Figure 8. The small GTPases are activated differentially in cells on TCD and PSF during odontoblast differentiation. MDPC-23 cells were cultured on TCD and PSF. The cells were treated either with rWnt5a or transfected with siRNA against RhoA or CDC42. The total and active RhoA as well as CDC42 were determined by western blot analysis after pull down assay.

V.4. Discussion

Here we provided evidence for the first time that the nanofibrous engineered matrix induces morphological alterations of odontoblast through noncanonical Wnt signaling pathway specifically Wnt5a. In our previous study we found that the nanofibrous engineered matrix induces odontoblast differentiation and specifically DSPP expression, further it acquired to determine the morphological alterations when cultured on the nanofibrous matrix.

Nanofibrous matrix can influence the cellular behavior such as, cell adhesion, migration, alignment, proliferation, cell morphology, and cytoskeleton organization. By understanding the aspect in which cells-matrix interaction affect cellular behavior and influence the complex cellular processes, it may be possible to control fabrication of substrates with unique properties. Recent development in nano and microfabrication techniques are being widely used to construct substrates of differing topographies that show its fibrillar structure and mimic the natural extracellular matrix (ECM) providing essential support for survival, cellular organization, and cellular function. In this regard, electrospinning technique is being used to create nanometer scale fibrous matrix [Li et al., 2002; Kunzler et al., 2007; Bettinger et al., 2009; Wang et al., 2010; DuFort et al., 2011]. The electrospun nanofibers hold high potential for cellular differentiation and tissue regeneration. In the case of bone biology, an effort has been made by the nanofiber to induce osteoblast differentiation and tissue regeneration. It has been reported previously that, the nanofibrous scaffolding promotes osteoblast and odontoblast differentiation and biomineralization [Woo et al., 2007; Wang et al., 2010]. It was unclear whether cells exhibit their specific morphological polarization

during differentiation when cultured on the nanofibrous matrix, and determined what mechanism is involved in this polarization. In our study, we fabricated the nanofibrous matrix by electrospinning and cultured dental pulp cells on it, and discovered the cellular polarization of dental pulp cells.

Odontoblast is similar to osteoblast in similar ways to secrete extracellular matrix protein. However, the relative proportion of these ECM proteins may differ dramatically among them during differentiation and tissue formation. The cells when differentiating into mature odontoblasts acquire a particular morphology with a long cell process and a cell body. Although the transduction mechanisms are highly complex and not fully understood. The odontoblast exhibited extended structure and showed a cytological polarization evidenced by the position of the nucleus that existed opposite to the secretory pole during differentiation and tooth engineering [Hilkens et al., 2013; Kokten et al., 2014]. It has been reported that polarized odontoblast cells are elongated, and their nucleus takes up an eccentric position [Lesot et al., 2014]. Our result demonstrated that the cells height increased significantly when cultured on PSF and was further increased with a time course. The number of cells exhibited nuclei at upper third part of cells increased significantly on PSF compared to control. To investigate whether PSF induces the morphological alterations of odontoblast, MDPC-23 were cultured for up to 7 days and then subjected to analyze the morphology using confocal microscopy. The cells displayed a columnar; elongated appearance has abundant cellular processes. With increasing the culture time, cells on PSF exhibited more columnar and more enriched fillopodial like cell processes structures.

To examine whether the characteristic cell processes of odontoblasts were

abundant after rWnt5a treatment, morphological analysis was performed. The cells after treatment with rWnt5a appeared strong cell processes formation on PSF, this kind of morphology were absent in the cells on TCD, while the cells on TCD increased stress fiber formation. Our study indicated the disappearance of cell processes structure after knockdown of Wnt5a by siRNA. Ror2 acts as an alternative receptor or as a coreceptor for Wnt5a to activate non-canonical Wnt signaling [Oishi et al., 2003; Mikels and Nusse, 2006]. After knockdown of Ror2, the cells on PSF showed similar disappearance of cell processes as of Wnt5a knockdown.

Odontoblasts express nestin that is considered as the intermediate filaments constituting the cytoskeleton. During tooth development, nestin is continuously expressed and disappears after development completed. In the mature tooth after cavity formation or with caries, nestin is re-upregulated in odontoblasts [Terling et al., 1995; About et al., 2000;]. Nestin is express in the odontoblast processes of fully differentiated cells [Fujita et al., 2006]. Thus, nestin is known to be related to odontoblast differentiation. Our result is consistent with the previous findings, demonstrated that the cells on PSF significantly increased nestin expression during odontoblast differentiation, and is further increased with time dependent manner compared to control group.

Odontoblasts are attached with gap junctions and junctional complexes. Tight junctions have been documented to play an important role in the polarization of odontoblasts. In developing teeth, the tight junctions contain abundant amount of ZO-1 (zona occludens-1) between differentiating odontoblast, while the transmembrane proteins such as occludin and claudins have characteristics to sealing properties of tight junctions [Joao and Arana.,

2003; Hoshino et al., 2008]. In another study, there is a high expression of ZO-1, and weaker expression of claudin-1 in mature human odontoblasts has been observed [Tjaderhane et al., 2013]. In our study, the expression of ZO-1 and claudin-1 increased significantly in cells on PSF compared to TCD.

Cell shape, structure, and polarity undergoes by actin cytoskeleton reorganization. Filopodia, lamellipodia, stress fibers, and focal adhesions constitute the structural framework of the actin cytoskeleton, which is mostly controlled by Rho GTPases [Murali and Rajalingam, 2014]. The Rho GTPase is a family of small signaling G proteins that regulates distinct steps during cytoskeletal dynamics and contributes in various cellular processes, including adhesion, cytokinesis, migration, proliferation, secretion, transformation, and cell polarity [Bar-Sagi and Hall, 2000; Schmitz et al., 2000; Etienne and Hall., 2002]. Rho GTPases are thus well known for their important role in the regulation of the actin cytoskeleton. The small GTPases have an important role in actin cytoskeleton and are activated by Wnt5a. CDC42 is a component of small GTPase family and is known to stimulate filopodia formation and in maintaining cell polarity. It has been observed that the CDC42 induces the formation of filopodia structure, and the RhoA induce stress fiber formation [Nobes et al., 1995; Bar and Hall, 2000; Etienne and Hall, 2002]. The cells on PSF increased cell processes formation after knockdown of RhoA, while the cells on TCD decreased stress fiber formation. However, after knockdown of CDC42 the cell processes formations on PSF were abrogated while increased the stress fiber formation. Further, we confirmed the activation of CDC42 and RhoA by pull down assay analysis, and determined that PSF-induced Wnt5a regulated activation of CDC42 while the cells on TCD increased the RhoA activation, and these

activations were further increased with rWnt5a treatment.

The phenotype of the odontoblasts may be defined by the cell morphology, the matrix secretion, and the pattern of its different genes expression. All these processes could be relatively independent from each other, such as IGF could only cause the cytological differentiation but not the functional differentiation while the BMPs could induce both the cytological as well as functional differentiation [Begue-Kirn et al., 1994]. It is for the first time we demonstrated in our study that PSF-induced Wnt5a regulates CDC42 activation followed by morphological alterations and specifically increases cell processes formation while RhoA activation increases stress fiber formation in cells on TCD.

V.5. Conclusion

In conclusion, our study demonstrated that nanofibrous engineered matrix induces the morphological alterations of MDPC-23 cells. We found that this morphological alteration is under the control of Wnt5a through small GTPases activation that we confirm by using inducers and inhibitors of noncanonical Wnt signaling pathway and knockdown of small GTPases such as RhoA and CDC42. The cells on PSF induce morphological alterations and specifically cell processes formation through CDC42, while the cells on TCD induces stress fiber formation when treated with rWnt5a or with knockdown of CDC42. Overall, our results demonstrate that nanofibrous engineered matrix induces morphological alterations of MDPC-23 cells through Wnt5a.

VI. Conclusion

Nano-biomaterial is a novel concept that mimics the natural ECM microenvironment and alters the interactive cellular activity. Electrospinning is one of the most up growing technology used to fabricate the nanofibrous materials that provide the nanometer scale fibrous structure to the surrounding cells. Here, we investigated the new developments that nanofibrous engineered matrix affect the cellular response to induce growth factors and transduce molecular events intracellularly that leads to odontoblast differentiation and has potential applications in biological research and tissue regeneration. The human dental pulp-derived (hDPSCs), bone marrow-derived (hBMSCs), and adipose-derived mesenchymal stem cells (hADSCs) were cultured on electrospun nanofibrous matrix, among them hDPSCs induces Wnt and BMP signaling molecules expression higher in cells cultured on nanofibrous matrix (PSF) compared to tissue culture dishes (TCD) during differentiation, as both substrates contain of same material. The hDPSCs induces DSPP expression higher on PSF while hBMSCs and hADSCs induce BSP and OCN expression higher on PSF compared to TCD. Further, we investigated that rhWnt3a treatment induces DSPP expression in hDPSCs on PSF. To determine the effect of nanofibrous engineered matrix in odontoblast differentiation and investigated the molecular mechanisms, we cultured MDPC-23 cells on TCd and PSF. An important difference observed in the extent of Alizarin Red Staining (ARS) analyzed qualitatively and quantitatively showed higher calcium concentration on PSF, indicating that odontoblast differentiation of the seeded MDPC-23 increased on PSF. DSPP is a dominant member of the non-collagenous matrix protein of dentin and is important for proper dentin

formation and biomineralization. . In our study, DSPP mRNA expression in MDPC-23 was increased higher on PSF than TCD. However, Wnt signaling pathway is a potent factor in tooth development and odontoblast differentiation. DSPP might be a direct target of canonical Wnt signaling pathway when cells seeded on nanofibrous engineered matrix. Based on these observations we examined genes expression of Wnt signaling molecules during odontoblast differentiation on PS nanofibrous matrix and TCD. In our study, we investigated that induction or inhibition of canonical Wnt signaling pathway by using inducers (rhWnt3a, LiCl) or inhibitors (DKK1, anti-Wnt3a antibody, siRNA against Wnt3a or β-catenin) alter DSPP gene expression in cells on PSF. Further, the in-vivo study shows that Wnt3a and DSP express higher in cells on PSF compared to TCD.

Nanofibrous engineered matrix can influence the cellular behavior such as, cell adhesion, migration, alignment, proliferation, cell morphology, and cytoskeleton organization. By understanding the aspect in which nanofibrous engineered matrix can affect morphological alterations during odontoblast differentiations and what mechanisms are involved was not well known. Our result demonstrated that the MDPC-23 cells height increases significantly and the number of cells exhibited nuclei at upper third part of cells increased significantly on PSF compared to control, as it has been reported that polarized odontoblast cells are elongated, and their nucleus takes up an eccentric position. MDPC-23 were cultured on TCD and PSF and then subjected to analyze the morphology of cells using confocal microscopy. The cells displayed a columnar; elongated appearance and have abundant cell processes formation on PSF. With increasing the culture time, cells on PSF exhibited more columnar and more enriched cell processes formation. In our

study, the nanofibrous engineered matrix induces Wnt5a expression during odontoblast differentiation. To examine whether the characteristics of odontoblasts were abundant after rWnt5a treatment, morphological analysis of cells was performed, as Wnt5a has an important role in cellular polarization. The cells after treatment with rWnt5a increased cell height and cell processes formation on PSF, this kind of morphology were absent in the cells on TCD, while the cells on TCD increased stress fiber formation. Our study indicated the disappearance of cell processes structure after knockdown of either Wnt5a or Ror2 (receptor of Wnt5a) by siRNA. Odontoblasts cells express nestin that is considered as the intermediate filaments and constituting the cytoskeleton. Nestin is express in the odontoblast processes of fully differentiated cells and is known to be related to odontoblast differentiation. Our result demonstrated that the cells on PSF significantly increased nestin expression during odontoblast differentiation and further increase with rWnt5a treatment of reduce its expression either with Wnt5a knockdown or Ror2 knockdown. Tight junctions have been documented to play an important role in the polarization of odontoblasts. In developing teeth, the tight junctions contain abundant amount of ZO-1 (zona occludens-1) between differentiating odontoblast, while the transmembrane proteins such as claudins have characteristic to sealing properties of tight junctions. In our study, the ZO-1 and claudin-1 genes expression increases significantly in cells on PSF compared to TCD and these expressions are further increased with rWnt5a treatment. Rho GTPase is a family of small signaling G proteins that regulates distinct events during cytoskeletal dynamics and contributes in various cellular processes, including adhesion, migration, proliferation, and cell polarity. Rho GTPases are thus well known for their essential role in the regulation of the actin cytoskeleton and are

activated by Wnt5a. Here, in our study we demonstrated that PSF-induced Wnt5a regulates CDC42 activation followed by morphological alterations and specifically increases cell processes formation while the cells on TCD activates RhoA that increases stress fiber formation, and these activities are further increased with rWnt5a treatment.

Overall, our results demonstrated that nanofibrous engineered matrix induces odontoblast differentiation through Wnt signaling pathways.

VII. References

About I, Laurent-Maquin D, Lendahl U, et al. Nestin expression in embryonic and adult human teeth under normal and pathological conditions. Am J Pathol 2000; 157:287–95.

Angers S & Moon RT. Proximal events in Wnt signal transduction. Nature Rev Mol Cell Biol 2009; 10:468–77.

Anselme K, Davidson P, Popa AM, Giazzon M, Liley M, Ploux L. The interaction of cells and bacteria with surfaces structured at the nanometre scale. Acta Biomater 2010; 6:3824-46.

Arinzeh, T. L., T. Tran, J. Mcalary, and G. Daculsi. A comparative study of biphasic calcium phosphate ceramics for human mesenchymal stem-cell-induced bone formation. Biomaterials 2005; 26:3631–8.

Atala A. Tissue engineering and regenerative medicine: concepts for clinical application. Rejuvenation Res 2004; 7:15-31.

Bao C, Chen W, Weir MD, Thein-Han W, Xu HH. Effects of electrospun submicron fibers in calcium phosphate cement scaffold on mechanical properties and osteogenic differentiation of umbilical cord stem cells. Acta Biomater 2011; 7:4037–44.

Bar-Sagi D, Hall A. Ras and Rho GTPases: a family reunion. Cell 2000; 103:227-38.

Batouli S, Miura M, Brahim J, Tsutsui TW, Fisher LW, Gronthos S, Robey PG, Shi S. Comparison of stem-cell-mediated osteogenesis and dentinogenesis. J Dent Res 2003; 82:976-81.

Begue-Kirn C, Krebsbach PH, Bartlett JD, Butler WT. Dentin sialoprotein, dentin phosphoprotein, enamelysin and ameloblastin : tooth-specific molecules that are distinctively expressed during murine dental differentiation. Eur J Oral Sci 1998; 106:963–70.

Bègue-Kirn C, Smith AJ, Loriot M, Kupferle C, Ruch JV, Lesot H. Comparative analysis of TGF beta s, BMPs, IGF1, msxs, fibronectin, osteonectin and bone sialoprotein gene expression during normal and in vitro-induced odontoblast differentiation. Int J Dev Biol 1994; 38:405-20.

Bettinger CJ, Langer R, Borenstein JT. Engineering substrate topography at the micro- and nanoscale to control cell function. Angew Chem Int Ed Engl 2009; 48:5406-15.

Biggs MJ, Richards RG, Gadegaard N, McMurray RJ, Affrossman S, Wilkinson CD, et al. Interactions with nanoscale topography: adhesion quantification and signal transduction in cells of osteogenic and multipotent lineage. J Biomed Mater Res A 2009; 91:195-208.

Bluteau G, Luder HU, De Bari C, Mitsiadis TA. Stem cells for tooth engineering. Eur Cell Mater 2008; 16:1-9.

Butler WT, Bhown M, Dimuzio MT, Linde A. Nonocollagenous proteins of dentin. Isolation and partial characterization of rat dentin proteins and proteoglycans using a three-step preparative method. Coll Relat Res 1981; 1:187–199.

Buttiglieri S, Pasqui D, Migliori M, Johnstone H, Affrossman S, Sereni L, Wratten ML, Barbucci R, Tetta C, Camussi G. Endothelization and adherence of leucocytes to nanostructured surfaces. Biomaterials 2003;

24:2731-8.

Buttler WT, Brunn JC, Qin C. Dentin extracellular matrix (ECM) proteins: comparison to bone ECM and contribution to dynamics of dentinogenesis. Connect Tissue Res 2003; 44:171-8.

Cavalcanti BN, Zeitlin BD, Nör JE. A hydrogel scaffold that maintains viability and supports differentiation of dental pulp stem cells. Dent Mater 2013; 29:97-102.

Chen H, Truckenmuller RK, Blitterswijk, CA van, Moroni L. Fabrication of nanofibrous scaffolds for tissue engineering applications. In: Nanomaterials in tissue engineering: Fabrication and applications. Series in Biomaterials (56). Woodhead Publishing 2013; 158-82. ISBN 9780857095961.

Chen J, Lan Y, Baek JA et al. Wnt/beta-catenin signaling plays an essential role in activation of odontogenic mesenchyme during early tooth development. Dev Biol 2009; 334: 174-85.

Chen JP, Chang YS. Preparation and characterization of composite nanofibers of polycaprolactone and nanohydroxyapatite for osteogenic differentiation of mesenchymal stem cells. Colloids Surf B Biointerfaces 2011; 86:169–75.

Clough BH, McCarley MR, Krause U, Zeitouni S, Froese JJ, McNeill EP, et al. Bone Regeneration with Osteogenically Enhanced Mesenchymal Stem Cells and Their Extracellular Matrix Proteins. J Bone Miner Res 2014. doi: 10.1002/jbmr.2320.

Conget PA, Minguell JJ. Phenotypical and functional properties of human

bone marrow mesenchymal progenitor cells. J Cell Physiol 1999; 181:67-73.

Cousins BG, Doherty PJ, Williams RL, Fink J, Garvey MJ. The effect of silica nanoparticulate coatings on cellular response. Journal of Materials Science: Materials in Medicine 2004; 15:355.

Dalby MJ, Gadegaard N, Tare R, Andar A, Riehle MO, Herzyk P, Wilkinson CD, Oreffo RO. The control of human mesenchymal cell differentiation using nanoscale symmetry and disorder. Nat. Mater 2007; 6:997–1003.

Daley WP, Peters SB, Larsen M. Extracellular matrix dynamics in development and regenerative medicine. J Cell Sci. 2008; 121:255-64.

DasGupta, R.Functional Genomic Analysis of the Wnt-Wingless Signaling Pathway. Science 2005; 308:826.

Dassule HR, Lewis P, Bei M, Maas R, McMahon AP. Sonic hedgehog regulates growth and morphogenesis of the tooth. Development 2000; 127:4775–85.

Davies OG, Cooper PR, Shelton RM, Smith AJ, Scheven BA. A comparison of the in vitro mineralization and dentinogenic potential of mesenchymal stem cells derived from adipose tissue, bone marrow and dental pulp. J Bone Miner Metab 2014; 10.1007/s00774-014-0601-y.

Ducy P, Karsenty G. The family of bone morphogenetic proteins. Kidney international 2000;57:2207-14.

DuFort CC, Paszek MJ, Weaver VM. Balancing forces: architectural control of mechanotransduction. Nat Rev Mol Cell Biol. 2011; 12:308-19.

El-Ghannam A, Ducheyne P, Shapiro IM. Porous bioactive glass and hydroxyapaite ceramic affect bone cell function in vitro along different time lines. J Biomed Mater Res 1997; 36:167–80.

Etienne-Manneville S, Hall A. Rho GTPases in cell biology. Nature 2002; 420:629-35.

Fan YW, Cui FZ, Hou SP, Xu QY, Chen LN, Lee IS. Culture of neural cells on silicon wafers with nano-scale surface topograph. J Neurosci Methods 2002; 120:17-23.

Feng JQ, Luan X, Wallace J, Jing D, Ohshima T, Kulkarni AB, et al. Genomic organization, chromosomal mapping, and promoter analysis of the mouse dentin sialophosphoprotein (Dspp) gene, which codes for both dentin sialoprotein and dentin phosphoprotein. J Biol Chem 1998; 73:9457–64.

Fisher LW, Torchia DA, Fohr B, Young MF, Fedarko NS. Flexible structures of SIBLING proteins, bone sialoprotein, and osteopontin. Biochem Biophys Res Commun 2001; 280:460–5.

Fleischmannova J, Matalova E, Tucker AS, Sharpe PT. Mouse models of tooth abnormalities. Eur J Oral Sci 2008; 116: 1–10.

Fujita S, Hideshima K, Ikeda T. Nestin expression in odontoblasts and odontogenic ectomesenchymal tissue of odontogenic tumours. J Clin Pathol 2006; 59:240-5.

Gentili C, Cancedda R. Cartilage and bone extracellular matrix. Curr Pharm Des 2009; 15:1334-48.

Gronthos S, Mankani M, Brahim J, Robey PG, Shi S. Postnatal human

dental pulp stem cells (DPSCs) in vitro and in vivo. Proc Natl Acad Sci U S A 2000; 97:13625-30.

Guo S, Lim D, Dong Z, Saunders TL, Ma PX, Marcelo CL, et al. Dentin Sialophosphoprotein: A Regulatory Protein for Dental Pulp Stem Cell Identity and Fate. Stem Cells Dev 2014 doi:10.1089/scd.2014.0066.

Guo H, Su J, Wei J, Kong H, Liu C. Biocompatibility and osteogenicity of degradable ca-deficient hydroxyapatite scaffolds from calcium phosphate cement for bone tissue engineering. Acta Biomater 2009; 5:268–78.

Hanks CT, Sun ZL, Fang DN, Edwards CA, Wataha JC, Ritchie HH, Butler WT. Cloned 3T6 cell line from CD-1 mouse fetal molar dental papillae. Connect Tissue Res 1998; 37:233–49.

Hilkens P, Gervois P, Fanton Y, Vanormelingen J, Martens W, Struys T,et al. Effect of isolation methodology on stem cell properties and multilineage differentiation potential of human dental pulp stem cells. Cell Tissue Res 2013; 353:65-78.

Hogan PG, Chen L, Nardone J, Rao A. Transcriptional regulation by calcium, calcineurin, and NFAT. Genes Dev 2003; 17:2205–32.

Holappa H, Nieminen P, Tolva L, Lukinmaa PL, Alaluusua S. Splicing site mutations in dentin sialophosphoprotein causing dentinogenesis imperfecta type II. Eur J Oral Sci 2006;114:381–4.

Hoshino M, Hashimoto S, Muramatsu T, Matsuki M, Ogiuchi H, Shimono M. Claudin rather than occludin is essential for differentiation in rat incisor odontoblasts. Oral Dis 2008; 14:606-2.

Huang B, Sun Y, Maciejewska I, Qin D, Peng T, McIntyre B, Wygant J, Butler WT, Qin C. Distribution of SIBLING proteins in the organic and inorganic phases of rat dentin and bone. Eur J Oral Sci 2008; 116:104–12.

Hubbell JA. Biomaterials in tissue engineering. Bio/Technology 1995; 13:565–76.

Hynes RO. The extracellular matrix: not just pretty fibrils. Science 2009; 326:1216-9.

Järvinen E, Salazar-Ciudad I, Birchmeier W, Taketo MM, Jernvall J, Thesleff I. Continuous tooth generation in mouse is induced by activated epithelial Wnt/beta-catenin signaling. Proc Natl Acad Sci U S A 2006; 103:18627-32.

Jiang N, Zhou J, Chen M, Schiff MD, Lee CH, Kong K, et al. Postnatal epithelium and mesenchyme stem/progenitor cells in bioengineered amelogenesis and dentinogenesis. Biomaterials 2014; 35:2172-80.

João SM, Arana-Chavez VE. Expression of connexin 43 and ZO-1 in differentiating ameloblasts and odontoblasts from rat molar tooth germs. Histochem Cell Biol 2003; 119:21-6.

Jose MV, Thomas V, Xu Y, Bellis S, Nyairo E, Dean D. Aligned bioactive multi-component nanofibrous nanocomposite scaffolds for bone tissue engineering. Macromol Biosci 2010; 10:433–44.

Kahn M. Can we safely target the WNT pathway? Nat Rev Drug Discov 2014; 13:513-32.

Katoh K, Kano Y, Ookawara S. Rho-kinase dependent organization of stress

fibers and focal adhesions in cultured fibroblasts. Genes Cells 2007; 5:623-38.
Katoh, M. WNT/PCP signaling pathway and human cancer. Oncol Rep 2005; 14:1583-8.

Kim TH, Bae CH, Lee JC, Ko SO, Yang X, Jiang R, et al. β-catenin is required in odontoblasts for tooth root formation. J Dent Res 2013; 92:215-21.

Kim TH, Lee JY, Baek JA, Lee JC, Yang X, Taketo MM, et al. Constitutive stabilization of β-catenin in the dental mesenchyme leads to excessive dentin and cementum formation. Biochem Biophys Res Commun 2011; 412:549-55.

Kim WS, Vacanti JP, Cima L, Mooney D, Upton J, Puelacher WC, Vacanti CA. Cartilage engineered in predetermined shapes employing cell transplantation on synthetic biodegradable polymers. Plast Reconstr Surg 1994; 94:233.

Kökten T, Bécavin T, Keller L, Weickert JL, Kuchler-Bopp S, Lesot H. Immunomodulation stimulates the innervation of engineered tooth organ. PLoS One 2014; 9:e86011.
Kratochwil K, Galceran J, Tontsch S, Roth W, Grosschedl R. FGF4, a direct target of LEF1 and Wnt signaling, can rescue the arrest of tooth organogenesis in Lef1 (-/-) mice. Genes Dev 2002; 16:3173–85.

Kshitiz, D.H., D.H. Kim, D.J. Beebe, and A. Levchenko. Micro- and nanoengineering for stem cell biology: The promise with a caution. Trends Biotechnol 2011; 29:399–408.

Kuhl M, Sheldahl LC, Park M, Miller JR, Moon RT. The Wnt/Ca2+pathway:

a new vertebrate Wnt signaling pathway takes shape. Trends Genet 2000; 16:279–83.

Kumada Y, Zhang S. Significant Type I and Type III collagen production from human periodontal ligament fibroblasts in 3D peptide scaffolds without extra growth factors. PLoS One 2010; 5:e10305.

Kunzler TP, Drobek T, Schuler M, Spencer ND. Systematic study of osteoblast and fibroblast response to roughness by means of surface-morphology gradients. Biomaterials 2007; 28:2175-82.

Lai SL, Chien AJ, Moon RT. Wnt/Fz signaling and the cytoskeleton: potential roles in tumorigenesis. Cell Res 2009; 19:532–45.

Langer RS, Vacanti JP. Tissue engineering: the challenges ahead. Sci Am 1999; 280:86-9.

Langer, R. & Tirrell, D.A. Designing materials for biology and medicine. Nature 2004; 428:487–92.

Lanza R, Langer PR, Vacanti JP. Principles of Tissue Engineering (2nd ed.). 2000. San Diego: Academic Press.

Lee EJ, Kasper FK, Mikos AG. Biomaterials for tissue engineering. Ann Biomed Eng 2014; 42:323-37.

Lee W, Oh JH, Park JC, Shin HI, Baek JH, Ryoo HM, et al. Performance of electrospun poly (ε-caprolactone) fiber meshes used with mineral trioxide aggregates in a pulp capping procedure. Acta Biomater 2012; 8:2986-95.

Lee SH, and Shin H. Matrices and scaffolds for delivery of bioactive molecules in bone and cartilage tissue engineering. Adv Drug Deliv Rev

2007; 59:339–59.

Lesot H, Hovorakova M, Peterka M, Peterkova R. Three-dimensional analysis of molar development in the mouse from the cap to bell stage. Aust Dent J 2014; 59:81-100.

Li WJ, Laurencin CT, Caterson EJ, Tuan RS, Ko FK. Electrospun nanofibrous structure: a novel scaffold for tissue engineering. J Biomed Mater Res 2002; 60: 613-21.

Lin M, Li L, Liu C, Liu H, He F, Yan F, Zhang Y, Chen Y. Wnt5a regulates growth, patterning, and odontoblast differentiation of developing mouse tooth. Dev Dyn 2011; 240:432-40.

Lin Y, Gallucci G, Buser D, Bosshardt D, Belser U, Yelick P. Bioengineered periodontal tissue formed on titanium dental implants. J Dent Res 2010; 90:251-6.

Linde A, Goldberg M. Dentinogenesis. Crit Rev Oral Biol Med. 1993; 4:679-728.

Liu F, Chu EY, Watt B, Zhang Y, Gallant NM, Andl T, et al. Wnt/β-catenin signaling directs multiple stages of tooth morphogenesis. Dev Biol 2008; 313:210-24.

Liu F, Millar SE. Wnt/β-catenin signaling in oral tissue development and disease. J Dent Res 2010; 89:318-30.

Logan CY, Nusse R. The wnt signaling pathway in development and disease. Annu Rev Cell Dev Biol 2004; 20:781-810.

Lutolf MP, Weber FE, Schmoekel HG, Schense JC, Kohler T, Müller R, et al.

Repair of bone defects using synthetic mimetics of collagenous extracellular matrices. Nat Biotechnol 2003; 21:513-8.

Lutolf MP, Hubbell JA. Synthetic biomaterials as instructive extracellular microenvironments for morphogenesis in tissue engineering. Nat Biotechnol 2005; 23:47-55.

Ma J, He X, Jabbari E. Osteogenic differentiation of marrow stromal cells on random and aligned electrospun poly(L-lactide) nanofibers. Ann Biomed Eng 2011; 39:14-25.

Ma PX. Biomimetic materials for tissue engineering. Adv Drug Del Rev 2008; 60:184-98.

Ma Z, Kotaki M, Inai R, Ramakrishna S. Potential of nanofiber matrix as tissue-engineering scaffolds. Tissue Eng 2005; 11:101-9.

MacDougall M, Simmons D, Luan X, Nydegger J, Feng J, Gu TT. Dentin phosphoprotein and dentin sialoprotein are cleavage products expressed from a single transcript coded by a gene on human chromosome 4. Dentin phosphoprotein DNA sequence determination. J Biol Chem 1997; 272:835–42.

Magloire H, Couble ML, Thivichon-Prince B, Maurin JC, Bleicher F. Odontoblast: a mechano-sensory cell. J Exp Zool B Mol Dev Evol 2009; 312:416-24.

Martin JY, Schwartz Z, Hummert TW, Schraub DM, Simpson J, Lankford J Jr, Dean DD, Cochran DL, Boyan BD. Effect of titanium surface roughness on proliferation, differentiation, and protein synthesis of human osteoblast-

like cells (MG63). J Biomed Mater Res 1995; 29:389-401.

Mata A, Geng Y, Henrikson KJ, Aparicio C, Stock SR, Satcher RL, et al. Bone regeneration mediated by biomimetic mineralization of a nanofiber matrix. Biomaterials 2010; 31:6004-12.

Matsuura T, Hosokawa R, Okamoto K, Kimoto T, Akagawa Y. Diverse mechanisms of osteoblast spreading on hydroxyapatite and titanium. Biomaterials 2000; 21:1121–1127.

Matthews, J.A., Wnek, G.E., Simpson, D.G., and Bowlin, G.L. Electrospinning of collagen nanofibers. Biomacromolecules 2002; 3:232.

Metallo CM, Mohr JC, Detzel CJ, de Pablo JJ, Van Wie BJ, Palecek SP. Engineering the stem cell microenvironment. Biotechnol Prog 2007; 23:18-23.

Mieszawska A, Fourligas N, Georgakoudi I, Ouhib N, Belton D, Perry C, Kaplan D. Osteoinductive silk–silica composite biomaterials for bone regeneration. Biomaterials 2010; 31:8902–10.

Mikels AJ, Nusse R. Purified Wnt5a protein activates or inhibits beta-catenin-TCF signaling depending on receptor context. PLoS Biol 2006; 4:e115.

Miura M, Gronthos S, Zhao M, Lu B, Fisher L, Robey P. SHED: stem cells from human exfoliated deciduous teeth. Proc Natl Acad Sci USA 2003; 100:5807-12.

Murali A, Rajalingam K. Small Rho GTPases in the control of cell shape and mobility. Cell Mol Life Sci 2014; 71:1703-21.

Nikkhah M, Edalat F, Manoucheri S, Khademhosseini A. Engineering microscale topographies to control the cell-substrate interface. Biomaterials 2012; 33:5230-46.

Nobes CD, Hall A. Rho, rac, and cdc42 GTPases regulate the assembly of multimolecular focal complexes associated with actin stress fibers, lamellipodia, and filopodia. Cell 1995; 81:53-62.
Nusse, R. Wnt signaling in disease and in development. Cell Res 2005; 15:28-32.

Oh JH, Seo J, Yoon WJ, Cho JY, Baek JH, Ryoo HM, et al. Suppression of Runx2 protein degradation by fibrous engineered matrix. Biomaterials 2011; 32:5826-36.

Oishi I, Suzuki H, Onishi N, Takada R, Kani S, Ohkawara B, et al. The receptor tyrosine kinase Ror2 is involved in non-canonical Wnt5a/JNK signalling pathway. Genes Cells 2003; 7:645-54.

Park SY, Ki CS, Park YH, Jung HM, Woo KM, Kim HJ. Electrospun silk fibroin scaffolds with macropores for bone regeneration: an in vitro and in vivo study. Tissue Eng Part A 2010; 16:1271-9.

Peng L, Dong G, Xu P, Ren LB, Wang CL, Aragon M, Zhou XD, Ye L. Expression of Wnt5a in tooth germs and the related signal transduction analysis. Arch Oral Biol 2010a; 55:108-14.

Peng L, Ren LB, Dong G, Wang CL, Xu P, Ye L, Zhou XD. Wnt5a promotes differentiation of human dental papilla cells. Int Endod J 2010b; 43:404–412.
Qin C, Brunn JC, Cadena E, Ridall A, Tsujigiwa H, Nagatsuka H, Nagai N,

Butler WT. The expression of dentin sialophosphoprotein gene in bone. J Dent Res 2002; 81:392–4.

Ravindran S, Zhang Y, Huang CC, George A. Odontogenic induction of dental stem cells by extracellular matrix-inspired three-dimensional scaffold. Tissue Eng Part A 2014; 20:92-102.

Rice JM, Hunt JA, Gallagher JA, Hanarp P, Sutherland DS, Gold J. Quantitative assessment of the response of primary derived human osteoblasts and macrophages to a range of nanotopography surfaces in a single culture model in vitro. Biomaterials 2003; 24:4799-818.

Ritchie HH, Li X. A novel rat dentin mRNA coding only for dentin sialoprotein. Eur J Oral Sci 2001; 109:342–7.

Ritchie HH, Li XR, Hanks CT, Knudtson K, Wang LH. The conservation and regulation of rat DSP-PP gene. Connect Tissue Res 2002; 43:331–7.

Ruch JV, Lesot H, Bègue-Kirn C. Odontoblast differentiation. Int J Dev Biol 1995; 39:51-68.

Saneyoshi T, Kume S, Amasaki Y, Mikoshiba K. The Wnt/ calcium pathway activates NF-AT and promotes ventral cell fate in Xenopus embryos. Nature 2002; 417:295–9.

Sarkar L, Sharpe PT. Expression of Wnt signalling pathway genes during tooth development. Mech Dev 1999; 85:197–200.

Sasaki T, Ito Y, Xu X, Han J, Bringas P Jr, Maeda T, et al. LEF1 is a critical epithelial survival factor during tooth morphogenesis. Dev Biol 2005; 278:130-43.

Schmitz AA, Govek EE, Böttner B, Van Aelst L. Rho GTPases: signaling, migration, and invasion. Exp Cell Res 2000; 261:1-12.

Shi S, Robey PG, Gronthos S. Comparison of human dental pulp and bone marrow stromal stem cells by cDNA microarray analysis. Bone 2001; 29:532-9.

Shin M, Yoshimoto H, Vacanti JP. In vivo bone tissue engineering using mesenchymal stem cells on a novel electrospun nanofibrous scaffold. Tissue Eng 2004; 10:33-41.

Shrivastaval A, Calame K. An analysis of genes regulated by the multi-functional transcriptional regulator Yin Yang-1. Nucleic Acids Res 1994; 22:5151-5.

Slinskey A, Barnes D, Pipas JM. Simian virus 40 large T antigen J domain and Rb-binding motif are sufficient to block apoptosis induced by growth factor withdrawal in a neural stem cell line. J Virol 1999; 73:6791–9.

Slusarski DC, Yang-Snyder J, Busa WB, Moon RT. Modulation of embryonic intracellular Ca^{2+}signaling by Wnt-5A. Dev Biol 1997; 182:114–20

Smith LA, Liu X, Hu J, Ma PX. The enhancement of human embryonic stem cell osteogenic differentiation with nano-fibrous scaffolding. Biomaterials 2010; 31:5526-35.

Sohier, J., G. Daculsi, S. Sourice, K. De Groot, and P. Layrolle. Porous beta tricalcium phosphate scaffolds used as a BMP-2 delivery system for bone tissue engineering. J Biomed Mater Res A 2010; 92:1105–14.

Sreenath T, Thyagarajan T, Hall B, Longenecker G, D_Souza R, Hong S, Wright JT, MacDougall M, Sauk J, Kulkarni AB. Dentin sialophosphoprotein knockout mouse teeth display widened predentin zone and develop defective dentin mineralisation similar to human dentinogenesis imperfect type III. J Biol Chem 2003; 278: 24874–80.

Taipale J, Keski-Oja J. Growth factors in the extracellular matrix. FASEB J 1997; 11:51–59.

Takai Y, Sasaki T, and Matozaki, T. Small GTP-binding proteins. Physiol Rev 2001; 81:153–208.

Takemoto M, Fujibayashi S, Neo M, Suzuki J, Kokubo T, Nakamura T. Mechanical properties and osteoconductivity of porous bioactive titanium. Biomaterials 2005; 26:6014–6023.

Tamer Uyar, Flemming Besenbacher. Electrospinning of uniform polystyrene fibers: The effect of solvent conductivity. Polymer 2008; 49:5336–43.

Terling C, Rass A, Mitsiadis TA, et al. Expression of the intermediate filament nestin during rodent tooth development. Int J Dev Biol 1995; 39:947–56.

Teti G, Salvatore V, Ruggeri A, Manzoli L, Gesi M, Orsini G, et al. In vitro reparative dentin: a biochemical and morphological study. Eur J Histochem 2013; 57:e23.

Thesleff I, Sharpe P. Signalling networks regulating dental development. Mech Dev 1997; 67:111–23.

Tjäderhane L, Koivumäki S, Pääkkönen V, Ilvesaro J, Soini Y, Salo T, et al.

Polarity of mature human odontoblasts. J Dent Res 2013; 92:1011-6.

Unterbrink A, O'Sullivan M, Chen S, MacDougall M. TGF beta-1 downregulates DMP-1 and DSPP in odontoblasts. Connect Tissue Res 2002; 43:354–8.

van Genderen C, Okamura RM, Fariñas I, Quo RG, Parslow TG, Bruhn L, et al. Development of several organs that require inductive epithelial-mesenchymal interactions is impaired in LEF-1-deficient mice. Genes Dev 1994; 8:2691-703.

Veeman MT, Axelrod JD, Moon RT. A second canon. Functions and mechanisms of β-catenin-independent Wnt signaling. Dev Cell 2003; 5:367–77.

Veis A, Perry A. The phosphoprotein of the dentin matrix. Biochem 1967; 6:2409–16.

Wang C, Ren L, Peng L, Xu P, Dong G, Ye L. Effect of Wnt6 on Human Dental Papilla Cells In Vitro. J Endod 2010; 36:238-43.

Wang J, Liu X, Jin X, Ma H, Hu J, Ni L, et al. The odontogenic differentiation of human dental pulp stem cells on nanofibrous poly(L-lactic acid) scaffolds in vitro and in vivo. Acta Biomater 2010; 6:3856-63.

Wang J, Ma H, Jin X, Hu J, Liu X, Ni L, et al. The effect of scaffold architecture on odontogenic differentiation of human dental pulp stem cells. Biomaterials 2011; 32:7822-30.

Wang Y, Li L, Zheng Y, Yuan G, Yang G, He F, et al. BMP activity is required for tooth development from the lamina to bud stage. J Dent Res

2012; 91:690-5.

Webster TJ, Ergun C, Doremus RH, Siegel RW, Bizios R. Specific proteins mediate enhanced osteoblast adhesion on nanophase ceramics. J Biomed Mater Res 2000; 51:475-83.

Wei G, Ma PX. Nanostructured biomaterials for regeneration. Advanced Functional Materials 2008; 18:3568–82.

Wnek GE, Carr ME, Simpson DG, Bowlin GL. Electrospinning of nanofiber fibrinogen structures. Nano Lett 2003; 3:213.

Woo KM, Chen VJ, Jung HM, Kim TI, Shin HI, Baek JH, et al. Comparative evaluation of nanofibrous scaffolding for bone regeneration in critical-size calvarial defects. Tissue Eng Part A 2009; 15:2155-62.

Woo KM, Jun JH, Chen VJ, Seo J, Baek JH, Ryoo HM, Kim GS, Somerman MJ, Ma PX. Nano-fibrous scaffolding promotes osteoblast differentiation and biomineralization. Biomaterials 2007; 28:335-43.

Xin X, Hussain M, Mao JJ. Continuing differentiation of human mesenchymal stem cells and induced chondrogenic and osteogenic lineages in electrospun PLGA nanofiber scaffold. Biomaterials 2007; 28:316-25.

Xue W, Krishna BV, Bandyopadhyay A, Bose S. Processing and biocompatibility evaluation of laser processed porous titanium. Acta Biomater 2007; 3:1007–18.

Yamaguchi TP, Bradley A, McMahon AP, Jones S. A Wnt5a pathway underlies outgrowth of multiple structures in the verte- brate embryo. Development 1999; 126:1211–23

Yamakoshi Y. Dentin Sialophophoprotein (DSPP) and Dentin. J Oral Biosci 2008; 50:33–44.

Yamakoshi Y. Dentinogenesis and Dentin Sialophosphoprotein (DSPP). J Oral Biosci 2009; 51:134.

Yamashiro T, Zheng L, Shitaku Y, Saito M, Tsubakimoto T, Takada K, Takano-Yamamoto T, Thesleff I. Wnt10a regulates dentin sailophosphoprotein mRNA expression and possibly links odontoblast differentiation and tooth morphogenesis. Differentiation 2007; 75:452-62.

Yang G, Yuan G, Ye W, Cho KW, Chen Y. An atypical canonical BMP signaling pathway regulates msh homeobox 1 (Msx1) expression during odontogenesis. J Biol Chem 2014: jbc.M114.600064.

Yang W, Harris MA, Cui Y, Mishina Y, Harris SE, Gluhak-Heinrich J. Bmp2 is required for odontoblast differentiation and pulp vasculogenesis. J Dent Res 2012; 9:58-64.

Yang X, Yang F, Walboomers XF, Bian Z, Fan M, Jansen JA. The performance of dental pulp stem cells on nanofibrous PCL/gelatin/nHA scaffolds. Journal of Biomedical Materials Research Part A 2009; 93:247-57.

Yokose S, Naka T. Lymphocyte enhancer-binding factor 1: an essential factor in odontoblastic differentiation of dental pulp cells enzymatically isolated from rat incisors. J Bone Miner Metab 2010; 28:650-8.

You MH, Kwak MK, Kim DH, Kim K, Levchenko A, Kim DY, Suh KY. Synergistically enhanced osteogenic differentiation of human mesenchymal stem cells by culture on nanostructured surfaces with induction media.

Biomacromolecules 2010; 11:1856–62.

Young C, Terada S, Vacanti J, Honda M, Bartlett J, Yelick P. Tissue engineering of complex tooth structures on biodegradable polymer scaffolds. J Dent Res 2002; 81:695-700.

Zayzafoon, M. Calcium/Calmodulin Signaling Controls Osteoblast Growth and Differentiation. J. Cell. Biochem 2006; 97:56–70

Zhang R, Yang G, Wu X, Xie J, Yang X, Li T. Disruption of Wnt/β-catenin signaling in odontoblasts and cementoblasts arrests tooth root development in postnatal mouse teeth. Int J Biol Sci 2013; 9:228-36.

Zhang X, Zhao J, Li C, Gao S, Qiu C, Liu P, et al. DSPP mutation in dentinogenesis imperfecta Shields type II. Nat Genet 2001; 27:151-2.

Zhu Z, Yin J, Guan J, Hu B, Niu X, Jin D, et al. Lithium Stimulates Human Bone Marrow-Derived Mesenchymal Stem Cell Proliferation Through GSK-3-beta-Dependent Beta-catenin/Wnt Pathway Activation. FEBS J 2014. doi: 10.1111/febs.13081.

Zuk PA, Zhu M, Ashjian P, De Ugarte DA, Huang JI, Mizuno H, Alfonso ZC, et al. Human adipose tissue is a source of multipotent stem cells. Mol Biol Cell 2002; 13:4279-95.

VII. Abstract in Korean

국문초록

Wnt 신호전달경로를 통한 나노섬유의 상아모세포 분화 조절

세이드 우르 라만
분자유전학 전공
치의과학과
서울대학교 대학원
지도교수: 우경미 (D.D.S., PhD)

생체재료는 조직공학의 주요 요소로서 생체재료의 표면구조(topography)는 세포 증식, 분화, 최종적인 조직 재생을 조절할 수 있음이 보고되고 있다. 본 연구는 생체 세포외기질을 형태학적으로 모방한 나노섬유 표면구조가 상아모세포의 분화에 미치는 영향과 그 기전을 밝히고자 수행하였다. 전기방사법을 이용하여 합성고분자 (polystryrene, polycaprolactone)로 나노섬유 기질을 제작하고, 사람 성체간엽줄기세포 (골수, 치수, 지방 유래)와 MDPC-23 상아모세포주에서 나노섬유에 대한 반응을 평탄면에 대한 반응과 비교하였다. 나노 섬유상의 치수 유래 중간엽 줄기세포에서 성장인자 중 Wnt-

3a, -5a, -10as와 BMP-2, -4, -7 발현이 높았다. 골분화 표지자들 중에선 분화배지에서 DSPP가 PSF 상의 hDPSCs에서 높게 나타났으며, hADPSCs의 경우 BSP가, hBMSCs에서는 OCN의 발현이 높게 나타났다. 이와 같은 결과는 여기서 나노섬유 인공기질이 같은 재질과 같은 배양 조건에서 중간엽 줄기세포의 성장인자 발현이 다르도록 유도함을 시사한다.

Wnt 신호 전달 경로는 *in vitro*와 *in vivo* 상에서 모두 상아모세포 분화에 중요한 역할을 하는 것으로 보고되어 왔다. 그러나 그 기전은 대부분 알려져 있지 않다. 우리는 여기서 나노 섬유 기질을 사용함으로써 Wnt3a가 canonical Wnt/β-catenin 세포 신호 전달 경로를 통해 직접적으로 DSPP 발현을 증가시킴을 확인하였다. 전기방사로 폴리스티렌 나노 섬유 (PSF)를 준비하였으며, 이 위에 MDPC23 전구 상아모세포를 배양하였다. PSF 상에서의 세포들은 높은 알리자린-레드 염색성과 DSPP와 DMP1의 발현을 나타내, 상아질 모세포 분화가 촉진되었음을 보여주었다. 다음으로 우리는 대표적인 Wnt 신호 전달 경로가 PSF에 의해 유도되는 DSPP 발현에 관련이 있는지 실험하였다. PSF 상에서 MDPC-23는 높은 수준의 β-catenin 발현을 유지하였으며, TCD 상에서 β-catenin이 세포막 근처에 머물러 있는 것

에 비해 PSF 상에서 배양된 세포에서는 핵 안으로 이동하였다. 더 나아가, 우리는 PSF가 LEF/TCF reporter의 활성을 촉진하는지 조사하였다. β-catenin 발현을 Knockdown 시키거나 재조합 Dkk1을 처리한 경우에는 PSF에 의한 DSPP 발현 증가가 억제되었으며, LiCl를 처리하여 LEF1의 발현을 증가시킨 경우에는 DSPP 발현이 증가하였다. 배양 시 재조합 Wnt3a 단백질을 넣어준 상아세포에서는 DSPP 발현이 증가하였다. 나아가 MDPC-23 세포가 배양된 PSF를 누드 마우스의 피하에 이식하는 실험을 통해, *in-vivo* 조건에서 PSF에 의해 촉진되는 Wnt3a 및 DSPP 발현을 확인하였다. 이와같은 결과는 PSF에 의해 유도된 Wnt3a가 상아모세포의 특징적인 분화표지자인 DSPP 발현을 canonical Wnt 신호전달경로를 통해 직접적으로 전사 활성을 증가시킴으로써 DSPP 발현을 유도함을 제시한다.

나노 섬유 기질에 의한 세포의 형태학적 변화와 액틴(actin)의 재구성에 대해 연구하였다. 세포의 극성 (polarization)은 상아모세포의 분화에서 나타나는 중요한 형태적 특징이다. 본 연구에서 Wnt5a 가 상아모세포 분화에 있어 형태적 변화에 관련이 있음을 확인하였다. PSF 상에서 세포의 높이와 세포 돌기 (cell process) 형성이 증가되었으며, 이는 재조합 Wnt5a 처리시 더욱

증가하였다. PSF 상에서 세포 융기 형성은 CDC42 에 의해 유도되는 한편, TCD 상에서 Stress fiber 는 RhoA 에 의해 유도되었다. Wnt5a, Ror2, CDC42 를 knockout 시켰을 때는 PSF 에 의해 유도된 세포 돌기가 감소하였다. 재조합 Wnt5a 의 처리는 TCD 상에서 배양된 세포의 Stress fiber 의 형성을 증가시켰으며 이는 RhoA 의 knockdown 에 의해 다시 감소하였다. PSF 상에서는 CDC42 의 활성이 증가하는 반면, TCD 에서는 RhoA 의 활성이 증가하였다. 나노섬유 인공기질에 의해 유도되는 이러한 변화는 나노섬유기질 위에서 배양된 세포의 Wnt5a 에 대한 차별적 반응성 즉, CDC42 의 활성화에 기인할 수 있음을 제시하였다.

이상의 결과를 종합하여 본 연구는 나노섬유기질이 Wnt 신호전달경로를 통하여 상아모세포 분화를 조절함을 입증하여주며, 이는 상아모세포 분화 조절과 재생 치료에 응용 가능성을 시사한다.

키워드: 나노 섬유, 상아모세포, Wnt3a, β-catenin, Wnt5a, CDC42

학번: 2009-31329